

**Biodiversity and microbial
activity in the epi-, meso- and
bathypelagic realms of the
ocean**

Doctoral Thesis 2017

Elisa Guerrero Feijóo



UNIVERSIDADE DA CORUÑA



Documento bajo licencia de Creative Commons
2017 – Elisa Guerrero Feijóo
Facultad de Ciencias, Universidad da Coruña

Fotografía de la cubierta: <https://www.carbonbrief.org/beneath-the-waves-how-the-deep-oceans-have-continued-to-warm-over-the-past-decade>

Biodiversity and microbial activity in the epi-, meso- and bathypelagic realms of the ocean

Elisa Guerrero Feijóo

TESIS DOCTORAL UDC 2017

Directora: Dra. Marta María Varela Rozados

Codirectora: Dra. Eva Sintés Elvelin

Tutora: Ana Insua Pombo



UNIVERSIDADE DA CORUÑA

Programa de doctorado en “Biología Celular y Molecular”



Dña. Marta María Varela Rozados, Investigadora en el Centro Oceanográfico de A Coruña del Instituto Español de Oceanografía, en colaboración con Dña. Eva Sintés Elvelin, Investigadora Post Doctoral del Departamento de Limnología y Oceanografía de la Universidad de Viena,

CERTIFICAN que el presente trabajo de investigación titulado “Biodiversity and microbial activity in the epi-, meso- and bathypelagic realms of the ocean” presentado por la Licenciada en Ciencias del Mar Elisa Guerrero Feijóo para optar al grado de Doctor por la Universidad de A Coruña, ha sido realizada bajo nuestra dirección, cumpliendo las condiciones exigidas para su presentación, la cual autorizamos.

Para que así conste a efectos oportunos firmamos la presente en A Coruña, a 31 de Julio de 2017.

Fdo. Marta M. Varela Rozados

Fdo. Eva Sintés Elvelin

Directora de la Tesis Doctoral Co-directora de la Tesis Doctoral

Dña. Ana María Insua, profesora contratada doctora del grupo de investigación Genética de organismos marinos (XENOMAR) del Departamento de Biología de la Universidade da Coruña y tutora de la presente memoria de Tesis Doctoral titulada: “Biodiversity and microbial activity in the epi-, meso- and bathypelagic realms of the ocean”, de la que es autora Elisa Guerrero Feijóo y que ha sido dirigida por la Dra. Marta María Varela Rozados, investigadora del Centro Oceanográfico de A Coruña del Instituto Español de Oceanografía, en colaboración con Dra. Eva Sintés Elvelin, Investigadora Post Doctoral del Departamento de Limnología y Oceanografía de la Universidad de Viena

AUTORIZA su presentación en la Universidad de A Coruña para su lectura y defensa.

Para que así conste, firmo la presente en A Coruña a 31 de Julio de 2017.

Fdo. Ana María Insua

Tutora de la Tesis Doctoral

A mis padres, mis hermanos, Lila e Iván

Project framework of the thesis

The work included in this doctoral thesis was carried out at the “Ecología Plantónica y Biogeoquímica (EPB)” group of the Instituto Español de Oceanografía (IEO). Financial support was provided by the projects “Biodiversidade funcional do microplanton nas profundidades mariñas de Galicia” (BIO-PROF, Ref. 10MMA604024PR, 2010-2012, Xunta de Galicia), “Fuentes de materia orgánica y diversidad funcional del microplanton en las aguas profundas del Atlántico Norte” (MODUPLAN, CTM2011-24008, Plan Nacional I+D+I) and RADIALES-PROFUNDAS (RAD-PROF, Instituto Español de Oceanografía).

Contents

| | |
|--|-----|
| SUMMARY / RESUMEN / RESUMO | 17 |
| Chapter 1. Introduction | 21 |
| Chapter 2. Methodology | 39 |
| Chapter 3. Optical properties of dissolved organic matter relate to different depth-specific patterns of archaeal and bacterial community structure in the north Atlantic ocean | 51 |
| Chapter 4. Changes in bacterial activity and community composition in response to size-fractionated dissolved organic matter | 93 |
| Chapter 5. High dark inorganic carbon fixation rates by chemolithoautotrophic microbes off the Galician coast (NW Iberian margin) | 123 |
| Chapter 6. Conclusions | 147 |
| Spanish summary / Resumen en español | 151 |
| Appendix | 170 |
| References | 181 |
| Acknowledgements | 209 |

Summary

This research thesis examined the vertical variation in microbial abundance, activity, community composition and structure, together with optical properties of the dissolved organic matter (DOM), along a longitudinal transect off the Galician coast (NW Spain, from 43°N, 9°W to 43°N, 15°W). The decrease of microbial activity (heterotrophic and autotrophic) with depth coincided with a change in the microbial community composition. Thaumarchaeota was the dominant archaeal (on average 83% of the total Archaea) group throughout the water column and decreased with depth, whereas the bacterial community was dominated by Proteobacteria (79% of the total Bacteria) throughout the water column. However, Cyanobacteria and Bacteroidetes contributed ~ 15% to the bacterial community in the epipelagic, and SAR202 accounted for ~ 5% in the deep waters. The DOM quality and quantity exhibited pronounced vertical variations strongly connected to the depth patterns of archaeal and bacterial community composition, assessed by fingerprinting analysis. Moreover, different size fractions of DOM stimulated the growth of specific bacterial groups, which were linked to changes in the optical indexes of the DOM. Finally, we identified several microbial groups involved in dark inorganic carbon fixation rates in the deep ocean. Taken together, our results highlight the strong link between DOM quality and quantity and specific microbial groups, and the potential for autotrophic carbon fixation by different groups of deep ocean microbes, indicating that the distribution of microbial groups in the ocean is determined by the availability of their preferred substrates and suggest a large metabolic potential of deep ocean microbes.

Resumen

Esta investigación examinó la variación vertical de la abundancia, la actividad, la estructura y la composición de las comunidades microbianas en relación con las propiedades ópticas de la materia orgánica disuelta (MOD) a lo largo de una sección longitudinal de la costa gallega (NO España, de 43°N, 9°O a 43°N, 15°O). El descenso de la actividad microbiana (heterotrófica y autotrófica) con la profundidad coincidió con un cambio en la composición de la comunidad microbiana. *Thaumarchaeota* dominó la comunidad de Arquea en la columna de agua (en promedio, 83% del total de Archaea) y su abundancia descendió con la profundidad, mientras que la comunidad de Bacteria estuvo dominada por Proteobacteria (79% de bacterias totales) en la columna de agua. Sin embargo, Cianobacteria y Bacteroidetes representan ~ 10% de la comunidad bacteriana epipelágica, mientras que SAR202 representó ~ 5% de la comunidad bacteriana profunda. La calidad y cantidad de MOD exhibió variaciones verticales fuertemente correlacionadas con el patrón de distribución vertical de la comunidad de arqueas y bacterias, evaluada por técnicas de huella dactilar. Además, el fraccionamiento molecular de la MOD estimuló el crecimiento de grupos de bacterianos específicos que estuvieron correlacionados con cambios en las propiedades ópticas de la MOD. Finalmente, identificamos varios grupos microbianos implicados en la fijación oscura de carbono inorgánico en el océano profundo. Nuestros resultados destacan el fuerte vínculo entre la calidad y cantidad de MOD con grupos específicos microbianos y el potencial para la fijación oscura de carbono de diferentes grupos microbianos del océano profundo, lo que indica que el patrón de distribución de los grupos microbianos en el océano está determinado por el sustrato disponible y sugiere un gran potencial metabólico de los microbios en el océano profundo.

Resumo

A presente investigación examinou a variación vertical da abundancia, actividade, estrutura e composición da comunidade microbiana en relación cás propiedades ópticas da materia orgánica (MOD) ó longo dunha sección lonxitudinal da costa galega (NO España, de 43°N, 9°O a 43°N, 15°O). O descenso da actividade microbiana (heterotrófica e autotrófica) coa profundidade coincidiu cun cambio na composición da comunidade microbiana. Thaumarchaeota dominou a comunidade de Arquea na columna de auga (en promedio, 83% do total de Archaea) e a súa abundancia descendeu coa profundidade, mentres a comunidade de Bacteria estivo dominada por Proteobacteria (79% de bacterias totais) na columna de auga. Cianobacteria e Bacteroidetes representaron ~ 10% da comunidade bacteriana epipeláxica, mentres SAR202 representou ~ 5% da comunidade bacteriana profunda. A calidade e cantidade da MOD exhibiu variacións verticais fortemente relacionadas co patrón de distribución vertical das comunidades de arquea e bacteria, avaliadas por técnicas de pegada dactilar. O fraccionamento molecular da MOD estimulou o crecemento de grupos bacterianos específicos, que estiveron correlacionados con cambios nas propiedades ópticas da MOD. Finalmente, identificamos varios grupos microbianos implicados na fixación escura de carbono inorgánico no océano profundo. Os nosos resultados destacan o forte vínculo entre a cantidade e calidade da MOD con grupos microbianos específicos e o potencial para a fixación oscura de carbono dos diferentes grupos microbianos no océano profundo, indicando que a distribución dos grupos microbianos no océano escuro está determinada pola preferencia do sustrato dipoñíbel e suxire un gran potencial metabólico dos microbios do océano profundo.



Chapter 1

Introduction

1.1. Role of microbial plankton in the ocean

The marine realm covers 70% of the earth's surface, and thus constitutes the largest habitat on earth. Marine microbes are found not only in the surface waters of the sea but down to abyssal depths. "Microorganisms" are characterized by their small size, they are invisible to the naked eye, and include viruses as well as members of the Bacteria, Archaea and Eukarya domains.

Archaea and Bacteria (Madigan et al. 2006) are unicellular organisms with low morphological diversity (varying from spherical to elongated rods) but with an enormous taxonomical diversity and range of metabolic capabilities. These microorganisms constitute a significant component of the marine plankton accounting for a major fraction in the marine environments (Giovannoni and Rappé 2000). The abundance of these microbes decrease with depth by one order of magnitude, while microbial heterotrophic activity decreases by two orders of magnitude from surface to deep waters (Arístegui et al. 2009). In general, Archaea and Bacteria exhibit opposite vertical distribution patterns in the ocean. Archaea increase their relative abundance towards the deep waters, while bacterial relative abundance decreases with depth (Karner et al. 2001; Teira et al. 2006a; Varela et al. 2008a, 2008b; Dobal-Amador et al. 2016; Guerrero-Feijóo et al. 2017). Within Archaea, Thaumarchaeota is the dominant phylum throughout the water column and generally increased with depth (Karner et al. 2001; Teira et al. 2006b; Guerrero-Feijóo et al. 2017). The bacterial community is dominated by Proteobacteria throughout the water column.

Cyanobacteria and Bacteroidetes are also relatively abundant in the upper water layer ($\approx 10\%$ and 5% , respectively), while Chloroflexi-related SAR202 cluster contributes a significant proportion (5%) to the bacterial communities below the chlorophyll maximum and in deep ocean.

Microbes play a crucial role in ecosystem function as they drive the fluxes of the major elements included in biological macromolecules (Falkowski et al. 2008). Half of the earth global primary production is mediated by the marine phototrophic microorganisms (cyanobacteria, diatoms and pico- and nano-phytoplankton) (Field et al. 1998). Although historically it was considered that a large part of the primary production was directly consumed by higher trophic levels and/or long-term stored into the deep ocean via sinking fluxes, we now know that an important fraction of the carbon fixed by primary producers is released as dissolved organic matter (DOM) and it can be processed by heterotrophic/mixotrophic microbes (Pomeroy 1974; Williams 1981). Adding up complexity to the view of carbon fluxes in the ocean, recent studies have found that some bacterioplankton groups use light (Gómez-Consarnau et al. 2007; Lami et al. 2009; DeLong and Béjà 2010; Palovaara et al. 2014) to obtain energy under conditions of low resource availability, and/or inorganic carbon occurs in the deep Atlantic waters (Varela et al. 2011; Swan et al. 2011).

The biological pump is the microbially mediated flux of carbon from the surface to the deep ocean (Herndl & Reinthaler, 2013). Autotrophic plankton utilizes the sunlight to convert

carbon dioxide into particulate organic carbon (Figure 1.1). This newly produced organic carbon can follow two pathways: (i) it can be remineralized again in the sunlit waters of the ocean; or (ii) a significant fraction (~ 1 to 40% of the photosynthetically fixed carbon) can be exported into the dark ocean, where it can supply energy and carbon to deep ocean prokaryotes. However, this settling organic matter is not sufficient to meet the energy demands of microbes in the dark realm of the ocean (Herndl and Reinthaler 2013). Thus, two other potential sources of organic matter for deep ocean prokaryotes have been suggested, neutrally buoyant organic matter (Baltar et al. 2010) and chemolithoautotrophic microorganisms inhabiting the deep ocean, which could represent a significant source of autochthonous carbon supply (Herndl and Reinthaler, 2013).

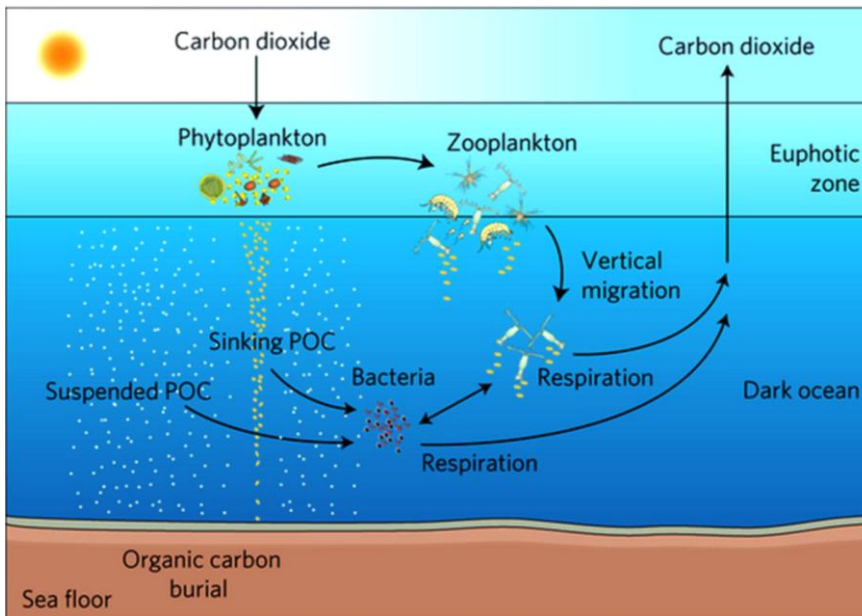


Figure 1.1. Representation of the biological pump in the ocean (Herndl and Reinthaler, 2013).

The chemolithoautotrophic microorganisms use the oxidation of different chemical compounds, such as ammonium (e.g., Konnecke et al. 2005; Wuchter et al. 2006), urea (e.g., Alonso-Sáez et al. 2012) or sulfur reduced compounds (e.g., Baltar et al. 2016; Swan et al., 2011) to generate energy for DIC fixation. Although this process has been considered of minor importance in the deep ocean, recent research indicates that the DIC fixation rates in deep ocean are in the same order of magnitude as heterotrophic activity (Reinthalder et al. 2010; Varela et al. 2011). Since mesophilic archaea were reported to be widely distributed in marine environments (DeLong 1998), several studies have suggested that ammonia oxidation by ammonia-oxidizing archaea (AOA) (Wuchter et al. 2006; Sintes et al. 2013) could substantially contribute to explain the rates of DIC fixation measured in the deep ocean. Additionally, specific marine bacterial taxa have been shown to uptake radiolabeled inorganic carbon (Swan et al. 2011; Guerrero-Feijóo et al. accepted). Thus, inorganic carbon fixation can be relevant for a wide range of metabolic groups, not only chemolithoautotrophs but also heterotrophs, which sustain inorganic carbon fixation via anaplerotic reactions.

1.2. Marine microbial diversity: current knowledge and molecular tools

1.2.1. Marine microbial diversity

Aquatic environments are inhabited by a wide variety of life. Marine microorganisms are not only abundant, but also exhibit a huge genetic diversity (Venter et al. 2004; Sogin et al.

2006) that affects the global biogeochemical cycles of matter and energy (Glöckner et al. 2012). The aquatic environments harbor a large range of microbial cellular densities ($10^4 - 10^7$ cells mL^{-1}) (Whitman et al. 1998). Global estimates indicated that the upper 200 m layer of the ocean contains 3.6×10^{28} cells, while the deep ocean (> 200 m depth) would contain 6.5×10^{28} cells (Whitman et al. 1998). The number of species of microorganisms on Earth has been estimated as high as 10^{12} (Locey and Lennon 2016). Thus, marine microbes represent the most diverse biological group phylogenetic and functional diversity (Sunagawa et al. 2015; Salazar et al. 2016).

1.2.2. Molecular approaches

The knowledge of marine microbial diversity has been hindered by methodological limitations, which until recently allowed the detection of only a “minor” fraction of the marine microbial diversity. Prior to the development of culture-independent approaches, only information on the so-called culturable microorganisms, representing less than 1% of the total diversity of the microbial communities, could be obtained. Early environmental studies of diversity based on culture-independent techniques used cloning and sequencing of specific genes (16S rRNA for prokaryotes and 18S rRNA for eukaryotes). Recently, advances in massive sequencing technologies and bioinformatic analysis have provided a more sensitive and increasingly cheaper approach to study the natural microbial communities at the DNA or RNA level. Metagenomic analyses of marine samples (e.g., GOS and Sorcerer cruises, and recently, Tara Oceans and Malaspina circumnavigation

expedition) have reported that between 50 - 80% of the genes sequenced are novel (Sunagawa et al. 2015; Salazar et al. 2016).

Different approaches can be used to characterize, the microbial communities at DNA/RNA level: (i) high-throughput sequencing of all the genetic information present in the DNA extracted from the environmental community (metagenomics, which includes not only phylogenetic but also functional characterization), (ii) high-throughput sequencing of selected genes previously amplified by polymerase chain reaction (PCR); and (iii) direct hybridization of the 16S rRNA using fluorescent probes targeting specific phylogenetic groups. To attain a more comprehensive knowledge of marine microbial diversity and ecosystem function, in this thesis we used a combination of several methods as described below.

1.2.2.1. Fingerprinting

Fingerprinting techniques are a set of molecular biology tools that can be used to rapidly profile microbial communities (Singh et al 2006; Sun et al 2012; Dorst et al 2014). Qualitative assessment of the microbial community structure in this thesis (Chapter 3) was assessed by traditional fingerprinting techniques, such as terminal restriction fragment length polymorphism (T-RFLP) (Moeseneder et al. 2001) and amplified ribosomal intergenic spacer analysis (ARISA) (Borneman and Triplett 1997). ARISA targets the hypervariable intergenic spacer (ITS) region (Brown and Furhman 2005), while T-RFLP was used in this study to target the 16S rRNA. The ITS region is lacking in many Archaea; thus, ARISA and T-RFLP were used to study bacterial and archaeal communities,

respectively (Yokokawa et al. 2010). Both approaches are culture independent techniques, robust, highly reproducible and time efficient (Bent et al. 2008). However, their main drawback is their low resolution, which hinders to identify the operational taxonomic units (OTU) with specific phylogenetic groups, and/or the lack of quantitative abundance data (Bent and Forney 2008). Some studies have used these techniques combined with cloning and/or sequencing in order to know the microbial phylogenetic composition (Sintes et al. 2013; Lekunberri et al. 2013).

1.2.2.2. Next generation sequencing

With the advent of next-generation sequencing (NGS) platforms, it became possible to recover the huge genetic microbial diversity. Sequencing technologies used for environmental studies have evolved from the Sanger sequencing (Sanger et al. 1977; Goldberg et al. 2006) to the high-throughput sequencing technologies such as 454 pyrosequencing (Venter et al. 2004; Chapters 3 and 4) and Illumina sequencing (Singh et al. 2009), among others. The NGS has been proven successful to recover the high diversity of microbes and the low abundance groups, coined as “rare biosphere”, in the deep waters of North Atlantic (Sogin et al. 2006). Thus, these NGS techniques can be used to infer the relative abundance of the different OTUs (Huber et al. 2007). However, pyrosequencing has also drawbacks, such as the high error rates especially in homopolimeric regions (Margulies et al. 2005; Quince et al. 2009). Up to 15% of the sequences obtained by pyrosequencing are artificial sequences (Gomez-Alvarez et al. 2009). Mende et al. (2012) reported a better resolution of metagenomic assembly

when using Illumina as compared to Sanger and pyrosequencing for the low and medium complexity metagenomes. This thesis used high performance pyrosequencing (Roche 454) to study the microbial 16S rRNA gene diversity. The 16S rRNA gene sequence is approximately 1550 bp long and contains 9 hypervariable regions with considerable sequence diversity (Van de Peer et al. 1996; Chakravorty et al. 2007). Three different hypervariable regions have been amplified and sequenced in the different chapters of this thesis: two hypervariable regions for Bacteria: V1-V3 (Chapter 3, Caporaso et al. 2010) and V3-V4 (Chapter 4, Herlemann et al. 2011), and the hypervariable region V3-V5 for Archaea (Chapter 3, Caporaso et al. 2010).

1.2.2.3. Real time PCR (qPCR)

The qPCR is a quantitative technique with high throughput potential. We used q-PCR to monitor the amplification of a target DNA sequence (e.g. *amoA* gene) in real-time from environmental samples (Chapter 5). The fluorescent signal associated to the DNA amplification can be obtained by using a probe labelled with a fluorochrome and a quencher, which is released as the probe binds to the product, or by a dye that binds to the double stranded DNA, such as SybrGreen (Bustin 2000). Target gene abundance derives from the number of PCR cycles required to exceed a certain fluorescence level. The use of this technique is widespread due to its linearity, sensitivity and the high-throughput.

1.2.2.4. Fluorescence *in situ* Hybridization

Fluorescence in Situ Hybridization (FISH) is a quantitative technique commonly used in combination with specific rRNA-target probes (DeLong et al. 1989; Amann et al. 1990). However, underestimation of the abundance of specific groups can result from the small size and slow growth of microbes. Thus, different modifications of the FISH technique have been developed to amplify the fluorescence signal, such as tyramide signal amplification (TSA), also known as catalyzed reported deposition (CARD). This enhanced technique was used to quantify the abundance of specific microbial groups, such as Bacteria, Thaumarchaeota, SAR11, SAR202, SAR324, SAR406 or Alteromonas, representing some of the most abundant taxa in the dark oceanic environments (Guerrero-Feijóo et al. 2017).

1.2.2.5. Microautoradiography combined with CARD-FISH (MICRO-CARD-FISH)

MICRO-CARD-FISH is a very powerful technique to study different metabolic capacities of microbial populations. Studies with this technique reported different uptake activities of selected compounds (such as amino acids) by specific microbial phylogenetic groups (Varela et al. 2008a, 2008b, Teira et al. 2017). The heterogeneity in microbial uptake patterns (Ouverney and Furhman 1999; Cottrell and Kirchman 2003; Teira et al. 2004, Alonso and Pernthaler, 2006) and the autotrophic capabilities of Archaea and Bacteria (Varela et al. 2011; Swan et al. 2011; Guerrero-Feijóo accepted) (Chapter 5) have been demonstrated by using this particular technique.

1.3. Vertical stratification of marine microbial diversity

Compelling evidence indicates that the distribution pattern of the main prokaryotic groups varies considerably with depth, however, little is known about the factors leading to this vertical stratification of microbial communities. Several physical and chemical parameters co-vary with depth, contributing most likely to the depth-stratification of prokaryotic communities (De Long et al. 2006; Galand et al. 2009; Ghiglione et al. 2012; Dobal-Amador et al. 2016). For instance, temperature, hydrostatic pressure and salinity correlate with the variation in abundance, activity and diversity of marine microbial communities (Fuhrman et al. 2006). Abundance of bacterial taxa in the Sargasso Sea is also explained by environmental variables, like chlorophyll-a and depth (Sjöstedt et al. 2014). However, few studies have examined how dissolved organic matter quantity and quality might shape microbial communities. Recent investigation reported that the microbial composition and abundance are not shaped by the quantity of dissolved organic carbon, but instead they reveal a strong connection with the DOM quality (Guerrero-Feijoo et al. 2017).

The variability of microbial community structure with depth has been shown using fingerprinting techniques (Yokokawa et al. 2010; Lekunberri et al. 2013; Dobal-Amador et al. 2016). A considerable fraction of the bacterial community is present throughout the water column, whereas some operational taxonomic units (OTUs) are specific for distinct water masses as shown by pyrosequencing (Agogué et al. 2011;

Ghiglione et al. 2012; Ferrera et al. 2015, Guerrero-Feijoo et al. 2017). The archaeal communities are less diverse than bacterial communities (Ferrera et al. 2015; Guerrero-Feijóo et al. 2017), however, they are also stratified (Kaneko et al. 2016; Guerrero-Feijóo et al. 2017). The description of the microbial diversity along the vertical dimension is critical to understand, model and predict the distributions of the microbial taxa in the ocean in the context of anthropogenic global change. In particular, it is important to ascertain to what extent climate change might impact the magnitude of specific processes rates. In turn, marine microorganisms could contribute to promote or alleviate the global change effect in hitherto unpredictable ways (Glöckner et al. 2012).

1.4. Interactions between dissolved organic matter and microbes

The marine DOM pool constitutes a continuum of compounds of different biological lability, ranging from highly labile (e.g. turnover time on the scale of minutes to days) to refractory (with turnover time on the scale of centuries to millennia) (Williams and Druffel, 1987; Bauer et al 1992). There are two important characteristics of the DOM that we assessed in this thesis in order to investigate the interaction between DOM and microbial communities: the optical properties and the molecular size/or weight of the DOM.

Optical properties of the DOM constitute an essential key to determine the quality and quantity of DOM as substrate for microbe utilization. DOM comprises a fraction of colored or

chromophoric compounds known as colored DOM (CDOM; Coble, 1996). CDOM compounds absorb light at different wavelengths, at the ultraviolet and visible. Throughout this work, three different wavelengths of CDOM were studied: (i) absorption coefficient of DOM at 254 nm; (ii) absorption coefficient of DOM at 340 nm; and (iii) absorption coefficient of DOM at 365 nm. Even though, the ecological significance of these indices of the DOM remains unclear, the differences between these indices depend on the nature of the CDOM. The conjugation/aromaticity characteristics increase with the absorption wavelength (Stedmon and Nelson, 2015). The spectral slope between 275 and 295 nm ($sCDOM_{275-295}$) has been frequently used to relate the optical features of the DOM with marine microbes, providing information on shifts in molecular weight and aromaticity of the DOM (Helms et al 2008). Nevertheless, more studies are needed to elucidate the specific compounds of the DOM that absorb at these wavelengths. Furthermore, a fraction of the CDOM can emit blue fluorescence when it is irradiated with ultraviolet light; it is termed fluorescent DOM (FDOM; Coble 1996, 2007). There are two main groups of FDOM substances depending on the excitation and emission wavelengths: (i) protein-like substances (FDOM-T) with fluorescence characteristics of the aromatic amino acids (Coble 1996), and considered as a proxy for labile DOM (Yamashita and Tanoue 2003; Nieto-Cid et al. 2006), and (ii) marine humic-like substances (FDOM-M), which are considered to be photo-labile and bio-refractory (Chen and Bada 1992; Nieto-Cid et al. 2006). Changes in the FDOM composition indicate both biological (Chen and Bada 1992; Nieto-Cid et al. 2006) and photochemical processes (Moran et al. 2000; Nieto-Cid et al. 2006) acting upon the bulk DOM pool.

Operationally, DOM comprises a low molecular weight (LMW-DOM <1 kDa) and a high molecular weight (HMW-DOM >1 kDa) fraction. Amon and Benner (1994) used ultrafiltration to separate DOM into these two fractions and incubate microbial communities, leading to the concept of the size-reactivity continuum of DOM. Higher bacterial production and respiration rates were obtained in HMW-DOM as compared to LMW-DOM incubations (Amon and Benner, 1994), suggesting that HMW-DOM is more bio-reactive and less diagenetically altered than the bulk of LMW-DOM. However, contrasting results were obtained by Khodse and Bhosle (2011). These authors indicated that the LMW-DOM was utilized more rapidly by microbial communities, and thus, it was suggested to be more bio-reactive than the HMW-DOM fraction. However, the DOM size is not the only factor driving the reactivity, but also biological processes control the size distribution (e.g. biosynthesis and biodegradation) (Benner and Amon, 2015). Consequently, the size-reactivity continuum model has been revised and suggests that the organic matter is a continuum from highly structured cellular state to seemingly random and complex molecular state (Benner and Amon, 2015).

The microbial-DOM interactions are central in biogeochemical cycles. The connection between microbial community composition and DOM composition has been scarcely studied, however, it is fundamental to understand the role and response of microbial communities to global change. The diversity and composition of DOM is one of the major factors driving the microbial community composition, and in turn the marine carbon cycle (Kirchman et al. 2004; Alonso-Sáez et al. 2007; Dinasquet et al. 2013; Landa et al. 2014;

Dobal-Amador et al. 2016; Guerrero-Feijóo et al. 2017). The archaeal communities are linked to labile and refractory DOM compounds in intermediate and deep waters, respectively (Guerrero-Feijóo et al. 2017). Specifically, Euryarchaeota-MGII was strongly connected to refractory compounds, while Thaumarchaeota-MGI revealed tight relations with the aromatic compounds in deep waters (Guerrero-Feijóo et al. 2017). Furthermore, bacterial communities were also related to vertical patterns of optical properties of DOM or size-reactivity (Dobal-Amador et al. 2016; Guerrero-Feijóo et al. 2017). Two abundant phylotypes of bacteria in the deep ocean, SAR202 and SAR406, were linked to refractory DOM compounds, while abundant phylotypes in upper waters, such as SAR11, were related to protein-like substances (Guerrero-Feijóo et al. 2017). Moreover, different size-fractions of DOM stimulated specific bacterial phylotypes (Guerrero-Feijóo et al. submitted).

1.5. Aims and outline of the thesis

The aim of this doctoral thesis was to advance our knowledge on the vertical variability of the microbial (Bacteria and Archaea) abundance, activity and community composition and their relationship with the abundance, and optical properties of the DOM in the epi- meso- and bathypelagic waters near the west coast off Galicia (NW Iberian Peninsula). The main goals of the present doctoral thesis can be summarized as follows:

Chapter 3. We studied the role of DOM quantity and quality in shaping the archaeal and bacterial community structure. A distance-based multivariate analysis for a linear model (DistLM) was used to study the associations between different optical properties of the DOM and archaeal and

bacterial community structure obtained with T-RFLP and ARISA, respectively. Additionally, a redundancy analysis (RDA) was used to link the different indices of the DOM and specific microbial 454-pyrosequencing phylotypes.

Chapter 4. Heterotrophic bacteria respond dynamically to variations in organic matter availability in the dark ocean. However, our knowledge on how the size and/or reactivity of dissolved organic matter (DOM) affect the bacterial community dynamics is still scarce. Chapter 4 aims to investigate the response of bacterial activity and community composition to filter and of size-fractionated DOM. We isolated a natural bacterial community from Mediterranean Water (1000 m depth) and inoculated it in molecular weight size-fractionated filtered seawater obtained by ultrafiltration. We measured bacterial abundance and production along with DOM optical properties over 6 days incubation, and linked these parameters to changes in bacterial community composition.

Chapter 5. Microbial chemolithoautotrophic activity in the deep ocean has been recently shown to be substantially larger than hitherto assumed, thus representing an alternative source of carbon for deep ocean microbes. We investigated several marine prokaryotic groups actively incorporating dissolved inorganic carbon by combining microautoradiography with catalyzed reporter deposition fluorescence in situ hybridization (MICRO-CARD-FISH). The dark inorganic carbon uptake is widespread among different bacterial phylotypes, suggesting a significant contribution of bacteria to the global dark ocean chemoautotrophy.



Chapter 2

Methodology

2.1. Study area

The study region in the Atlantic ocean off the Galician coast (from 43°N, 9°W to 43°N, 15°W) is a dynamic area characterized by seasonal upwelling pulses, which support both the exportation offshore and sinking fluxes of organic matter. Mixing of different water masses reaches down to the mesopelagic waters that flows northwards along the western Iberian Peninsula (Ruíz-Villareal et al. 2006), and may influence the abundance and composition of the microbial communities inhabiting the dark ocean. The mesopelagic realm is characterized by the interaction between North Eastern Atlantic Central Water (NEACW), rich in dissolved oxygen, and Mediterranean water (MW), characterized by higher salinity and lower oxygen concentration than NEACW. The MW flows through the west Iberian slope and its core is located at around 1000 m depth. Underlying the MW flows the Labrador Sea Water (LSW), characterized by a relative minimum of salinity, temperature and oxygen concentration. The LSW enters the Biscay Bay (Paillet et al. 1998) and the western part of the Iberian margin. The core of LSW is detected in the channel between the Galician continental shelf and the Galician Bank (VACLAN, Climatic Variability in the North Atlantic).

2.2. Sampling

2.2.1. *In situ* measurements

Sampling was conducted during two oceanographic cruises, BIO-PROF-1 (August 2011, 11-28) and BIO-PROF-2

(September 2012, 11-20) on board R/V Cornide de Saavedra off Cape Finisterre (Figure 2.1). A total of 43 stations were sampled during the BIO-PROF cruises (22 and 21 stations in BIO-PROF-1 and BIO-PROF-2, respectively). These stations corresponded to the same stations sampled during the time series RADIALES-PROFUNDOS/VACLAN, led by the Instituto Español de Oceanografía (IEO) (<http://www.seriestemporales-ieo.com>). Vertical profiles of temperature, salinity and oxygen concentration were obtained down to >5000 m depth. Samples were collected with Niskin bottles mounted on a conductivity-temperature-depth (CTD) rosette sampler from different water masses according to their temperature and salinity.

Water samples were collected to determine of the variables listed below (Table 2.1). The methods used are described in detail in Chapters 3, 4 and 5:

- Inorganic dissolved nutrients: nitrate, nitrite, silicate and phosphate
- Concentration of dissolved organic carbon (DOC)
- Fluorescence of dissolved organic matter (FDOM)
- Absorbance of dissolved organic matter (aCDOM)
- Prokaryotic abundance (PA)
- High nucleid acid content cells (HNA)
- Leucine incorporation rates (Leu. incorp.)
- Bulk microbial heterotrophic production
- Bulk dissolved inorganic carbon (DIC) fixation rates (DIC fixation)
- Nucleid acid double staining (NADS) for assessing membrane integrity of microbial cells (%live)
- CTC reduction to identify actively respiring cells (%CTC+)

- Catalyzed reported deposition-fluorescence in situ hybridization (CARD-FISH)
- Microautoradiography combined with CARD-FISH (MICRO-CARD-FISH)
- DNA extraction
- Automated ribosomal intergenic spacer analysis (ARISA).
- Terminal restriction fragment length polymorphism (T-RFLP).
- 454 pyrosequencing.
- Quantitative PCR (qPCR) of specific genes

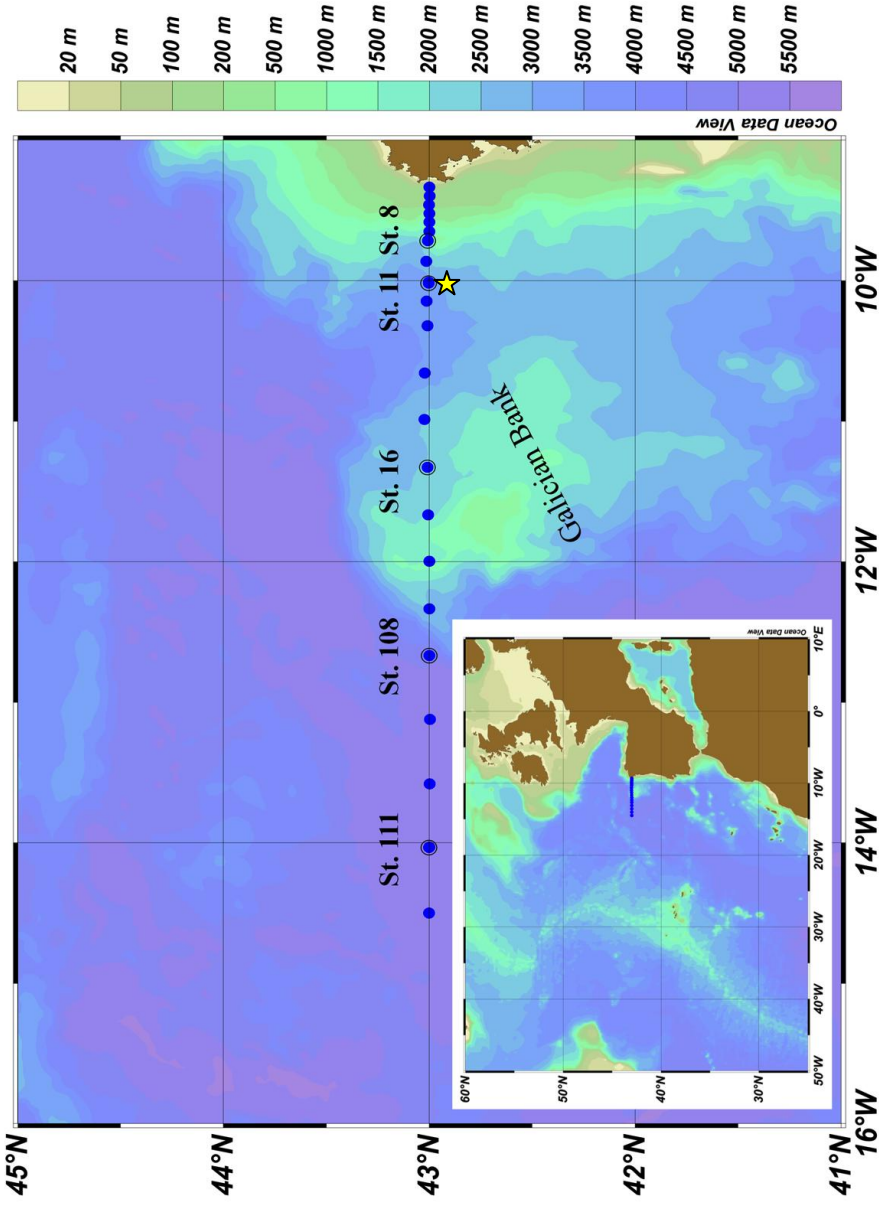


Figure 2.1. Map showing the stations along the Finisterre Section located in the NW Atlantic Ocean off the Galician coast. Dots represent the stations where the physico-chemical data was collected. The stations 8, 11, 16, 108 and 111 correspond to the biological stations highlighted in the map (Chapter 3 and 5). Yellow star indicates the station where the water was collected to perform the molecular weight experiment (Chapter 4).

Table 2.1. Set of variables measured in this doctoral thesis (1: BIO-PROF-1; 2, BIO-PROF-2; 3, MODUPLAN)

| Variable | Abbreviation | Cruise | Units |
|---|-------------------------------|---------|---|
| Concentration of nitrite | NO ₂ ⁻ | 1, 2, 3 | umol kg ⁻¹ |
| Concentration of nitrate | NO ₃ ⁻ | 1, 2, 3 | umol kg ⁻¹ |
| Concentration of phosphate | PO ₄ ³⁻ | 1, 2, 3 | umol kg ⁻¹ |
| Concentration of silicate | SiO ₄ ⁻ | 1, 2, 3 | umol kg ⁻¹ |
| Concentration of DOC | DOC | 1, 2, 3 | umol kg ⁻¹ |
| Protein-like fluorescence | FDOM-T | 1, 2, 3 | OSU |
| Humic-like fluorescence | FDOM-M | 1, 2, 3 | OSU |
| Absorption coefficient at 254 nm | aCDOM254 | 1, 2, 3 | OSU |
| Absorption coefficient at 340 nm | aCDOM340 | 1, 2, 3 | OSU |
| Absorption coefficient at 365 nm | aCDOM365 | 1, 2, 3 | OSU |
| Optical slope between 275 and 295 nm | sCDOM275-295 | 1, 2, 3 | OSU |
| Prokaryotic abundance | PA | 1, 2, 3 | cells mL ⁻¹ |
| High nucleic acid content | HNA | 1, 2, 3 | % |
| Low nucleic acid content | LNA | 1, 2, 3 | % |
| Leucine incorporation rates | Leu incorn. | 1, 2, 3 | nmol Leu cell ⁻¹ h ⁻¹ |
| Bulk microbial heterotrophic production | MHP | 1, 2, 3 | umol C m ⁻³ d ⁻¹ |
| Bulk DIC fixation rates | DIC fixation | 1, 2 | umol C m ⁻³ d ⁻¹ |
| Percentage of active cells | %CTC+ | 3 | % |
| Percentage of actively respiring cells | %live | 3 | % |
| Fluorescence in situ Hybridization | CARD-FISH | 1, 2 | % probe + cells |
| Microautoradiography | MICRO-CARD-FISH | 2 | % dami + cells with silver grain |
| Automated Ribosomal Intergenic Spacer Analysis | ARISA | 1, 2 | presence/absence OTUs |
| Terminal Restriction Fragment Length Polymorphism | T-RFLP | 1, 2 | presence/absence OTUs |
| 454 nt-sequencing | 454 | 2, 3 | abundance of 16S rRNA |
| Quantitative PCR | qPCR | 1, 2 | copies mL ⁻¹ |

2.2.2. Experimental approach

Mediterranean water (MW, 1000m depth) was collected at the station 11 (43° N 9° W to 43° N 14° W, Fig. 2.1) during the MODUPLAN cruise on board R/V Sarmiento de Gamboa (<https://moduplansarmiento2014.wordpress.com/>, MODUPLAN project) to set up the experimental approach described in Chapter 4. The bacterial community from the MW was inoculated to (i) 0.1 µm–filtered seawater (DOM); (ii) low-molecular-weight fraction (LMW-DOM) and (iii) the recombined low- and high-molecular-weight fractions (H+L-DOM) obtained from the size-fractionation of DOM. The scheme of size fractionation of DOM utilized in this experimental approach is shown in Figure 2.2.

The 0.1 µm filtered seawater (used also as CONTROL) entered the tangential flow ultrafiltration system by the exterior of the 1 kDa membrane (blue line; Figure 2.2). As the flow rate is reduced at the top of this membrane, the sample is pressed (5 psi) to the centre, and the tangential flow of the material smaller than the molecular weight cut-off passes through the membrane and reaches the centre and it is collected into the low molecular weight carboy (LMW-DOM, red line; Figure 2.2). Finally, the small flux that cannot go through the membrane constitutes the high molecular weight fraction of the DOM (HMW-DOM, green line; Figure 2.2). The H+L-DOM treatment was prepared by recombining the LMW-DOM and HMW-DOM in the same proportion as the original sample water (see details in Chapter 4).

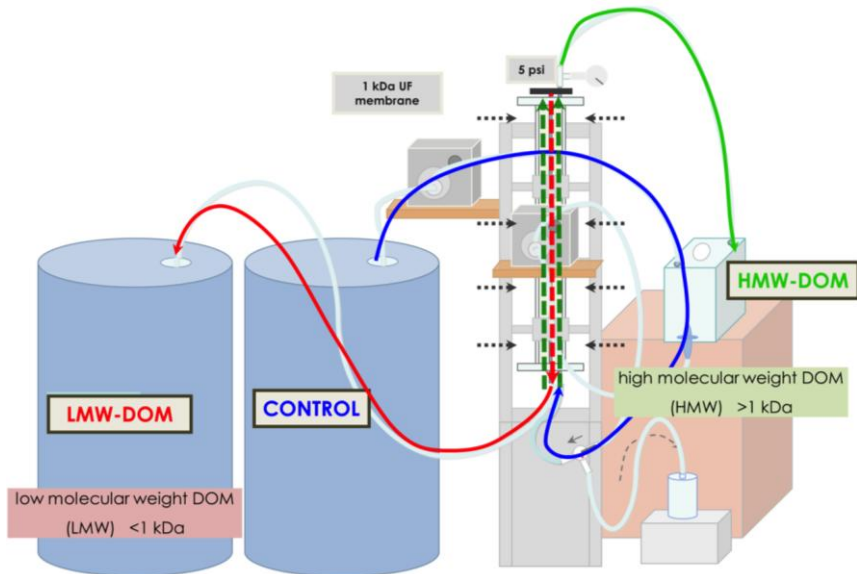


Figure 2.2. Scheme of the ultrafiltration approach used to produce size fractionated- DOM. Abbreviations: LMW-DOM, low-molecular-weight fraction of DOM (DOM<1kDa); HMW-DOM, high-molecular-weight of DOM (DOM>1kDa); CONTROL, 0.1 μm filtered seawater.

2.3. Data analysis

2.3.1. Bioinformatics analyses

Bioinformatics analyses of 454 pyrosequencing data were performed using the Quantitative Insights Into Microbial Ecology (QIIME) pipeline (<https://qimme.org>; Caporaso et al. 2010) (Chapter 3 and Chapter 4). Firstly, the raw reads were demultiplexed and quality filtered to eliminate the low quality pyrotags. The remaining sequences were denoised to remove sequencing errors such as long sequences of homopolymers. OTUs were assigned as the sequences sharing 97% identity. A representative sequence for each OTU was chosen by selecting

the most abundant sequence in the cluster. Subsequently, chimera sequences were removed with ChimeraSlayer implemented in MOTHUR (Schloss et al. 2009; Haas et al. 2011). Phylogenetic affiliation of the 16S rRNA sequences was assigned using the blast classifier implemented in QIIME (Wang et al. 2007). Sequences identified as chloroplast and mitochondria were removed. Additionally, rarefaction analysis was used to verify that the number of sequences obtained in each sample showed a tendency of plateauing.

Subsequently, the resulting OTU tables were subsampled to ensure an equal number of sequences per sample to allow comparisons between samples (Chapter 3 and Chapter 4). Richness and diversity indices such as Chao1 (Chao, 1987; Chapter 3 and Chapter 4) and Shannon (Hill, 1973; Chapter 4) were calculated. Clustering of samples was tested for significance with ANOSIM analysis. Furthermore, MOTHUR was used to generate venn diagrams (Chapter 4).

Pyro-sequences have been deposited in the National Center for Biotechnology Information (NCBI) Sequence Read Archive (PRJNA317990 and PRJNA318014 for BIO-PROF samples) and (PRJNA385510 for MODUPLAN samples).

2.3.2. Statistical analysis

Student's t-test analyses were performed to determine significant differences of the physico-chemical characteristics and DOM variables between BIO-PROF-1 and BIO-PROF-2 (Chapter 3 and Chapter 5), and to test for significant differences in biological measurements between the different water masses

(Chapter 3 and Chapter 4) (Sokal and Rohlf 2013). Furthermore, Spearman correlation was performed to analyse the relationship between microbial communities and environmental variables (Chapter 3 and Chapter 5). All statistical analyses were performed using Sigmaplot 11.0.

Presence/absence OTU tables and normalized abundance were used to perform a hierarchical cluster (Chapter 3 and 4, respectively) when using fingerprinting assessment of the community composition. A distance-based linear model (DistLM) was used to study the relationships between the resemblance matrix of microbial community structure (fingerprinting analysis) and normalized DOM-related variables (Chapter 3). The marginal tests showed the percentage of contribution of each DOM related variable taken separately, while the sequential test indicated the cumulative effect of each variable once the previous variable(s) had been counted for (Chapter 3; Guerrero-Feijóo et al. 2017). These analyses were carried on in PRIMER6 and PERMANOVA+ (Anderson et al. 2008). Redundancy analysis (RDA) implemented in XLSTAT was used to analyse the relationships between normalized abundance of the OTUs obtained by 454 pyrosequencing and normalized data of optical properties of DOM (Chapter 3 and Chapter 4).



Chapter 3

Optical properties of dissolved organic matter relate to different depth-specific patterns of archaeal and bacterial community structure in the north Atlantic ocean

Abstract

Abundance, activity and prokaryotic community composition were studied in the euphotic, intermediate and deep waters off the Galician coast (NW Iberian margin) in relation to the optical characterization of dissolved organic matter (DOM). Microbial (Archaea and Bacteria) community structure was vertically stratified. Among the Archaea, Euryarchaeota, especially Thermoplasmata, was dominant in the intermediate waters and decreased with depth, whereas marine Thaumarchaeota, especially Marine Group I, was the most abundant archaeal phyla in the deeper layers. The bacterial community was dominated by Proteobacteria through the whole water column. However, Cyanobacteria and Bacteroidetes occurrence was considerable in the upper layer and SAR202 was dominant in deep waters. Microbial composition and abundance were not shaped by the quantity of dissolved organic carbon, but instead they revealed a strong connection with the DOM quality. Archaeal communities were mainly related to the fluorescence of DOM (which indicates respiration of labile DOM and generation of refractory sub-products), while bacterial communities were mainly linked to the aromaticity/age of the DOM produced along the water column. Taken together, our results indicate that the microbial community composition is associated to the DOM composition of the water masses, suggesting that distinct microbial taxa have the potential to use and/or produce specific DOM compounds.

3.1. Introduction

Marine microbes are major components of plankton and play a significant role in the oceanic biogeochemical cycles. Prokaryotic abundance and activity decrease with depth by one and two orders of magnitude, respectively (Arístegui et al. 2009; Furrman et al. 2015). Such pattern is determined by the vertical variability of the physical and chemical features of the pelagic environment, which also contribute to the vertical stratification of the microbial community composition (DeLong et al. 2006; Martín-Cuadrado et al. 2007; Agogué et al. 2011).

Sequencing (Sanger and 454 pyrosequencing) of rRNA gene is a valuable tool to characterize the microbial community structure in the water column (Giovannoni et al. 1996; DeLong et al. 2006; Yokokawa et al. 2010; Agogué et al. 2011; Lekunberri et al. 2013). Based on these techniques, several recent investigations have shown a vertical stratification of the microbial populations in the deep waters of the Atlantic Ocean (Agogué et al. 2011; Lekunberri et al. 2013; Ferrera et al. 2015; Frank et al. 2016) and Pacific Ocean (Schmidt et al. 1991; DeLong et al. 2006). In addition, variations of Archaea and Bacteria relative abundances among different water masses have also been well established by catalyzed reporter deposition fluorescence *in situ* hybridization (CARD-FISH) enumeration of specific phylogenetic groups. CARD-FISH studies revealed increasing relative abundance of archaeal cells with depth while Bacteria shows the opposite pattern (Karner et al. 2001; Teira et al. 2006a; Varela et al. 2008a, 2008b; Dobal-Amador et al. 2016). Similarly, the distribution of specific groups of Bacteria varies considerably with depth (Varela

et al. 2008b; Lekunberri et al. 2013; Dobal-Amador et al. 2016). However, variation of the microbial community's composition with depth is not only attributable to the most abundant taxa, but also to the less abundant phylotypes. Recent results from next generation sequencing of the 16S rRNA gene indicate the existence of microbial phylotypes specific to the deep water masses of the Atlantic Ocean (Agogué et al. 2011; Ferrera et al. 2015).

Temperature, hydrostatic pressure and salinity correlate with the variation in abundance, activity and diversity of the microbial communities (Sjöstedt et al. 2014; Fuhrman et al. 2015; Dobal-Amador et al. 2016). The amount and quality of organic matter in marine ecosystems is also recognized as a major factor that affects the metabolism, distribution and dynamics of prokaryotic communities (Cottrell and Kirchman 2000; Kirchman et al. 2004; Dobal-Amador et al. 2016). However, our knowledge on the sources of DOM in the intermediate and deep waters and the link between the composition and diversity of DOM and microbial communities, particularly Archaea, in the dark ocean is still limited.

The Galician coast (NW Spain) is a dynamic area characterized by seasonal upwelling pulses, which support the exportation offshore and sinking of organic matter. Hence, this ecosystem represents an ideal study area to investigate how the composition and diversity of DOM might shape the microbial communities. Results from a previous exploratory study in the same area indicated that the bacterial community structure assessed by automated rRNA intergenic spacer analysis (ARISA) fingerprinting was related not only to physico-chemical

parameters but also to DOM quality (Dobal-Amador et al. 2016). The aim of the present study was to extend these previous results and investigate the role of DOM quality and quantity in shaping the archaeal community structure as compared to Bacteria, by using terminal restriction fragment length polymorphism (T-RFLP/ARISA) fingerprinting and sequencing of the bacterial and archaeal 16S rRNA gene, along a longitudinal section off the eastern north Atlantic. We hypothesized that vertical variation in the different indices of the DOM results in different depth-related patterns in archaeal community structure as compared to Bacteria. We used the distance-based multivariate analysis for a linear model (DISTLM) and redundancy analysis (RDA) to identify the best set of optical properties of organic matter explaining the variations in the Archaea community structure and composition as compared to Bacteria in the euphotic, intermediate and bathypelagic waters of the eastern north Atlantic.

3.2. Material and methods

3.2.1. Sampling

Sampling was conducted during the cruises BIO-PROF-1 (August 11th – 28th, 2011) and BIO-PROF-2 (September 11th – 20th, 2012), on board R/V Cornide de Saavedra from 43°N, 9°W to 43°N, 14°W off Cape Finisterre (NW Spain) (Figure 3.1). Samples were collected with Niskin bottles mounted on a CTD (conductivity-temperature-depth) rosette sampler from different depths based on their temperature and salinity: euphotic zone (EZ, 3 samples, 5, 50 and 100 m depth); Eastern North Atlantic Central Water (ENACW, 2 samples, 250-300 and 500-900 m depth), the

layer of the oxygen minimum zone (OMZ, ≈ 900 m); Mediterranean Water (MW, 1 sample, 1000 m depth); Labrador Sea Water (LSW, 1 sample, 1800 m depth); Eastern North Atlantic Deep Water (ENADW, 1 sample, 2750 m depth) and Lower Deep Water (LDW, 1 sample, >4000 m depth). A total of 43 stations were sampled (22 and 21 stations for BIO-PROF-1 and BIO-PROF-2, respectively) to perform the physical and chemical analysis (Figure 3.1; Table 3.1). Seawater samples from six stations (5, 8, 11, 16, 108, 111, Figure 3.1) were collected for dissolved organic matter measurements, and four stations (11, 16, 108 and 111, Figure 3.1) were additionally sampled for microbial

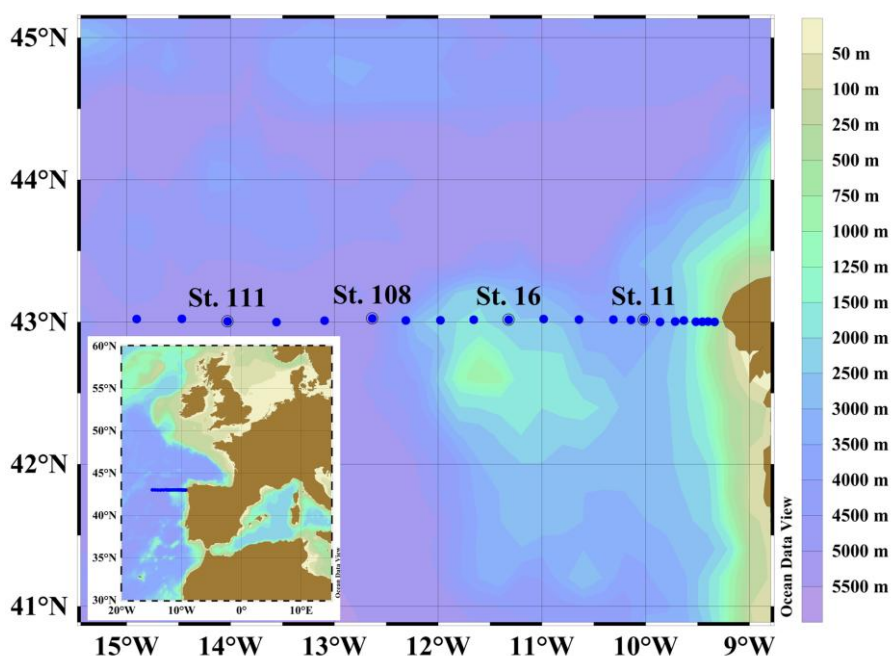


Figure 3.1. Map showing the stations along the Finisterre Section located in the NW Atlantic Ocean off the Galician coast. Dots represent the stations where the physicochemical data were measured. The stations where the biological measurements were conducted are also indicated (St 11, St 16, St 108 and St 111).

analysis, including abundance, activity, structure and composition of the prokaryotic communities in both cruises.

3.2.2. Chemical analysis

Samples for the analysis of dissolved oxygen measurements were collected in pyrex “iodine titration” flasks with flared necks and ground glass stoppers, with a nominal volume of about 115 mL. Following Langdon (2010), the samples were measured by the winkler potentiometric method. Nutrient salts (nitrate, nitrite, phosphate and silicate) were collected in rinsed polyethylene bottles and frozen at -20 °C until further analysis by standard colorimetric methods on a segmented flow analyser Bran-Luebbe analyser following the procedures of Hansen and Koroleff (1999).

All DOM samples above 200 m were filtered under positive pressure using an acid-clean all-glass system and combusted (450 °C, 4 h) GFF filters. Water samples for the analysis of dissolved organic carbon (DOC) were collected in combusted (450 °C, 12h) glass ampoules, and acidified with H₃PO₄ to pH <2. The ampoules were heat-sealed and DOC was determined with a Shimadzu TOC-CSV analyser by high temperature Pt-catalytic oxidation (Alvarez-Salgado and Miller 1998). DOM fluorescence intensity was measured on board within 2-3 hours at two pair of fixed excitation/emission wavelengths: 320 nm/410 nm (FDOM-M), characteristic of marine “refractory” humic-like substances; and 280 nm/350 nm (FDOM-T), characteristic of “labile” protein-like materials, using a Perkin Elmer LS55 to following Nieto-Cid et al. (2006). Samples were calibrated against quinine sulphate and results given in quinine

Table 3.1. Physical and chemical characteristics of the main water masses sampled during the cruises BIO-PROF-1 and BIO-PROF-2 along Northwestern of Iberian Peninsula (Fisterra Cape), Euphotic Zone (EZ); Eastern North Atlantic Central Water – Oxygen Minimum Zone (ENACW-OMZ); Mediterranean Water (MW); Labrador Sea Water (LSW); Eastern North Atlantic Deep Water (ENADW), Lower Deep Water (LDW).

| Water masses | Depth (m) | Temperature (°C) | Salinity | Oxygen ($\mu\text{mol kg}^{-1}$) | Nitrate ($\mu\text{mol kg}^{-1}$) | Silicate ($\mu\text{mol kg}^{-1}$) | Phosphate ($\mu\text{mol kg}^{-1}$) |
|--------------|-----------|------------------|-------------|------------------------------------|-------------------------------------|--------------------------------------|---------------------------------------|
| EZ | ≤100 | 12.47-20.45 | 35.73-36.11 | 189.81-269.16 | 0.10-8.71 | 0.22-4.40 | 0.10-0.72 |
| ENACW-OMZ | 250-900 | 10.11-12.92 | 35.54-36.11 | 180.47-243.71 | 7.31-19.50 | 2.12-8.07 | 0.51-1.11 |
| MW | 1000 | 3.6-11.42 | 35.03-36.15 | 180.58-261.7 | 13.03-21.44 | 6.64-12.69 | 0.72-1.31 |
| LSW | 1800-2000 | 3.56-7.25 | 34.96-35.21 | 197.50-261.78 | 15.54-19.49 | 9.63-15.23 | 0.91-1.31 |
| ENADW | 2500-2900 | 2.51-3.50 | 34.92-35.04 | 235.13-255.94 | 14.63-22.96 | 10.59-35.12 | 1.02-1.49 |
| LDW | ≥4000 | 2.47-2.54 | 34.89-34.91 | 232.03-243.70 | 18.30-23.23 | 32.82-47.10 | 1.24-1.56 |

sulphate units (QSU). UV-visible absorption spectra of the chromophoric DOM were acquired on a Beckman Coulter DU800 spectrophotometer equipped with 10cm quartz cuvettes also in a time frame of 2-3 hours after collection. Spectral scans were recorded from 250 to 700 nm, using the sample average absorbance between 600 and 700 nm to correct for offsets (Green and Blough 1994). Absorption coefficients were calculated following Green and Blough (1994) at several wavelengths along the spectra aCDOM₂₅₄ (absorption coefficient at 254 nm), aCDOM₃₄₀ (absorption coefficient at 340 nm), and aCDOM₃₆₅ (absorption coefficient at 365 nm). Differences between these indices lay on the nature of the colored DOM, as the intensification of the conjugation/aromaticity increases with the absorption wavelength (Stedmon and Nelson, 2015). Thus, absorption coefficients at wavelength larger than 300 nm would only gather information of complex/aromatic molecules and would not be related to relatively simple compounds. In addition, the shape of the absorption spectra was explored by means of the spectral slopes between 275 and 295 nm (sCDOM₂₇₅₋₂₉₅), calculated from the linear regression of log-transformed absorption spectra, and providing information on shifts in molecular weight and DOM aromaticity (Helms et al. 2008). In general terms, absorption coefficients are considered "quantitative" variables, as they are a proxy of the concentration of colored DOM, while the slope of the spectra is assessed as a "qualitative" variable, indicating changes in colored DOM composition (Stedmon and Nelson, 2015).

3.2.3. Prokaryotic abundance

Following Gasol et al. (1999) samples for prokaryotic abundance (PA) were determined by flow cytometry. A volume of 1.8 mL per water sample was preserved with 1% paraformaldehyde (final concentration), shock-frozen in liquid N₂ for 10 min and stored at -80 °C. Samples were thawed to room temperature and stained with Syto13 (Life Technologies) in the dark for 10 min. Subsequently, 1 µm fluorescent latex beads (approximately 1x10⁵ mL⁻¹) (Molecular Probes, Invitrogen, Carlsbad, CA) were added to all the samples as internal standard. The prokaryotes were counted using a FACSCalibur flow cytometer (Becton Dickinson, Franklin Lakes, NJ) according to their signature in right angle light scatter and green fluorescence.

3.2.4. Leucine incorporation rates

Leucine incorporation (Leu incorp.) rates from the microbial communities from the euphotic and upper intermediate waters (up to 500m) were measured by adding 5 nmolL⁻¹ [³H]-leucine (final concentration, specific activity 160 Ci mmol L⁻¹, GE Healthcare, Amersham, Bucks, UK) to triplicate 1.2 mL samples. Duplicate TCA (trichloroacetic acid)-killed blanks (5% final concentration) were treated in the same way as the samples (Simon and Azam 1989). Samples and blanks were incubated in the dark and in situ temperature in temperature-controlled chambers for 2–6 h, depending on the expected activity. Incubations were terminated by adding TCA (5% final concentration) to the samples. Bacterial proteins were precipitated by two successive centrifugation steps (12000 rpm, 10 min), including a washing step with 1 mL of 5% TCA following

Kirchman (1985) with slight modifications (Smith and Azam 1992).

Leu incorp. from the lower intermediate and deep waters (below 1000m) was determined by adding 5 nmol L⁻¹[³H]-leucine (final concentration, specific activity 160 Ci mmol L⁻¹, GE Healthcare, Amersham, Bucks, UK) to duplicate 40 mL samples and duplicate formaldehyde-killed blanks (2% final concentration) (Simon and Azam 1989). The incubation of samples and blanks was carried out in the dark and in situ temperature for 10 - 24 h, depending on the expected activity. The incubations were finished by adding formaldehyde (2% final concentration) to the samples. Samples and blanks were filtered onto 0.2 µm polycarbonate filters (25 mm filter diameter, Millipore). Afterwards, the filters were rinsed with 10 mL 5% ice-cold TCA and air-dried before liquid scintillation cocktail was added to the vials. After 18 h, the radioactivity was quantified in a scintillation counter (LBK Wallac). The disintegrations per minute (DPMs) of the blanks were subtracted from the mean DPMs of the respective samples and the resulting DPMs converted into leucine incorporation rates. The cell-specific activity was estimated dividing Leu incorp by PA.

3.2.5. DNA extraction of the prokaryotic community

A volume of 10 - 15 L of water was filtered through sterile Sterivex 0.22 µm pore size filters (Millipore, USA). 1.8 mL of lysis buffer (40 mM EDTA, 50 mM Tris-HCl, 0.75 M sucrose) was added to the filter cartridge and stored at -80 °C. DNA extraction was performed by enzymatic lysis of the cells with lysozyme and proteinase K, followed by phenol-chloroform

extraction. DNA was precipitated by the addition of isopropanol. The pellet was washed with 70% ethanol and resuspended in sterile TE buffer. DNA samples were quantified and quality checked (according to the A260/A280 ratio) using a Nanodrop spectrophotometer (Thermo Scientific, USA).

3.2.6. T-RFLP and ARISA fingerprinting of archaeal and bacterial communities

Two different fingerprinting techniques, T-RFLP and ARISA, were performed to study archaeal and bacterial community structure, respectively. Both techniques can be used to quickly profile the structure of microbial communities. The ITS region used for ARISA is more variable than the 16S rRNA used for T-RFLP. Slightly higher total numbers of bacterial OTUs have been obtained with ARISA as compared to T-RFLP (Yokokawa et al. 2010). Thus, ARISA has been suggested to be more effective than T-RFLP on the 16S rRNA for estimating diversity of prokaryotic assemblages (García-Martínez et al. 1999). However, several Archaea harbours very short or even lack intergenic transcribed spacer (Moreira et al. 2004, Leuko et al. 2008). Taking these previous findings into account, we used ARISA fingerprinting to assess the bacterial community structure and T-RFLP was performed to assess the archaeal community structure.

T-RFLP fingerprinting was carried out on a standard amount of DNA (2 µL) from each sample by using the primer set 27F-FAM (FAM-6'-AGA GTT TGA TCC TGG CTC AG-3') and 958R-VIC (VIC-5'-YCC GGC GTT GAM TCC ATT T-3'; DeLong 1992). PCR conditions and chemicals were applied as described by Moeseneder et al. (2001). PCR product was purified

and subsequently digested at 37 °C overnight with the tetrameric restriction enzyme (HhaI). The restriction enzyme was heat inactivated and the digested DNA was precipitated. Fluorescently labelled fragments were separated and detected in an ABI Prism 310 capillary sequencer (Applied Biosystems). The internal size standard used were LIZ 1200 (20-1200 pb, Applied Biosystems). The output from the ABI Genescan software was analysed with the FINGERPRINTING II software (BIO-RAD) to determine the peak height.

Automated rRNA intergenic spacer analysis (ARISA)-PCR was conducted on a standard amount of DNA (2 µl) from each sample. Bacterial ARISA was performed using ITSF, 5'-GTC GTA ACA AGG TAGGCC GTA-3', and ITSReub, 5'-GCC AAG GCA TCC ACC 3', primer set (Thermo Scientific) as previously described (Cardinale et al. 2004). ARISA fingerprinting conditions have been previously reported (Dobal-Amador et al. 2016). ARISA fragments were separated using the ABI Prism 3730XL (Applied Biosystems) genetic analyzer applying the internal standard LIZ 1200 (20 – 1200 pb, Applied Biosystems). Obtained peaks with height value <20 fluorescence units were removed from the output peak matrix before statistical analyses. Each ARISA peak was defined as a different operational taxonomic unit (OTU).

3.2.7. Pyrosequencing of the archaeal and bacterial 16S rRNA gene

Pyrosequencing was performed for Archaea and Bacteria only at station 111 during the BIO-PROF 2 cruise. We analysed 7

samples, representative of the different water masses in this region. A subsample of the DNA extracted was used for pyrosequencing at the Research and Testing Laboratory (Lubbock, TX, USA: <http://medicalbiofilm.org>) using 454 GL FLX technology. The Bacteria specific primers 28F (5'GAGTTTGATCNTGGCTCAG) and 519R (5'GTNTTACNGCGGCKGCTG) were used to generate amplicons from V1 to V3 regions of the bacterial 16S rRNA gene (~500 bp). Archaeal specific primers 341F (5'-GYGCASCAGKCGMGAAW-3') and 958R (5'-GGACTACVSGGGTATCTAAT-3') were used to amplify the region spanning the V3 to V5 regions (~600 bp). Subsequent analyses were performed using Quantitative Insights Into Microbial Ecology (QIIME) pipeline (<http://qiime.org>) (Caporaso et al. 2010).

A quality check was performed to minimize low quality pyrotags, eliminating sequences with 50bp sliding window Phred average below 25, ambiguous bases and sequences with length <100-125 bp after trimming. The remaining sequences were run into Denoiser to detect the pyrosequencing errors (Reeder and Knight 2010). The curated sequences were grouped into operational taxonomic units (OTUs) with a 97% similarity threshold. A representative sequence from each phylotype was chosen by selecting the most abundant sequence in each cluster. MOTHUR was used to remove chimeras by ChimeraSlayer (Schloss 2009; Haas et al. 2011) based on the alignment file SILVA 108 (<http://www.arb-silva.de>). Blast Classifier (Wang et al. 2007) implemented in QIIME determined the identity of 16S rRNA phylotypes. OTUs assigned to chloroplast or mitochondria were removed from our analysis. In addition, the rarefaction

curves were plotted to verify that the sequences obtained in each sample showed a tendency of plateauing for the most samples of Archaea (Supplementary Figure 3.1 A) and Bacteria (Supplementary Figure 3.1 B). Pyrotag sequences have been deposited in the National Center for Biotechnology Information (NCBI) Sequence Read Archive (SRA) under PRJNA317990 and PRJNA318014 bioproject numbers.

One OTU table was built for Archaea and another one for Bacteria. Both tables were subsampled to ensure an equal number of sequences per sample (1436 and 3511 sequences for Archaea and Bacteria, respectively).

3.2.8. CARD-FISH and FISH

CARD-FISH was used to quantify the abundance of the major of prokaryotic groups at four stations (11, 16, 108 and 111) following the method described by Pernthaler et al. (2002). Immediately after collecting the samples from the Niskin bottles, 20–80 mL of seawater were preserved with paraformaldehyde (2% final concentration) and stored at 4 °C in the dark. About 12–18 h later, the samples were filtered onto 0.2 µm polycarbonate filters (Millipore GTTP, 25-mm filter diameter) supported by nitrocellulose filters (Millipore, HAWP, 0.45 µm), washed twice with 10 mL Milli-Q water, dried and stored in a microfuge vial at -20 °C until further analysis. Filters were cut in sections and hybridized with horseradish peroxidase (HRP)-labelled oligonucleotide probes (Supplementary Table 3.1), followed by tyramide-Alexa488 signal amplification. Cells were counter-stained with a DAPI-mix [5.5 parts of Citifluor (Citifluor), 1 part of Vectashield (Vector Laboratories) and 0.5 parts of phosphate-

buffered saline (PBS) with DAPI (final concentration $2 \mu\text{g mL}^{-1}$)]. Quantification of DAPI-stained cells and cells stained with the specific probes was carried out under a Nikon Eclipse 80i epifluorescence microscope equipped with Hg lamp and appropriate filter sets for DAPI, Cy3 and Alexa448. A minimum of 500 DAPI-stained cells was counted per sample.

3.2.9. Statistical Analysis

All t-test analysis was performed using Sigmaplot 8.0. Hierarchical cluster analysis (CLUSTER) was carried out to explore similarities between samples, based on Bray-Curtis similarity matrix obtained by T-RFLP and ARISA fingerprintings of archaeal and bacterial communities. Significant differences in microbial community composition between samples were investigated by permutational analysis of variance with PRIMER software (Primer-E v. 6; Anderson et al. 2001). The differences in alpha diversity among water masses (by using the 454 pyrosequencing data) were tested statically using ANOSIM analysis of the PRIMER software.

A distance-based linear model (DistLM) analysis was used to study the relationship between the resemblance matrix of microbial community structure and DOM-related variables. Previously, all variables were tested for co-linearity (Spearman correlation matrix) and those with determination coefficients (R^2) higher than 0.95 were eliminated. The contribution of each variable was assessed, firstly using “marginal test” to assess the statistical significance and percentage contribution of each variables taken separately. Secondly, a “sequential test” was employed to evaluate the cumulative effect of each variable once

the previous variable(s) had been accounted for. All variables were introduced in the model with the “step wise” selection procedure of the DistLM model, using the “Akaike” information criterion (AIC). Such procedure allows us to find the best combination of variables that explain the variability from the microbial resemblance matrix. All statistical tests were performed with PRIMER6 & PERMANOVA+ (Anderson et al. 2008). In addition, a redundancy analysis (RDA) was performed to examine the associations among DOM-variables and specific microbial groups obtained using 454-pyrosequencing with XLSTAT software.

3.3. Results

3.3.1. Environmental parameters

The main water masses along a section off the Galician coast (Figure 3.1) were identified according to their temperature and salinity signals (Prieto et al. 2013). The physical and chemical characteristics of these water masses are summarized in Table 3.1. No significant differences were detected for the physico-chemical variables among the two cruises (t-test, $p > 0.5$, $n = 555$ for temperature, salinity and oxygen; t-test, $p > 0.5$, $n = 371$ for nitrate, silicate and phosphate). The Lower Deep Water (LDW) was found below 4000 m depth. LDW is characterized by low temperature (2.5 °C; Table 3.1), low salinity (34.4; Table 3.1), high dissolved oxygen (250 $\mu\text{mol kg}^{-1}$; Supplementary Figure 3.2 A-B), nitrate (20 $\mu\text{mol kg}^{-1}$ Supplementary Figure 3.2 C-D), phosphate (1.5 $\mu\text{mol kg}^{-1}$; Supplementary Figure 3.2 E-F) and silicate concentration (32.8 – 44.94 $\mu\text{mol kg}^{-1}$; Supplementary

Figure 3.2 G-H). The Eastern North Atlantic Deep Water (ENADW) was identifiable by slightly higher temperature (2.5 – 3.5 °C; Table 3.1) and higher oxygen concentration (Supplementary Figure 3.2 A-B; Prieto et al. 2013; Dobal-Amador et al. 2016). Two types of intermediate waters were found, the Labrador Sea Water (LSW; 1800-2000 m) showed a minimum of salinity (35.0 – 35.4; Table 3.1) and a relatively high oxygen concentration (197.5 – 262.8 $\mu\text{mol kg}^{-1}$; Supplementary Figure 3.2 A-B). The Mediterranean Water (MW; 1000 m depth) was clearly identifiable by the highest salinity values (35.0 - 36.2; Prieto et al. 2013; Table 3.1) as compared to the other water masses. The Eastern North Atlantic Central Water was found between 250 – 900 m depth and the Oxygen Minimum Zone (ENACW-OMZ) was located east of the Galician bank at around 900 m depth characterized by the lowest oxygen concentrations (180 – 241 $\mu\text{mol kg}^{-1}$, Supplementary Figure 3.2 A-B). The lowest concentrations of nitrate, phosphate and silicate (0.1 – 8.7, 0.1 – 0.7 and 0.2 – 4.4 $\mu\text{mol kg}^{-1}$, respectively) were found in the Euphotic Zone (EZ; 0-100 m depth).

3.3.2. Elemental and optical characterization of the DOM

The DOC concentration decreased from subsurface towards the deeper layers (Figure 3.2 A-B) with no significant differences between BIO-PROF-1 and BIO-PROF-2 cruises (t-test, $p=0.19$, $n=107$). The lowest DOC concentrations (42 – 44 $\mu\text{mol L}^{-1}$) were determined in the LDW. The fluorescence of protein-like substances of the DOM showed significant differences between the two cruises (t-test, $p<0.01$, $n=107$), being lower during BIO-PROF-1. FDOM-T also decreased with depth, from 1.84 QSU at the EZ and reaching values of about 0.30 QSU

in LDW (Figure 3.2 C-D). By contrast, the fluorescence of marine humic-like substances increased from ~0.60 QSU in EZ to 1.00 in LDW (Figure 3.2 E-F) and did not exhibit significant differences between the two cruises (t-test, $p=0.13$, $n=107$).

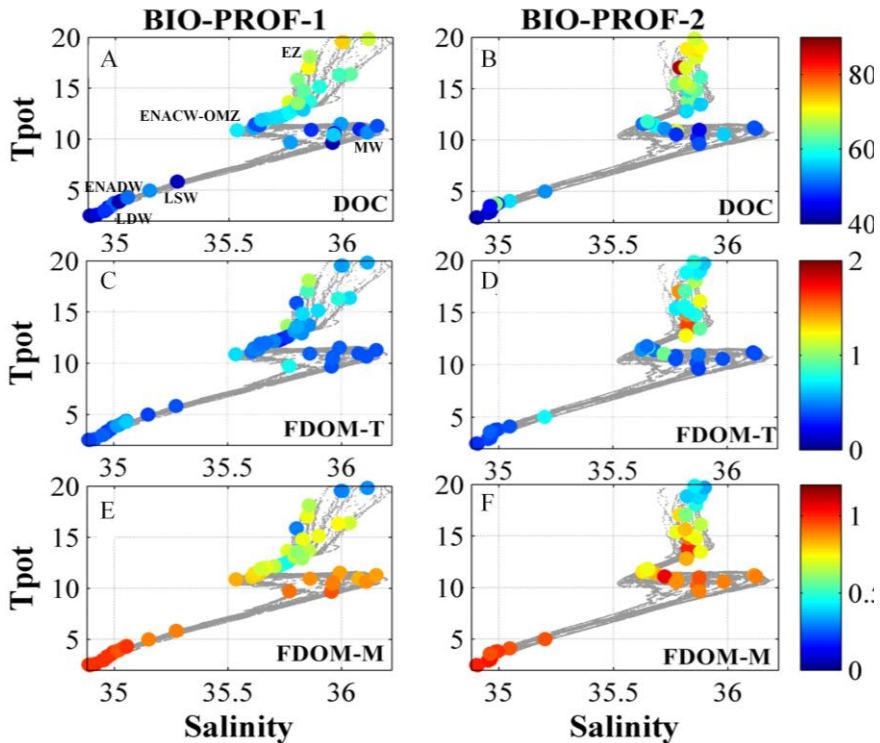


Figure 3.2. Potential temperature (T_{pot} , °C) - salinity diagrams every 2 dbars for the BIO-PROF-1 (Left) and BIO-PROF-2 (Right), with superimposed values from discrete depths of: (A, B) DOC in $\mu\text{mol kg}^{-1}$; (C, D) protein-like fluorescence, FDOM-T; (E, F) humic-like fluorescence, FDOM-M.

The absorption coefficient at 254 nm ($a_{CDOM254}$) (Figure 3.3A-B) ranged from 1.32 at EZ to 0.84 at LDW with no significant differences between both cruises (t-test, $p=0.52$, $n=107$). On the other hand, $a_{CDOM340}$ and $a_{CDOM365}$ (Figure 3.3 C-F) did not show any clear vertical trend, presenting average

values of 0.13 and 0.09, respectively. However, significant differences were found between both cruises (t-test, $p < 0.01$, $n = 107$), as both coefficients were higher in the shallower waters during BIO-PROF-2. The $sCDOM_{275-295}$ decreased from 0.033 in the EZ to 0.027 in the LDW and significant differences were found between both cruises (t-test, $p < 0.01$, $n = 54$).

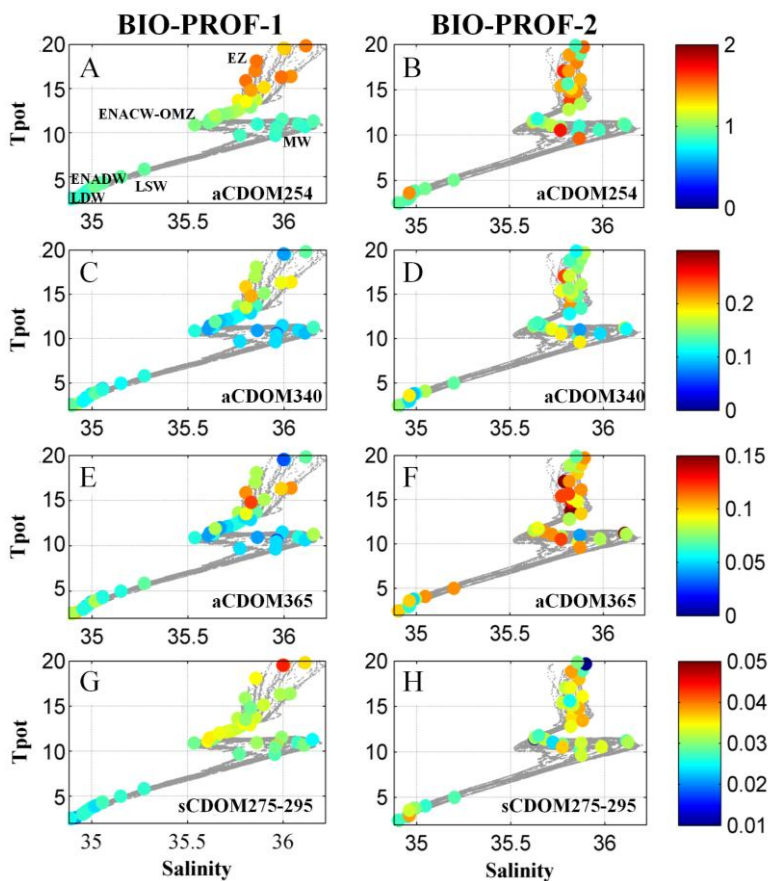


Figure 3.3. Potential temperature (T_{pot} , °C) - salinity diagrams every 2 dbars for the BIO-PROF-1 (Left) and BIO-PROF-2 (Right), with superimposed values from discrete depths of: (A, B) absorption coefficient at 254 nm, (C, D) absorption coefficient at 365 nm and (E, F) optical slope between 275 and 295 nm.

3.3.3. Prokaryotic abundance and leucine incorporation

The highest prokaryotic abundance (PA) occurred in the EZ ($2.33 \pm 0.8 \times 10^5$ cells mL⁻¹; Figure 3.4A-B), decreasing exponentially with depth at all stations during both BIO-PROF-1 and BIO-PROF-2 cruises. No significant differences among PA

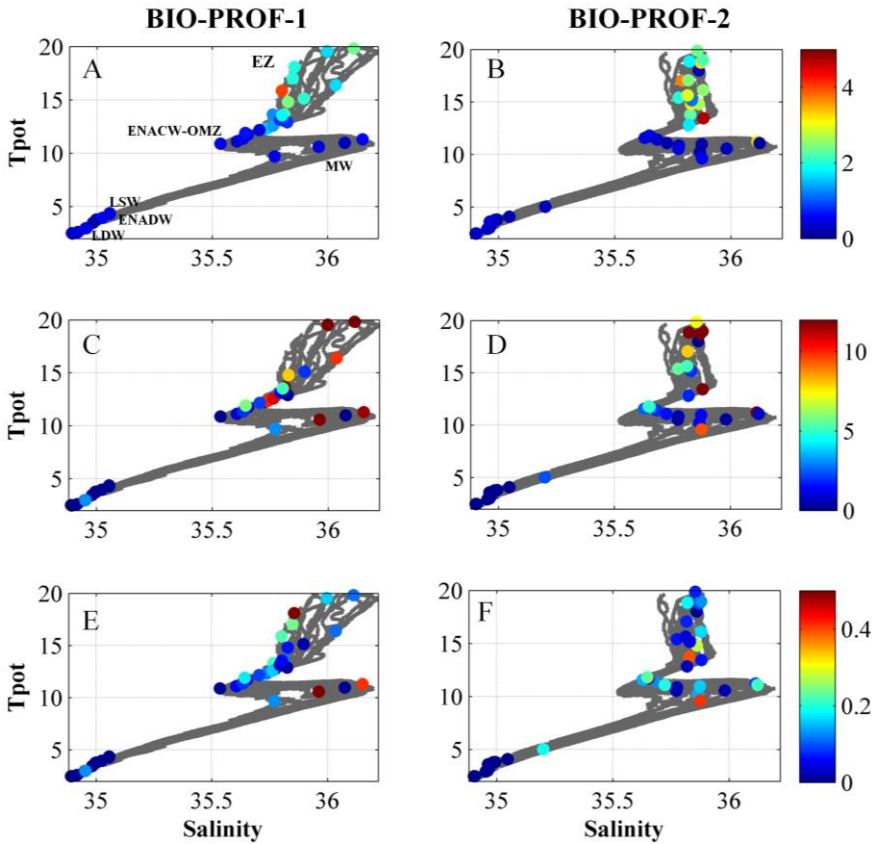


Figure 3.4. Potential temperature (T_{pot} , °C) - salinity diagrams every 2 dbars for the BIO-PROF-1 (Left) and BIO-PROF-2 (Right), with superimposed values from discrete depths of: (A, B) prokaryotic abundance (10^5 cells mL⁻¹); (C, D) leucine incorporation rate ($\text{pmol Leu L}^{-1} \text{h}^{-1}$); (E, F) cell-specific activity (10^{-4} $\text{pmol Leu cell}^{-1} \text{h}^{-1}$).

distribution in the two cruises were observed (t-test, $p=0.67$, $n=58$). The minimum values were found in the ENADW ($1.84 \pm 0.94 \times 10^4$ cells mL^{-1} ; Figure 3.4B) during BIO-PROF-2 cruise.. The rates of leucine incorporation (Leu incorp.) showed a similar vertical trend at both cruises, decreasing three orders of magnitude from the EZ (7.85 ± 5 fmol Leu $\text{L}^{-1} \text{day}^{-1}$; Figure 3.4C-D) to the LDW ($6.68 \pm 6.75 \times 10^{-3}$ fmol Leu $\text{L}^{-1} \text{day}^{-1}$; Figure 3.4C-D).

Cell-specific activity decreased from the euphotic zone to the intermediate and deep waters; however, it varied between cruises (Figure 3.4E-F). Maximum cell-specific activity was $1.46 \pm 1.5 \times 10^{-5}$ fmol Leu $\text{cell}^{-1} \text{day}^{-1}$ in the EZ during the BIO-PROF-1 cruise (Figure 3.4E). Generally, cell-specific activity was more variable in the intermediate and deep waters, particularly during the BIO-PROF-2 cruise, but always within one order of magnitude. In the intermediate and deep waters, the minimum cell-specific activity was $9.81 \pm 6.98 \times 10^{-6}$ fmol Leu $\text{cell}^{-1} \text{day}^{-1}$ in the LDW during BIO-PROF-1, while the maximum was $1.13 \pm 1.04 \times 10^{-3}$ fmol Leu $\text{cell}^{-1} \text{day}^{-1}$ in the EZ during BIO-PROF-2.

3.3.4. Microbial community structure determined by fingerprinting techniques

The terminal restriction fragment length polymorphism (T-RFLP) pattern of the archaeal community revealed a total of 133 OTUs at the 16S rRNA gene level, ranging from 46 to 918 bp. The T-RFLP fingerprints of specific water masses showed 106 OTUs in the EZ, 49 OTUs in the ENACW-OMZ, 68 OTUs in the MW, 56 OTUs in the LSW, 67 OTUs in the ENADW and 26 OTUs in the LDW. The 14% of the 135 OTUs were present in all water masses. By contrast, 35% were unique to specific water

masses. The archaeal community clustered according to different water masses (Supplementary Figure 3.3 A): (i) the first cluster corresponded to archaeal communities inhabiting the euphotic zone (labelled in blue, Supplementary Figure 3.3 A); (ii) the second set corresponded to archaeal communities in intermediate waters, ENACW-OMZ and MW (labelled in orange, Supplementary Figure 3.3 A); and (iii) the third cluster corresponded to the deep waters, represented by LSW, ENADW and LDW (labelled in green, Supplementary Figure 3.3 A).

On the other hand, the automated ribosomal intergenic spacer analysis (ARISA) patterns of the bacterial community revealed in total 290 different bacterial taxa (OTUs) on the internal transcribed spacer (ITS) region, ranging from 101 to 1017 bp. The ARISA profiles for the different water masses comprised 206 OTUs in the EZ, 172 OTUs in the ENACW-OMZ, 151 OTUs in the MW, 154 OTUs in the LSW, 169 OTUs in the ENADW and 124 OTUs in the LDW. The 16% of the 290 OTUs were present in all water masses; by contrast, 21% were unique to specific water masses. These specific OTUs led to a clear separation of bacterial communities according to three main groups of water masses: (i) one cluster comprised bacterial communities inhabiting in EZ (labeled in blue, Supplementary Figure 3.3 B); (ii) the second cluster consisted of bacterial communities inhabiting the intermediate water masses, ENACW-OMZ and MW (labeled in orange, Supplementary Figure 3.3 B); (iii) and the third cluster comprised the bacterial communities from the deep waters, comprised by LSW, ENADW and LDW (labeled in green, Supplementary Figure 3.3 B).

3.3.5. Microbial community composition assessed by 454-pyrosequencing

A total of 29336 archaeal (on average 4191 sequences per sample, range 1436 – 8043) and 80659 bacterial (on average 13443 sequences per sample, range 3511 – 45269) sequences were obtained by 454 pyrosequencing from 7 samples, after quality check and denoising of the raw sequences. The total number of OTUs for Archaea and Bacteria was 275 and 1309 respectively. The highest richness (Chao1 richness index) of Archaea occurred in ENACW-OMZ (141) decreasing towards the ENADW, which showed the minimum value of richness (41, Supplementary Table 3.2). Subsequently, the richness increased again at LDW (51). Similarly, Bacteria also revealed a maximum of Chao1 index richness in the ENACW-OMZ (638) and decreased towards deep reaching the minimum in the LDW (222, Supplementary Table 3.2).

The taxonomy of Archaea (Figure 3.5 A) and Bacteria (Figure 3.5 B) was studied at the order and family level. The archaeal community was composed by the phyla Euryarchaeota and Thaumarchaeota contributing 17 and 83% to the total archaeal 16S rRNA gene sequences, respectively. Euryarchaeota was dominated by Thermoplasmata, mainly by the Marine Group II (MGII) with an average relative abundance among all water masses of 14%, and relative abundances up to 40% in the ENACW-OMZ and in the LSW. Additionally, on average 3% of the sequences were identified as Marine Group III (MGIII). The most abundant order of Thaumarchaeota was Marine Group I (MGI 81%) with the maximum relative abundance located in the EZ and in the MW (Figure 3.5 A).

The bacterial community showed a larger number of different phyla compared to Archaea (Figure 3.5 B). Taking into account the whole Bacteria dataset, we found that most sequences belonged to the phyla Proteobacteria (80%). The most abundant classes of Proteobacteria were the Alphaproteobacteria (56%) with the highest abundance found in the EZ (82%). Delta- and Gammaproteobacteria made up to 14 and 8% of total Bacteria, respectively. Delta- accounted for 24% of total Proteobacteria in the LSW, while Gammaproteobacteria showed the highest abundance located in the LDW (36% of total Proteobacteria). Interestingly, Vibrionaceae accounted for 3.5% of total bacterial sequences, however, 24.3% of Vibrionaceae sequences were found in the LDW. Cyanobacteria sequences, belonging to *Prochlorococcus*, were on average 6% of the total bacterial community, and showed the maximum relative abundance in the ENACW-OMZ. Additionally, SAR202 (4%) was the dominant group within the Chloroflexi class, with maxima relative abundance in the ENADW and in the LDW. Other less abundant groups were Bacteroidetes (3%), Actinobacteria (2%), Deferribacteres (1%) and Planctomycetes (1%). Despite the majority of the samples were dominated by Proteobacteria, differences between the different water masses were observed at lower phylogenetic levels. Flavobacteriaceae was present in the ENACW-OMZ (3%; Figure 3.5 B). Within Alphaproteobacteria, we found three members of SAR11 at family level (SAR11clade, SAR11 surface and SAR11 deep). SAR11clade and SAR11 surface were more abundant in the EZ and in the ENACW-OMZ (Figure 3.5 B) as compared to SAR11 deep or SAR11clade. However, SAR11 deep showed the highest relative abundance in the LSW (Figure 3.5 B). Rhodospirillaceae had higher relative abundance in the MW and in the LSW than Rickettsiales, which

peaked in the ENADW and in the LDW (Figure 3.5 B). Nitrospinaeae, the second most abundant group of Deltaproteobacteria, was relatively more abundant in the EZ and in the MW (Figure 3.5 B) than in deep waters. Within Gammaproteobacteria, the most frequent phylotypes at family level were Colwellia, JL-ETNP-Y6 (Oceanospirilla), Oceanospirillaceae and Vibrionaceae. These phylotypes showed their maximum relative abundance in the LDW (Figure 3.5 A-B). The relative abundance of Mariprofundaceae (Zetaproteobacteria) ranged between 0.1 – 1% of total bacteria, with maximum values located in the MW and in the ENADW.

3.3.6. Bacterial and archaeal abundance assessed by CARD-FISH

The contribution of Bacteria to the total prokaryotic community decreased from the euphotic zone (~60%) to the deep waters (~45%) (Table 3.2). By contrast, the relative abundance of Thaumarchaeota (% of DAPI, Table 3.2) tended to increase with depth. The highest relative abundance was found in the oxygen minimum zone and deep waters, however, Thaumarchaeota never reached values higher than ~15%. The abundance of both, Thaumarchaeota and Bacteria, did not show significant differences among BIO-PROF-1 and BIO-PROF-2 (t-test, $p > 0.05$, $n=22$).

Table 3.2. Relative abundance of the major groups of prokaryotes, Thaumarchaeota and Bacteria (% of DAPI) in the different water masses off the Galician coast (Fisterra Cape). For water-mass abbreviations see Table 3.1.

| Water mases | Bacteria | Thaumarchaeota |
|--------------------|-----------------|-----------------------|
| EZ | 54.58±15.08 | 5.34±2.42 |
| ENACW-OMZ | 48.85±5.18 | 9.52±2.82 |
| MW | 43.70±7.03 | 9.36±3.48 |
| LSW | 41.78±5.55 | 8.22±2.18 |
| ENADW | 37.83±5.11 | 12.98±3.89 |
| LDW | 44.51±2.17 | 14.09±2.17 |

3.3.7. DOM variables influencing the microbial communities

Marginal test were calculated to explain the contribution of each DOM-variable separately on the archaeal community structure using T-RFLP fingerprinting and bacterial community structure using ARISA fingerprinting results. DOC, FDOM-T, FDOM-M, aCDOM254, sCDOM275-295 and depth were significantly related with the archaeal community composition (Supplementary Table 3.3). The FDOM-M and FDOM-T were the main explanatory factors identified by DistLM of the archaeal community structure (Table 3.3) for the whole dataset (n=48), explaining together 18% of the total variability. However, different depth layers showed different predictor variables. The main predictor factor for the variability in archaeal community structure in the euphotic zone (n=11) was aCDOM254, explaining 22.3% of the total variation. Alternatively, FDOM-T, aCDOM254, depth, sCDOM275-295, DOC and FDOM-M explained most of the variability in archaeal community structure in the intermediate waters (54.4%, n=19). In the deep waters

(n=18), FDOM-M was the only significant variable, accounting for 11.7% of the variation in archaeal community structure (Table 3.3).

Table 3.3. Multivariate regression analysis (DistLM) of variables contributing to explain the archaeal community structure with “step-wise” selection procedure on the AIC as selection criterion (sequential test). P: represents the significance level; %Variation: corresponds to the percentage of variation explained by each variable; %Cumul: shows the cumulative percentage variance.

| Depth layer | Variable | Pseudo-F | P | %Var. |
|-------------------------------------|--------------|----------|--------------|-------|
| Total | FDOM-M | 7.1726 | 0.001 | 13.49 |
| (n=48) | FDOM-T | 2.7069 | 0.014 | 4.91 |
| Euphotic Zone (EZ) | aCDOM254 | 2.585 | 0.015 | 22.31 |
| (n=11) | FDOM-T | 2.4385 | 0.040 | 12.55 |
| Intermediate | aCDOM254 | 2.3295 | 0.042 | 11.12 |
| (ENACW-OMZ, MW) | Depth | 2.3541 | 0.024 | 10.36 |
| (n=19) | sCDOM275-295 | 2.1236 | 0.035 | 8.69 |
| | DOC | 1.5705 | 0.131 | 6.18 |
| | FDOM-M | 1.4421 | 0.187 | 5.48 |
| Deep(LSW, NEADW, LDW) (n=18) | FDOM-M | 2.1115 | 0.042 | 11.66 |

Similarly, the marginal test for bacterial communities revealed significant effects of DOC, FDOM-T, FDOM-M, sCDOM275-295 and depth (SupplementaryTable 3.4). Considering the whole water column (n=63), the DistLM

sequential test showed that FDOM-M, depth, aCDOM365, aCDOM340, FDOM-T and sCDOM275-295 were related with the bacterial community composition, explaining 36% of the total variation (Table 3.4). However, depth was the only variable that

Table 3.4. Multivariate regression analysis (DistLM) of variables that contribute to explain the bacterial community structure with “step-wise” selection procedure on the AIC as selection criterion (sequential test).; P: represents the level of significance; %Var.: corresponds to the percentage of variation explained by each variable; %Cumul.: shows the cumulative variance percentage.

| Depth layer | Variable | Pseudo-F | P | %Var. |
|---------------------------|--------------|----------|--------------|-------|
| | FDOM-M | 10.541 | 0.001 | 14.73 |
| Total | Depth | 5.2119 | 0.001 | 6.81 |
| (n=63) | aCDOM365 | 3.7877 | 0.001 | 4.73 |
| | aCDOM340 | 3.7000 | 0.001 | 4.42 |
| | FDOM-T | 2.3326 | 0.016 | 2.72 |
| | sCDOM275-295 | 2.3070 | 0.012 | 2.63 |
| Euphotic Zone (EZ) | Depth | 2.4216 | 0.016 | 13.15 |
| (n=18) | | | | |
| Intermediate | sCDOM275-295 | 4.7230 | 0.002 | 17.04 |
| (ENADW-OMZ, | Depth | 3.7751 | 0.001 | 12.15 |
| MW) (n=25) | aCDOM340 | 1.8321 | 0.090 | 5.68 |
| Deep | Depth | 2.5866 | 0.017 | 12.57 |
| (LSW, NEADW, | sCDOM275-295 | 2.4778 | 0.044 | 11.12 |
| LDW) (n=20) | aCDOM365 | 1.8587 | 0.067 | 7.94 |

significantly explained the variation in the bacterial community structure from the euphotic zone (13.2%; n=18). sCDOM₂₇₅₋₂₉₅, depth and aCDOM₃₄₀ accounted for 29.2%, 12.1% and 5.7% of the total variation in bacterial community structure from the intermediate waters (n=25). The main predictor factors for the variability in bacterial community from the deep waters (n= 20) were the aCDOM₃₆₅, depth and sCDOM₂₇₅₋₂₉₅, with 7.9%, 11.1% and 12.6%, respectively (Table 3.4).

Redundancy analysis (RDA) was performed to examine how DOM-variables were associated to specific microbial 454-pyrosequencing phylotypes (Figure 3.6). Microbial phylotypes in the different water masses were associated to different DOM-variables. Axes 1 and 2 were interpreted as (i) depth/DOM quantity and (ii) DOM quality, respectively. The FDOM-M showed positive correlation with both axes. Depth presented a positive correlation with axis 1 and negative correlation with axis 2. sCDOM₂₇₅₋₂₉₅, aCDOM₃₆₅, aCDOM₃₄₀, aCDOM₃₅₄ and FDOM-T displayed a negative correlation with axis 1 and positive with axis 2. In addition, Euryarchaeota-MGIII, which had its highest relative abundance in ENADW, was significantly associated to FDOM-M. Furthermore, sCDOM₂₇₅₋₂₉₅ was connected to Thaumarchaeota-MGI and also to the bacterial groups Acidobacteria and SAR324 clade. Flavobacteria and OCS116 clade were related to aCDOM₃₆₅. RDA also suggests a strong link between aCDOM₂₅₄ and bacterial members inhabiting ENACW-OMZ, i.e. SAR11 clade, Rhodobacterales, SAR116 SAR116 clade and Verrucomicrobia. Additionally, the DOC concentrations were correlated with the relative abundance of Nitrospirillaceae. By contrast, the increasing relative abundance of SAR202 clade, SAR406 clade, SAR286 clade,

Rickettsiales and Rhizobiales with depth were related to FDOM-M.

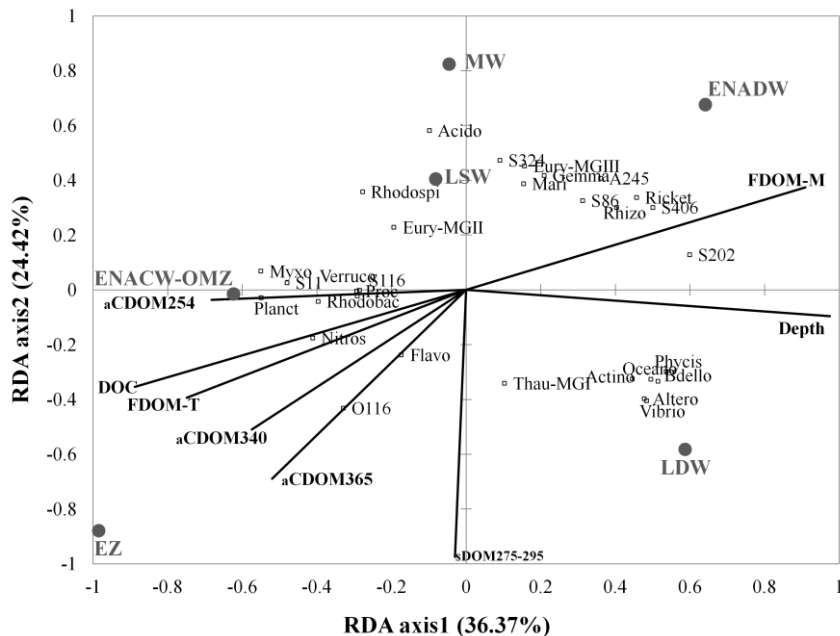


Figure 3.6 Redundancy Analysis (RDA) of microbial groups obtained with 454-pyrosequencing and DOM-variables. The filled circles represent the water masses sampled and the stars represent the microbial phylogenetic groups. The direction of the rows indicates the direction of increase in the variable and the length corresponds to DOM-variables. For water mass abbreviations see Table 1. Microbial groups' abbreviations are Acido, Acidobacteria; Actino, Actinobacteria; Flavo, Flavobacteria; Proc, Prochlorococcus; Gemma, Gemmatimonadetes; Phycis, Phycisphaeraceae; Planct, Planctomycetes; A245, AEGAN-245; Rhizo, Rhizobiales; Rhodobac, Rhodobacteraceae; Rhodosp, Rhodospirillales; Ricket, Rickettsiales; Bdello, Bdellovibrionaceae; Nitros, Nitrospinaceae; Myxo, Myxococcales; Altero, Alteromonadales; Oceano, Oceanopirillaceae; Vibrio, Vibrionaceae; Mari, Mariprofundaceae; Verru, Verrucomicrobia; Eury-MGII, Euryarchaeota-MGII; Eury-MGIII, Euryarchaeota-MGIII; Thau, Thaumarchaeota.

3.4. Discussion

Archaeal and Bacterial communities inhabiting the euphotic, intermediate and deep waters has been described for the first time in the euphotic and dark waters off the Galician coast. The microbial abundance, activity and community composition showed clear vertical trends consistent with the vertical stratification of environmental and optical characterization of DOM. As expected, most of DOM variables (DOC, FDOM-T and aCDOM₂₅₄) presented higher concentrations at the surface that decreased with depth, whereas FDOM-M, increases with depth, showing the highest values at the deeper layers, as described previously (Carlson and Hansell 2015; Stedmon and Nelson 2015). Globally, all the DOM values were consistent with previous measurements in this region (Lønborg and Álvarez-Salgado, 2014).

Correspondingly, the highest abundance and leucine incorporation of the prokaryotic communities was found in the euphotic zone, characterized by a highest temperature, oxygen and organic matter bioavailability that facilitate the growth of microbes. On the other hand, the abundance and activity decreases with increasing depth by 2 and 3 orders of magnitude, respectively, and environmental conditions may only allow the growth of specific microbes associated to dark waters.

3.4.1. Vertical distribution of specific archaeal and bacterial phylotypes

Vertical microbial distribution patterns suggest habitat partitioning, where Bacteria is dominant at the surface waters and

Archaea is more abundant in OMZ and deeper waters, as previously reported for other regions of the North Atlantic ocean (Herndl et al. 2005; Teira et al. 2006a; Varela et al. 2008b; Agogué et al. 2011). Thaumarchaeota dominated over Euryarchaeota and exhibited a patchy vertical distribution. The high abundance of Thaumarchaeota-MGI found in the EZ and in the ENADW waters have also been observed in previous studies (Herndl et al. 2005; Teira et al. 2006a; Varela et al. 2008b). Ferrera et al. (2015) found all Euryarchaeota related to the class Thermoplasmata in northeastern Atlantic Ocean in agreement with our results off the Galician coast. The Euryarchaeota-MGII vertical distribution, with maximum relative abundance in OMZ, indicates an adaptation of members of this group to low oxygen concentrations. The highest abundance of Thaumarchaeota in this area is found in layers with lower oxygen concentrations as compared to surface and deep waters, in agreement with previous studies in ocean ecosystems (Francis et al. 2005; Lam et al. 2007). These decreased oxygen layers are suitable to harbour redox processes, such as ammonia oxidization (Zehr and Ward 2002; Konneke et al. 2005; Sintes et al. 2013) and, consequently, the organisms inhabiting them can potentially exhibit autotrophic metabolism (Guerrero-Feijoo et al. accepted). However, Thaumarchaeota also showed high relative abundance in the euphotic zone and the deeper layers linked to the highest DOC concentration, suggesting mixotrophic metabolism and different substrate preferences for different Thaumarchaeota ecotypes (Sintes et al. 2016; Smith et al. 2016).

Our results support that members of the SAR11 clade of Alphaproteobacteria are the most abundant and ubiquitous bacterial organisms in the ocean, indicating high competition for

available resources, particularly in the ocean surface (Giovanni and Rappé, 2000; Morris et al. 2002; DeLong et al. 2006; Dobal-Amador et al. 2016). By contrast, the Gammaproteobacteria were the dominant group in the deeper waters, particularly in the LDW, in accordance with current knowledge of bacterial communities from marine ecosystems (Lopez-Garcia et al. 2001; Sogin et al. 2006; Lauro and Bartlett 2008). *Alteromonas* identified by 16S rRNA gene 454 sequences showed a patchy distribution as compared to CARD-FISH counts from the same cruise which showed a decreasing relative abundance with depth (Dobal-Amador et al. 2016). Both 454 pyrosequencing of these study and CARD-FISH counts (Dobal-Amador et al. 2016) methods showed a clear increasing trend of SAR324 clade with depth (maximum relative abundance was located in the LSW). The enrichment of this group could reflect an important role of the chemoautotrophic metabolism in the deep water masses, since previous studies based on single cell genomic analyses have shown that members of the SAR324 clade contain sulphur oxydizing genes in the intermediate and deep waters and are capable of inorganic carbon fixation (Swan et al. 2011; Sheik et al. 2014). SAR202 clade has been described as a deep bacterial phylotype in the deep north Atlantic waters (Varela et al. 2008b) and an r-strategist, which can rapidly exploit nutrient patches in the dark ocean (Varela et al. 2008b). Another prominent group in deep waters off the Galician coast was SAR406 clade, in agreement with previous reports (Gordon and Giovannoni 1996; Gallagher et al. 2004; Pham et al. 2008; Galand et al. 2010). SAR406 members contain inorganic sulfur metabolic pathways (Yamamoto and Takai 2011), suggesting a possible role of these organisms as sulfate-reducers. Bacteroidetes is more abundant in surface than deep waters

(Chauhan et al. 2009), in agreement with their ability to use high molecular weight DOM biopolymers (Kirchman 2001).

Although a correlation between the results obtained by the CARD-FISH analysis (Dobal-Amador et al. 2016) and the 16S rRNA gene amplicon 454-pyrosequencing could not be performed as these different techniques target different 16S gene regions, we found a good correspondence between the vertical distributions of the specific groups of Bacteria by both methodologies. The contribution of SAR324 and SAR406 to the bacterial community as determined by CARD-FISH and pyrosequencing was close to the 1:1 line (data not shown), indicating that both techniques retrieved this cluster with similar efficiency. By contrast, the relative abundance of SAR11 was higher in the pyrosequencing dataset than with CARD-FISH (data not shown, t-test, $p < 0.05$). *Alteromonas* and SAR202 contributed disproportionately more to bacterial abundance using CARD-FISH than using pyrosequencing (data not shown, t-test, $p < 0.05$). These different patterns could be explained either by the different number of samples analysed with the two methodologies or due to the PCR-bias associated to the pyrosequencing approach as compared to CARD-FISH, where the probes target directly the 16S rRNA.

3.4.2. Importance of DOM-related variables influencing the microbial community structure and composition

Microbial community composition correlates with a variety of abiotic parameters (such as temperature and salinity) of the water masses (Yokokawa et al. 2010; Agogu e et al. 2011; Sj ostedt et al. 2014; Dobal-Amador et al. 2016). Moreover, microbial community composition varies according to DOM

composition (Kirchman et al. 2004). Several studies have found that the microbial production of recalcitrant DOM (mostly humic substances) as a sub-product of the remineralisation processes adds up complexity to this relationship (Jiao et al. 2010; Nieto-Cid et al. 2006). Standard physico-chemical variables were the main factor explaining the variability of the bacterial community vertical distribution in the deep waters of the Galician coast (Dobal-Amador et al. 2016). However, in this previous study it was also indicated that some optical DOM characteristics further explain the variability in the bacterial community structure through the water column (Dobal-Amador et al. 2016). Nevertheless, our knowledge on DOM composition and the link between microbial communities and the DOM acting as substrate/sub-product of bacterial and archaeal metabolism in the deep ocean remains enigmatic. Both labile and refractory compounds, represented by FDOM-T and FDOM-M, respectively, related differently with the microbial communities off the Galician coast. Whereas, the archaeal communities from the intermediate layers are linked to more labile molecules (protein-like material), which could be preferentially respired by these organisms, the archaeal communities of the deep waters are related to more refractory compounds. The strong positive correlation among FDOM-M and the relative abundance of Archaea, particularly Euryarchaeota-MGII, support the concept of the microbial carbon pump (MCP; Jiao et al. 2010), as these deep-ocean microbial communities are more connected to the refractory DOM (humic-like compounds) generated by themselves as sub-products of their respiratory metabolism.

Variations in bacterial community structure of the samples from the EZ are associated with depth, which is probably related

to temperature and other physical parameters (Yokokawa et al. 2010; Sjöstedt et al. 2014), as well as chlorophyll a and the DOM availability (Walsh et al. 2015). The sCDOM₂₇₅₋₂₉₅ was the main explanatory DOM-related variable for bacterial community structure in the intermediate and deep waters, suggesting a tight coupling between the bacteria and the aromaticity and molecular weight of the DOM (Helms et al. 2008). This finding would indicate that the molecular weight of the DOM, very likely associated to DOM ageing in the water masses (Helms et al. 2008), is linked to the changes in the bacterial community structure within the dark ocean. The strong relationship of Acidobacteria and SAR324 clade, typical deep-sea groups, with sCDOM₂₇₅₋₂₉₅, suggests a higher contribution of these organisms to transform DOM into older, bigger and more aromatic compounds. Furthermore, the relationship of bacterial communities from intermediate waters with aCDOM₃₄₀ (mainly Nitrospirae) and the relationship of the bacterial communities inhabiting the deeper layers with aCDOM₃₆₅ (Mariprofundaceae and Gemmatimonadetes) suggest that the deep water bacterial communities metabolize DOM with a higher degree of aromaticity (more refractory) than the bacterial communities of the intermediate waters (absorption wavelength of 365 nm versus 340 nm; Stedmon and Nelson 2015). The relationships between DOM variables and the distribution patterns of Flavobacteria, Myxococcales, SAR11 clade, SAR86 clade, SAR116 clade, SAR202 clade, SAR324 clade, SAR406 clade, Rhodobacteraceae, Rickettsiales, Planctomycetes and Verrucomicrobia, support the notion of a heterotrophic (or mixotrophic) lifestyle of these groups. Flavobacteria (Bacteroidetes) and SAR86 (Gammaproteobacteria) have been reported before as important players in DOM cycling, especially from the high molecular

weight fraction of DOM (Kirchman et al. 2002; Nikard et al. 2014). Nevertheless, several bacterial groups, such as SAR202 clade (Chloroflexi), SAR406 clade (Deferribacteres), Rickettsiales (Alphaproteobacteria) and Rhizobiales (Alphaproteobacteria), showed also a strong correlation with FDOM-M indicative of their potential to generate refractory compounds of DOM (humic-like compounds), as sub-products of the remineralization processes.

Our data suggest that both archaeal and bacterial communities are coupled to compositional changes in the DOM pool. The increasing/decreasing patterns of FDOM-M and FDOM-T with depth are the main variables related to the vertical stratification of microbial communities; however, the absorption coefficients at 254, 340 and 365 nm are also affected by the stratification of microbial communities in the eastern North Atlantic Ocean. Some phylotypes, such as SAR202 and SAR406 might be able to relate to both labile and refractory-DOM, while others, such as Thaumarchaeota-MGI, display preferential relations with aromatic compounds in the deep waters.



Chapter 4

Changes in bacterial activity and community composition in response to size-fractionated dissolved organic matter

Abstract

Heterotrophic bacteria plays a pivotal role in the cycling of marine dissolved organic matter (DOM), yet our understanding of DOM-microbe interactions is limited. Here, we studied the response of Bacteria to the degradability of filtered and size-fractionated DOM in relation to the optical properties of DOM. A natural bacterial community from the Mediterranean Water (1000 m depth) was isolated and grown in (i) 0.1 μm seawater (DOM), (ii) the low-molecular-weight fraction (LMW-DOM) and (iii) the recombination of low- and high-molecular-weight fractions (H+L-DOM). Bacterial abundance and activity were consistently higher in H+L-DOM than LMW-DOM at the end of the experimental treatment, suggesting a different bioavailability of DOM fractions. Moreover, the bacterial community composition in the different experimental treatments varied due to the exposure to the different DOM-fractions. Colwelliaceae, Shewanellaceae and Oleiphilaceae were selectively stimulated by H+L-DOM treatment. Together with the relationship with protein-like fluorescence, it suggests their preference for very labile substances. Alternatively, Flavobacteriaceae, Rhodospirillales and Rhodobacteraceae increased relatively in the LMW-DOM as compared to the CONTROL and the H+L-DOM treatments. Our results suggest that the size-fractionation of DOM, defined by specific DOM optical properties in the treatments, stimulated specific bacterial phylotypes.

4.1. Introduction

The dissolved organic matter (DOM) pool constitutes the major source of carbon and energy in the aquatic ecosystems (Hansell et al. 2009). Marine heterotrophic microbes utilize DOM differentially depending on both molecular size and biochemical composition (Amon and Benner, 1996; Covert and Moran, 2001; Logue et al. 2016). However, the molecular structure and chemical composition of marine DOM size fractions remains enigmatic. DOM exhibits a continuum of reactivity (Hansell 2013), which is strongly dependent on environmental parameters such as inorganic nutrients or temperature (Arnosti et al. 2011). DOM is primarily originated from phytoplankton either via extracellular release or via zooplankton grazing and viral lysis (Buchan et al. 2014). A significant fraction of this DOM is remineralized in surface waters; however, about 1 to 40% is exported into the dark realm of the ocean (Buchan et al. 2014). The high molecular weight fraction of DOM (HMW-DOM) dominates the material released by phytoplankton. This fraction is more labile and thus can be rapidly utilized by marine microbes (Amon and Benner, 1996). Conversely, the low molecular-weight fraction of DOM (LMW-DOM), through humification, generates refractory compounds (Amon and Benner, 1996) that together with the microbial remains (e.g remains of cell walls, lipids) (Kaiser and Benner, 2009) add to the complexity of the DOM. However, the knowledge on the biochemical composition of DOM and the interaction between the diversity and composition of DOM and bacterial communities in the dark ocean is still limited.

Remineralization and transformation of DOM by marine microbes have large impact on global carbon cycle (Carlson, 2002; Kujawinski, 2011). Several studies have focused on specific aspects of this interaction, such as the linkages between microbes and DOM in surface coastal waters (Kirchman et al. 2002; Kirchman et al. 2004; Alonso-Sáez et al. 2007), in relation to phytoplankton blooms (Pinhassi et al. 2004; West et al. 2008), during enrichment experiments (Gómez-Consarnau et al. 2012), after photochemical transformation (Lonborg et al. 2016), or in continuous cultures (Landa et al. 2013; 2014). Recently, the relationship between some specific microbial groups and the DOM optical properties was described in the North Atlantic ocean, suggesting the relation of SAR324 with the degradation of aged DOM in deep waters, and of SAR202 and SAR406 with refractory DOM compounds (Dobal-Amador et al. 2016, Guerrero-Feijóo et al. 2017).

The Galician coast is a dynamic area characterized by seasonal upwelling pulses, which supports the exportation offshore as well as sinking fluxes of organic matter. The mix layer reaches down to the mesopelagic layer, where the Mediterranean Water (MW) is located flowing northwards along the western Iberian Peninsula at ~1000 m depth (Ruíz-Villareal et al. 2006), where it may influence the abundance and composition of the microbial communities inhabiting the dark waters of this ecosystem. The main goal of our study is to investigate the effect of filtered and size-fractionated DOM on: (i) bacterioplankton richness; (ii) bacterioplankton community structure and (iii) bacterioplankton community composition using an experimental approach. Our hypothesis is that different size-fractionated DOM

selects for bacterial communities that differ in their diversity, structure and phylogenetic composition.

4.2. Material and methods

4.2.1. Sampling and experimental set-up

A natural bacterial community isolated and grown in Mediterranean Water (MW; 1000 m depth) was collected during the MODUPLAN cruise, carried out between 4th and 24th August 2014 on board R/V Sarmiento de Gamboa. Seawater was sampled at St. 11 (43°N, 10°W) using 12 L Niskin bottles mounted on a CTD (conductivity-temperature-depth) rosette and collected in acid-washed polycarbonate (PC) carboys (Nalgene, Thermo Fisher Scientific, Waltham, MA, USA). Firstly, 75 L of seawater were filtered through 0.1 µm membrane filters (142 mm diameter, Supor-100, Pall Corporation). Following, 50 L of the filtrate were filtered through a tangential flow ultrafiltration system with a 1 kDa ultrafiltration membrane (GE Series, GE Power & Water), size-fractionating the sample in high (1.75 L, >1kDa) and low (48.25 L, <1kDa) molecular weight fractions. The concentration factor was low (~28). Subsequently, 3 different treatments were established in triplicate: (i) the CONTROL treatment consisted of 0.1 µm filtered seawater; (ii) the LMW-DOM treatment consisted of low-molecular-weight seawater; and (iii) the H+L-DOM treatment was prepared by recombining the high and low-molecular-weight fractions in the original proportions. The inoculum for the different treatments consisted of 0.6 µm filtered seawater (142 mm diameter, polycarbonate hydrophilic membranes) collected from the same station and depth. Dilution cultures were prepared for each treatment in

triplicate by adding 700 mL of 0.6 μm filtered seawater to 6.3 L of the corresponding DOM fraction. Additionally, 2 L of the 0.6 μm filtered seawater were immediately filtered onto 0.2 μm polycarbonate filters to assess the initial bacterial community composition. The filters were flash-frozen in liquid nitrogen and stored at $-80\text{ }^{\circ}\text{C}$ until DNA extraction. All treatments were kept in a dark cold room at in situ temperature ($10\text{ }^{\circ}\text{C}$) to mimic the environmental conditions of the mesopelagic waters. Cultures were monitored over 6 days. Bacterial growth was assessed daily by determining bacterial abundance and production until the stationary phase was reached.

4.2.2. Inorganic nutrients

Water samples for nutrient salts (nitrate, nitrite, and phosphate) analysis were collected and stored frozen ($-20\text{ }^{\circ}\text{C}$) until measured in the base laboratory using a QuAAtro auto-analyzer from SEAL Analytical. The protocols from SEAL analytics Q-126 R1 and Q-125 were used for nitrite and nitrate, and phosphate concentration analysis, respectively.

4.2.3. Optical properties of DOM

DOM optical properties were measured on board by pouring small aliquotes of the sample (5-25 mL) directly into the corresponding optical cell. On one hand, fluorescence intensity was measured with a Perkin Elmer LS55 following Nieto-Cid et al. (2006) at two excitation/emission wavelengths pairs: (i) 320 nm/410 nm (FDOM-M), characteristic of marine humic-like substances, and (ii) 280 nm/350 nm (FDOM-T), characteristic of protein-like materials. Samples were calibrated against quinine sulphate and results are given in quinine sulphate units (QSU). On

the other hand, absorption spectra of the chromophoric DOM were acquired on a Beckman Coulter DU800 spectrophotometer equipped with 10 cm quartz cells. Spectral scans were collected from 250 to 700 nm providing the following indices (Green and Blough 1994): aCDOM₂₅₄ (absorption coefficient at 254 nm), aCDOM₃₄₀ (absorption coefficient at 340 nm), aCDOM₃₆₅ (absorption coefficient at 365 nm), sDOM₂₇₅₋₂₉₅ (slope of the absorption spectrum between 275 and 295 nm). For more details see Guerrero-Feijóo et al. (2017).

4.2.4. Total microbial abundance

Microbial abundance (MA) was quantified by flow cytometry according to Gasol et al. (1999). Briefly, water samples (1.8 mL) were fixed with 1% paraformaldehyde + 0.05% glutaraldehyde (final concentration) for 10 min, flash-frozen in liquid N₂ and kept at -80 °C until analysis on board. Prior to the measurement with the flow cytometer, the samples were thawed to room temperature and the prokaryotic cells stained with Syto13 in the dark for 10 min. Subsequently, fluorescent latex beads (approximately $1 \times 10^5 \text{ mL}^{-1}$) (Molecular Probes, Invitrogen, Carlsbad, CA) were added to all the samples as internal standard. The prokaryotes were enumerated using a FACSCalibur flow cytometer (Becton Dickinson, Franklin Lakes, NJ). Low nucleic acid content (LNA) and high nucleic acid (HNA) content bacteria were differentiated according to their signature in right angle light scatter and green fluorescence. The proportion of HNA bacteria in the total assemblage (%HNA) is the number of HNA bacteria divided by the total prokaryotic abundance (LNA+HNA) (Morán and Calvo-Díaz, 2009).

4.2.5. Enumeration of microbes with different cell-membrane integrity

We follow the protocol described in Grégori et al. (2001) to evaluate the cell-membrane integrity of microbes using nucleic acid double staining (NADS) with SYBR Green I (Molecular Probes, ref. S-7563) and propidium iodide (PI, Sigma, ref. P-4170). Water samples (0.4 mL) were stained for 15 min in the dark at room temperature with 1x SYBR Green I and 10 $\mu\text{g mL}^{-1}$ PI. Subsequently to the addition of the beads solution as internal standard, they were run in a FACSCalibur flow cytometer. Cells impermeable to PI and cells permeable to PI (i.e., cells with intact and damaged membranes, respectively) were distinguished according to their signature in red and green fluorescence. The terms “live” and “dead” were subsequently used to designate cells with intact and damaged membranes, respectively. To obtain a coherent dataset, the percentage of live cells (%live) was calculated as the number of live cells relative to the sum of live and dead cells rather than to total bacteria previously quantified with Syto13-staining (Morán and Calvo-Díaz, 2009).

4.2.6. Actively respiring microbial cells

We used the redox dye 5-Cyano-2,3-di-(p-tolyl)tetrazolium chloride (CTC, Polysciences, ref. 19292) to identify actively respiring cells. Water samples (0.25 mL) were incubated with CTC at a final concentration of 5 mmol L^{-1} for c. 90 min in dark at in situ temperature as described in Gasol and Arístegui (2007). Subsequently, the samples were immediately run on the flow cytometer, and the CTC+ cells were identified according to their signature in red vs. orange fluorescence. The proportion of CTC+ cells (%CTC+) was calculated for each

sample as the number of CTC+ cells versus the total microbial counts estimated with Syto-13 (Morán and Calvo-Díaz, 2009).

4.2.7. Microbial leucine incorporation rates

Leucine incorporation rates were estimated by adding 5 nmol L⁻¹ [³H]-leucine (final concentration, specific activity 160 Ci mmol L⁻¹, GE Healthcare, Amersham, Bucks, UK) to triplicate 1.2 mL samples. Duplicate TCA (trichloroacetic acid)-killed blanks (5% final concentration) were treated in the same way as the samples (Simon and Azam, 1989). Samples and blanks were incubated in the dark at in situ temperature in temperature-controlled chambers for 2–6 h, depending on the expected activity. Incubations were terminated by adding TCA (5% final concentration) to the samples. Bacterial cells were pelleted by two successive centrifugation steps (12000 rpm, 10 min), including a washing step with 1 mL of 5% TCA following Kirchman (1985) with slight modifications (Smith and Azam, 1992). Scintillation cocktail was added to pellets and after 18 h, the radioactivity was determined in a scintillation counter (LKB Wallac). The mean disintegrations per minute (DPM) of the blanks were subtracted from the mean DPM of the respective samples and the resulting DPM converted into leucine incorporation rates.

4.2.8. Bacterial diversity

Samples for DNA analysis were collected from the initial bacterial community and from the community at the end of the experiment (day 6) in the three different treatments. A volume of 2 L of water was filtered onto a 0.2 µm polycarbonate filter (Millipore) and the filters were subsequently stored at -80 °C until DNA extraction. Briefly, total DNA extraction was performed by

PowerSoil DNA Isolation Kit (MO BIO). In total, 10 samples were extracted, quantified (via Nanodrop, Thermo Scientific) and sent for 454-pyrosequencing to the Research and Testing Laboratory (Lubbock, TX, USA; <https://www.researchandtesting.com>). Primers 341F (CCTACGGGNGGCWGCAG) and 805R (GACTACHVGGGTATCTAATCC) (Herlemann et al. 2011) generated amplicons spanning the V3 to V4 regions of the bacterial 16S rRNA gene. Sequences were analyzed and processed using the Quantitative Insights Into Microbial Ecology (QIIME) pipeline (<https://www.qiime.org>) (Caporaso et al. 2010). A quality check was performed to minimize low quality pirotags, eliminating sequences with 50 bp sliding window Phred average below 25, ambiguous bases and sequences with length shorter than 100 bp after trimming. The remaining sequences were denoised to reduce the pyrosequencing errors (Reeder and Knight, 2010). The curated sequences were clustered into operational taxonomic units (OTUs) with 97% similarity threshold. A representative sequence from each phylotype was chosen by selecting the most abundant sequence in each cluster. The chimeric sequences were removed using ChimeraSlayer implemented in MOTHUR (Schloss 2009; Haas et al. 2011) based on the alignment file SILVA108 (<http://www.arb-silva.de>). Blast Classifier (Wang et al. 2007) implemented in QIIME assign the phylogenetic identity of 16S rRNA phylotypes. OTUs assigned to chloroplast, mitochondria or Archaea were removed from our analysis. In addition, rarefaction analysis was conducted to assess if the sequences from the different samples tended to plateau (Supplementary Figure 4.1). Pyrotag sequences have been deposited in the National Center for Biotechnology Information (NCBI) Sequence Read Archive (SRA) under PRJNA385510

bioproject number. Sequencing data was downsized to 1817 sequences per sample by random re-sampling to allow comparison of samples. All further analyses, alpha and beta diversity estimations were performed with the subsampled OTU table.

4.2.9. Statistical analysis

Hierarchical cluster analysis based on Bray-Curtis similarity matrix was performed to explore similarities between treatments. Additionally, the differences in alpha diversity between treatments (using 454-pyrosequencing data) were statistically evaluated by ANOSIM analysis. A redundancy analysis (RDA) was performed for testing the association between changes in the DOM optical properties and single-cell physiological properties along with the bacterioplankton community composition shift in the different treatments. Variables included FDOM-M, FDOM-T, aCDOM₂₅₄, aCDOM₃₄₀, aCDOM₃₆₅, sCDOM₂₇₅₋₂₉₅, %CTC+ and %live. All statistical analyses were performed using XLSTAT software.

4.3. Results

4.3.1. Inorganic nutrients and optical properties of the DOM

At the beginning of the experiment, the concentrations of nutrient salts ($\text{NO}_3^- + \text{NO}_2^-$ and PO_4^{3-}) showed similar values in all the treatments. PO_4^{3-} concentration did not change significantly during the 6-day incubation. Inorganic nitrogen ($\text{NO}_3^- + \text{NO}_2^-$) concentrations varied in the different treatments. CONTROL and H+L-DOM treatments showed a significant decrease (mean \pm SD) of -0.23 ± 0.05 and $-0.24 \pm 0.09 \mu\text{mol kg}^{-1}$, respectively, while the

values in the LMW-DOM treatment increased in 0.18 ± 0.01 $\mu\text{mol kg}^{-1}$ (Supplementary Table 4.1).

The average change in the optical properties of the DOM (mean \pm SD) for each treatment between the initial and final time point of the experiment are summarized in Table 4.1. Regarding the fluorescence of the DOM, FDOM-M did not display any significant change for any treatment, and FDOM-T presented significant changes only for the CONTROL and H+L-DOM treatments. FDOM-T increased in 0.7 ± 0.6 and 0.9 ± 0.5 QSU in CONTROL and H+L-DOM treatments, respectively. The absorp-

Table 4.1. Average change of the optical properties of the DOM in the three treatments between day 0 and day 6. See abbreviations of each treatment in Figure 1. Abbreviations of optical properties: FDOM-M, marine humic-like substances; FDOM-T, protein-like substances; aCDOM254, absorption coefficient at 254 nm; aCDOM340, absorption coefficient at 340 nm; aCDOM365, absorption coefficient at 365 nm; sCDOM275-295, slope of the absorption spectrum between 275 and 295 nm.

| Variables | CONTROL | H+L-DOM | LMW-DOM |
|--|-------------------|-------------------|-------------------|
| FDOM-M (QSU) | 0.01 ± 0.04 | -0.01 ± 0.06 | 0.00 ± 0.06 |
| FDOM-T (QSU) | 0.7 ± 0.6 | 0.9 ± 0.5 | 0.1 ± 0.6 |
| aCDOM254 (m^{-1}) | -0.05 ± 0.03 | -0.10 ± 0.07 | -0.07 ± 0.03 |
| aCDOM340 (m^{-1}) | -0.03 ± 0.01 | -0.06 ± 0.01 | -0.04 ± 0.03 |
| aCDOM365 (m^{-1}) | -0.02 ± 0.01 | -0.03 ± 0.03 | -0.03 ± 0.02 |
| sCDOM275-295 | 0.001 ± 0.001 | 0.003 ± 0.003 | 0.004 ± 0.000 |

tion coefficient of the DOM at 254nm (aCDOM₂₅₄) decreased with time in all three treatments (-0.05 ± 0.03 , -0.10 ± 0.07 , -0.07 ± 0.03 m⁻¹ for CONTROL, H+L-DOM and LMW-DOM, respectively; Table 4.1). Similarly, aCDOM₃₄₀ and aCDOM₃₆₅ decreased in the three treatments at the end of the experiment. In the case of the absorption slope (sCDOM₂₇₅₋₂₉₅) only the LMW-DOM treatment exhibited an increase of 0.004 ± 0.000 .

4.3.2. Bulk and single-cell microbial properties

Microbial abundance (MA) was higher in H+L-DOM compared to CONTROL and LMW-DOM treatments at the beginning of the experiment ($2.10 \pm 0.83 \times 10^4$, $0.69 \pm 0.11 \times 10^4$ and $0.37 \pm 0.03 \times 10^4$ cells mL⁻¹, respectively) (Figure 4.1 A-C). MA increased exponentially in the three treatments until day 6. The CONTROL and LMW-DOM treatment yielded lower abundance ($4.73 \pm 0.28 \times 10^4$ and $5.84 \pm 1.03 \times 10^4$ cells mL⁻¹, respectively) at the end of the experiment as compared to H+L-DOM ($15.80 \pm 3.80 \times 10^4$ cell mL⁻¹) (Figure 4.1 A-C). The percentage of high nucleic acid content microbial cells (%HNA) dominated the community throughout the time span of the experiment (Figure 4.1 A-C), with relative abundance >50% in the majority of the samples. Live microbial cells (%live) were more abundant than dead cells through the time span of the experiment, with a proportion of >50% in the majority of the samples. The proportion of live cells generally increased throughout the experiment, reaching slightly higher values in the CONTROL and H+L-DOM than in LMW-DOM treatment (Figure 4.1 D-F). The percentage of actively respiring cells (%CTC+) represented a variable fraction of the total community, with %CTC+ cells generally increasing during the experiment

(Figure 4.1 D-F). %CTC+ was <50% at the beginning of the experiment in all treatments and peaked on day 4, with higher values in the CONTROL ($79 \pm 8\%$ of CTC+) and LMW-DOM ($72 \pm 6\%$ of CTC+) as compared to H+L-DOM ($56 \pm 7\%$ of CTC+) (Figure 4.1 D-F). However, all treatments showed similar proportion of actively respiring cells at the end of experiment, ranging among 45-50% (Figure 4.1 D-F).

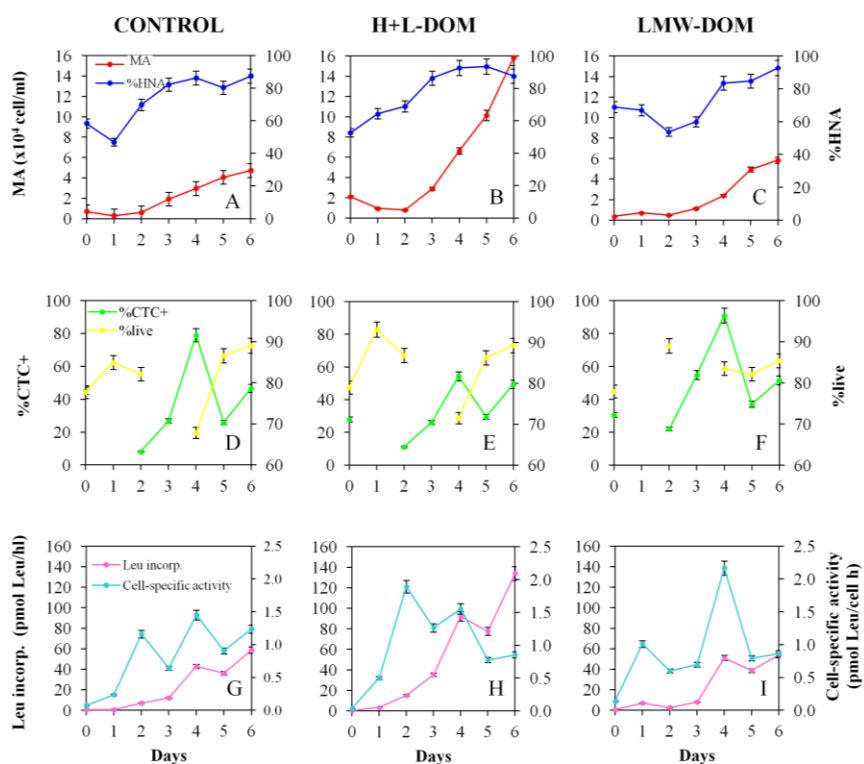


Figure 4.1. Time course of bulk and single-cell microbial properties during the experiment. Microbial abundance (MA) and % of high nucleic content cells (%HNA) present in CONTROL (A), H+L-DOM (B) and LMW-DOM (C). The % of actively respiring cells (%CTC+) and % of live cells (%live) in CONTROL (D), H+L-DOM (E) and LMW-DOM (F). Leucine incorporation rate and cell-specific activity in CONTROL (G), H+L-DOM (H) and LMW-DOM (I).

Leucine incorporation rates (Leu incorp.) increased in all treatments during the experiment and showed 3-fold higher rates in H+L-DOM on day 6 ($1.34 \pm 0.30 \times 10^2$ pmol Leu L⁻¹ h⁻¹) as compared to CONTROL and LMW-DOM ($0.59 \pm 0.07 \times 10^2$ and $0.54 \pm 0.17 \times 10^2$ pmol Leu L⁻¹ h⁻¹, respectively) (Figure 4.1 G-I). Leu incorp. per cell generally increased in all treatments from the beginning of the experiment to day 4, with a slightly higher response for LMW-DOM compared to the other treatments (Figure 4.1 G-I). However, Leu incorp. per cell slightly decreased from day 4 to day 6, down to ~ 1 pmol Leu cell⁻¹ h⁻¹ in all treatments at the end of the experiment (Figure 4.1 G-I).

4.3.3. Effects of size-fractionated DOM on bacterioplankton richness

The initial community had the highest Shannon ($H' = 4.2$) and Chao1 (Chao1 = 212.5; Chao, 1987) indexes (Table 4.2), and the largest number of singletons and doubletons. Chao 1 index abruptly decreased as compared to the initial community after 6 days of incubation. Chao1 was rather similar between the three treatments (Table 4.2). Similarly, Shannon index also decreased in all treatments at day 6 (Table 4.2).

Table 4.2. Average bacterial richness estimates using Chao1 and Shannon diversity indexes at the initial community and the end of experiment on the three treatments: CONTROL, H+L-DOM and LMW-DOM.

| Treatment | Chao1 | Shannon |
|-------------------|------------|---------|
| Initial community | 212.5 | 4.2 |
| CONTROL | 129.6±12.9 | 2.5±0.1 |
| H+L-DOM | 130.6±3.6 | 2.8±0.0 |
| LMW-DOM | 134.3±6.8 | 2.3±0.0 |

4.3.4. Effects of size-fractionated DOM on bacterial community structure

A venn diagram was build to show the number of unique and shared OTUs at the initial community and at day 6 in the three size-fractionated DOM treatments (Figure 4.2). The initial community revealed the highest number of unique OTUs. While the treatments showed similar number of unique OTUs, especially CONTROL and H+L-DOM treatments; the LMW-DOM accounted for the lowest number of unique OTUs (Figure 4.2). However, the number of shared OTUs among treatments was 78, while the initial community only shared 4 OTUs with the three treatments (Figure 4.2).

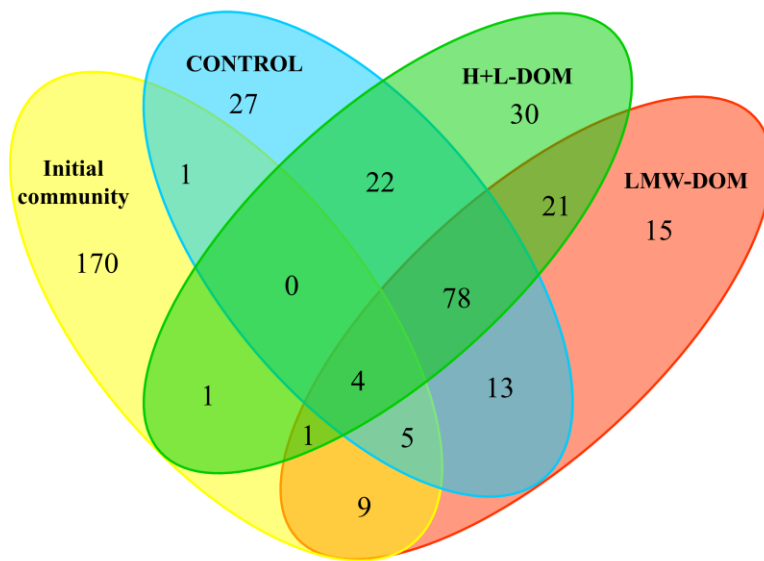


Figure 4.2. Venn diagram showing the shared bacterial OTUs between the environmental initial community and each of the different experimental treatments. The number of OTUs in the different treatments at the end of the experiment is an average of the three replicates.

4.3.5. Effects of size-fractionated DOM on bacterial community composition

The bacterial community composition growing in H+L-DOM and LMW-DOM was strikingly different from those found at the initial environmental community (Figure 4.3 A-B). A total of 17 bacterial taxa (phyla and classes) were identified in the initial environmental community (Figure 4.3 A). The most abundant taxa at the initial community were Chloroflexi (20%), Alphaproteobacteria (15%), Deltaproteobacteria (24%) and Gammaproteobacteria (14%) (Figure 4.3 A). The initial community changed over the time course of the experiment in the three DOM treatments. At the day 6 of experiment, Gammaproteobacteria and Alphaproteobacteria were the dominant classes in the three treatments and a low proportion of abundance was related to Bacteroidetes (1-8% of total abundance; Figure 4.3 A). At lower taxonomic levels (order and family), we found several phylotypes with low abundances at the initial community which increased their abundance at the end of experiment in all treatments, e.g. Rhodobacteraceae (Alphaproteobacteria), Alteromonadae, Colwelliaceae, Shewanellaceae, Oceanospirillaceae, Oleiphilaceae and Vibrionaceae (belong to Gammaproteobacteria; Figure 4.3 B). However, other phylotypes showed a differential response in the different DOM-treatments. While Flavobacteriaceae increased in the LMW-DOM, Pseudoalteromonas showed higher abundance in the CONTROL and H+L-DOM treatments as compared to LMW-DOM (Figure 4.3 B). Although members of Alteromonadaceae, Colwelliaceae, Oceanoasprillaceae, Oleiphilaceae, Phyllobacteriaceae and Rhodobacteraceae occurred in all the

samples, they were represented by different OTUs depending on the treatment (Supplementary Figure 4.2 A-C).

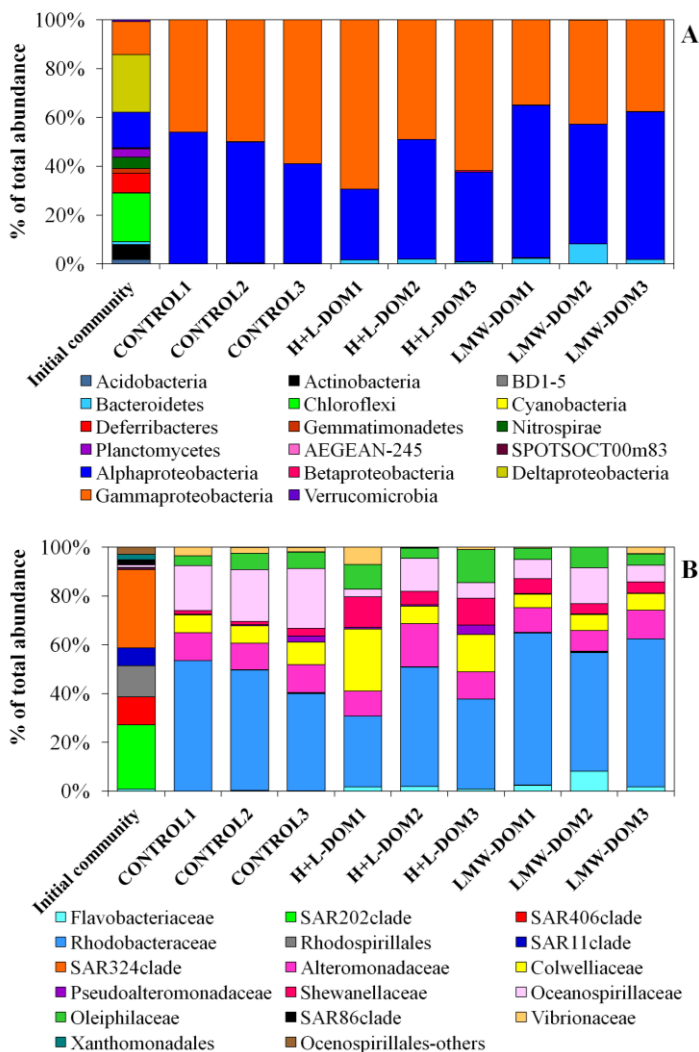


Figure 4.3. Taxonomical composition at phylum and class level (A) and order and family level (B) of the bacterial community in the environmental initial community and in the CONTROL, H+L-DOM and LMW-DOM treatments at the end of the experiment.

The relative abundance of Flavobacteriaceae increased slightly (0-4%) in H+L-DOM and LMW-DOM as compared to CONTROL treatment, more intensely in the LMW-DOM2 with an increase of 8-12% (Figure 4.4). Rhodobacteraceae, Rhodospirillales and SAR11clade (from Alphaproteobacteria) increased their relative abundance as compared to the CONTROL in the LMW-DOM treatment and decreased in the H+L-DOM as compared to CONTROL1 and CONTROL2 (Figure 4.4). The Rhodobacteraceae family increased their relative abundance between 12-24% in LMW-DOM as compared to the CONTROL. Other bacterial groups as Rhodospirillales or SAR11 clade increased slightly only in the LMW-DOM, between 0-4% as compared to the CONTROL. Gammaproteobacteria members exhibited an increase in the H+L-DOM (Figure 4.4) as compared to the CONTROL, with the exception of Oceanospirillaceae that decreased in both DOM treatments. Alteromonadaceae, Colwelliaceae, Shewanellaceae and Oleiphilaceae increased their relative abundance between 8-20% in the H+L-DOM as compared to the CONTROL (Figure 4.4). Pseudoalteromonadaceae and Vibrionaceae also increased slightly (0-4%) in the H+L-DOM treatment as compared to the CONTROL. CONTROL, H+L-DOM and LMW-DOM treatments had 28, 31 and 24 unique OTUs, respectively, while 82 OTUs were shared between the three treatments (Supplementary Figure 4.2 A). Unique OTUs from Alteromonadaceae, Colwelliaceae, Oceanospirillaceae, Oleiphilaceae and Rhodobacteraceae were present in all treatments (Supplementary Figure 4.2 B). Unique OTUs from Flavobacteriaceae, Rhodospirillales, SAR324, SAR86 and Verrucomicrobia occurred in LMW-DOM and unique OTUs of Betaproteobacteria, Gemmatimonadetes and Shewanellaceae were present in H+L-DOM (Supplementary Figure 4.2 B). The majori-

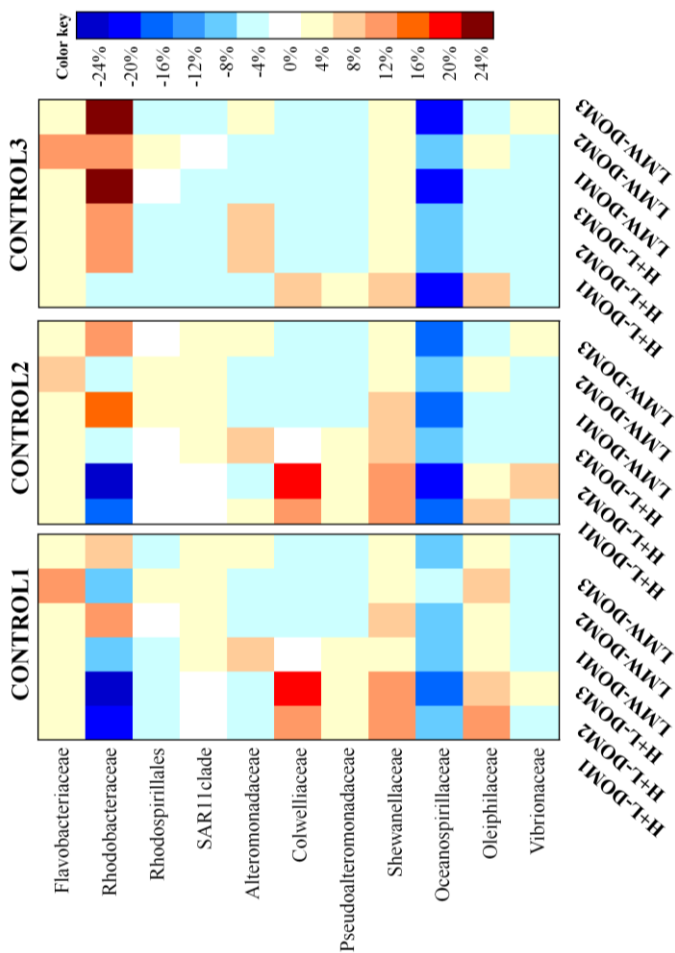


Figure 4.4. Heatmap visualizing the changes of the most abundant bacterial phylotypes growing in H+L-DOM and LMW-DOM as compared to the CONTROL. The change in relative abundance is illustrated by the color key for the three different replicates of each treatment. The different shades of blue represent decreasing relative abundance compared to CONTROL. The different shades of warm color represent increasing relative abundance as compared to the CONTROL.

ty of the 82 shared OTUs between the treatments were classified as Alteromonadaceae, Colwelliaceae, Flavobacteriaceae, Oceanospirillaceae, Oleiphilaceae, Pseudoalteromonadaceae, Rhodobacteraceae, Shewanellaceae and Vibrionaceae (Supplementary Figure 4.2 C).

4.3.6. Links between the bacterial community composition growing on different DOM and DOM properties

We evaluated the links between the most abundant bacterial phylotypes and the optical properties of DOM and biotic parameters in the different size-fractionated DOM treatments, using redundancy analysis (RDA, Figure 4.5). Axis 1 explained ~41% of the variability of the bacterial communities, while axis 2 explained ~34% of the variability. The FDOM-T was positively correlated with both axes. The sCDOM₂₇₅₋₂₉₅, aCDOM₃₄₀ and aCDOM₃₆₅ were negatively correlated with both axes. The proportion of live cells and of CTC+ cells, the aCDOM₂₅₄ and FDOM-M were negatively correlated with axis 1 and positively correlated with axis 2. RDA indicated that sCDOM₂₇₅₋₂₉₅ and aCDOM₃₆₅ were the main DOM indexes differentiating the CONTROL vs. the H+L- and/or LMW-DOC bacterial communities. H+L-DOM communities were associated to protein-like substances and included mainly Gammaproteobacteria, such as Shewanellaceae, Oleiphilaceae, Pseudoalteromonadaceae, Colwelliaceae and Vibrionaceae (Figure 4.5). In contrast, aCDOM₂₅₄, FDOM-M and %CTC+ were highly associated with the LMW-DOM communities (Figure 4.5), and correlated with members of Alphaproteobacteria, such as Rhodospirillales and Rhodobacteraceae, and Bacteroidetes, mainly Flavobacteria.

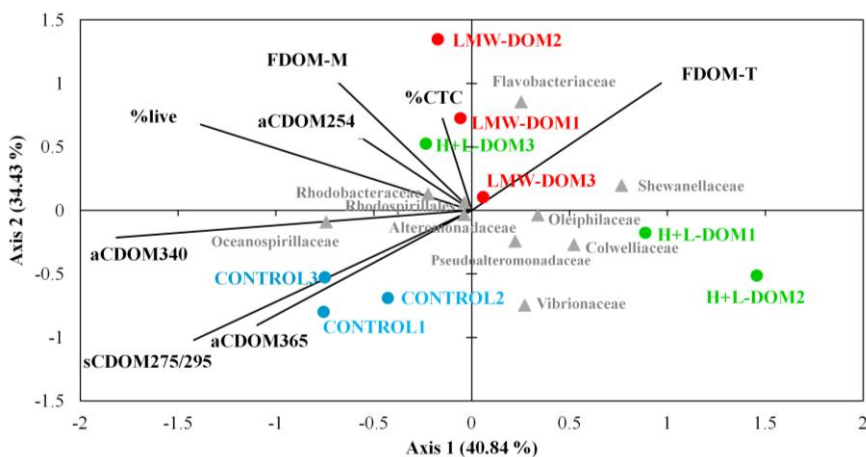


Figure 4.5. Redundance Analysis (RDA) of bacterial phylotypes, the different optical indices of the DOM and the bulk bacterial parameters. Black squares represented the replicates of the CONTROL treatment, white squares represented the H+L-DOM treatment and grey squares represented the LMW-DOM treatment replicates. The direction of the rows indicates the increase of the different variables.

4.4. Discussion

The size-reactivity continuum model for organic matter decomposition in aquatic environments was proposed by Amon and Benner (1994; 1996), based on their experimental results on bacterial utilization of high- and low-molecular weight DOM. Later, some other studies also focused on the bacterial degradation of natural DOM size fractions (e.g. Covert and Moran 2001; Khodse and Bhosle 2011). Ammon and Benner (1994, 1996) suggested that the bulk of HMW-DOM is more bioreactive and less diagenetically altered than the bulk of LMW-DOM, supported by higher bacterial abundance and respiration rates in the LMW-DOM as compared to the HMW-DOM incubations. Contrasting results were observed in other studies, which

suggested that the LMW-DOM was more biologically reactive, i.e. it was utilized more rapidly, than the HMW-DOM (Covert and Moran 2001; Khodse and Bhosle 2011), in agreement with some studies of size-based bioavailability (Meyer et al. 1987). Recently, Benner and Amon (2015) revised their model and suggested that the biodegradation processes might shape the size distribution of organic matter and the nature of the small dissolved molecules that persist in the ocean. To shed light on the link between microbes and DOM in the deep ocean, we designed an experiment to investigate the response of a natural bacterial community isolated and grown in filtered and size-fractionated DOM Mediterranean Water (1000 m depth).

Our results indicated that the ultrafiltration system affected the integrity of DOM (breaking up the continuum) as supported by the differences in the optical properties of DOM between CONTROL vs. H+L-DOM treatments. The changes in optical properties of DOM over the time course of the experiment in the CONTROL and H+L-DOM treatment were comparable; however, they differed from the changes in the LMW-DOM treatment. The decrease in aCDOM₂₅₄, a proxy for DOC concentrations (Lonborg and Álvarez-Salgado, 2014; Guerrero-Feijóo et al. 2015, person. comun.), together with the increase in inorganic nitrogen in the LMW-DOM treatment could suggest efficient mineralization of DOM in this treatment. In addition, the molecular-weight of the DOM decreased during the incubation (as indicated by the higher absorption slope at the end), indicating that the relatively higher-molecular-weight DOM available in this treatment (LMW-DOM, <1 KDa) was preferentially used. Correspondingly, microbial abundance, % of live cells and leucine incorporation rates were consistently higher in H+L-DOM than

CONTROL suggesting that breaking the DOM continuum affected the microbial communities growing in the H+L-DOM treatment. Additionally, these results would support previous findings suggesting that the HMW-DOM fraction is more bioavailable for bacteria than the LMW-DOM fraction (Amon and Benner, 1994, 1996; Benner and Amon, 2015; Guerrero-Feijóo et al. 2015, person. comun., Amon 2016), however in disagreement with studies indicating the opposite trend (Covert and Moran, 2001; Khodse and Bhosle, 2011).

Previous studies in the same area of the North Atlantic suggested that the quality of the DOM affects the heterotrophic community structure in the open ocean (Dobal-Amador et al. 2016; Guerrero-Feijóo et al. 2017), and thus would support that the size-fractionation of DOM can shape the bacterial community composition. Interestingly, the present study found that the highest richness displayed in our MW experiment occurred in LMW-DOM treatment, which some authors have linked to a larger bioavailability of the DOM (Covert and Moran 2001, Khodse and Bhodse 2011). However, it has to be taken into account that “size” is not the only variable shaping the DOM reactivity, also the chemical composition of different size classes of DOM adds up to the DOM complexity (Benner and Amon, 2015), and consequently affects the availability of this DOM. Moreover, different microbes could act in concert to facilitate the degradation of less bio-available DOM, suggesting that some bacteria could start metabolize specific compounds and release other compounds that then would become available for other microbes (Logue et al. 2016). With these considerations in mind, it is not so clear that higher richness of the bacterial communities would correspond to more bioavailable DOM.

The bacterial community composition inhabiting the filtered and size-fractionated DOM treatments was strikingly different from the initial environmental community. Several abundant bacterial taxa from the initial community, such as SAR324, SAR202, SAR406, Rhodospirillales or Actinobacteria, disappeared after 6 days in all treatments. This change in community composition is common in experimental incubations (Christian and Capone, 2002). The experimental incubations favor microbes that have low relative abundance under natural conditions, the so-called rare microbes, but which also harbor opportunistic capabilities to rapidly grow under changing environmental conditions and outcompete other microbes that were originally more abundant in the natural community (e.g., Colwelliaceae) (Lauro et al. 2009; Landa et al. 2013). However, although at the family level, we could not find significant changes in the bacterial communities that developed in the different treatments, these treatments not only differed from the initial community, but they showed changes in the relative abundance of some specific phylotypes associated to the filtered and size-fractionated DOM.

Gammaproteobacteria, with the exception of Oceanospirillaceae, increased relatively in the three treatments in agreement with previous results from experimental incubations (Pinhassi and Berman 2003; Nelson and Carlson 2012) and supporting the opportunistic life style of the members of this group, characterized by fast growth and metabolic potential for a wide range of substrates (Lauro et al. 2009; Landa et al. 2013). Alternatively, the bacterial communities inhabiting in the LMW-DOM treatment were mainly composed by phylotypes related to

Flavobacteriaceae and Alphaproteobacteria. In particular, Flavobacteriaceae had higher relative abundance in the LMW-DOM as compared to the H+L-DOM treatment, in disagreement with the reported preference of Bacteroidetes for high-molecular-weight DOM compounds (Pinhasi et al. 2004, West et al. 2008, Fernández-Gómez et al. 2013). The sCDOM₂₇₅₋₂₉₅ was the main DOM optical property that differentiated the CONTROL from size-fractionated DOM treatments, suggesting a tight coupling between bacteria and the aromaticity and molecular mass of DOM in this treatment (Helms et al. 2008). H+L-DOM communities were only associated to protein-like substances (represented by labile compounds) suggesting a connection between the FDOM-T and members of Gammaproteobacteria, such Pseudoaltetomonadaceae, Colwelliaceae and Vibrionaceae, growing in the H+L-DOM (with the exception of the H+L-DOM3). In contrast, LMW-DOM populations were connected to FDOM-M and aCDOM₂₅₄ indicative either of older/more reworked DOM (Martínez-Pérez et al. 2017) or of the bacterial potential (of specific groups such as Rhodospirillales and Rhodobacteraceae, or Flavobacteria), to generate refractory compounds (humic-like compounds) as subproducts of the remineralization processes.

In summary, our results suggest an association of specific phylogenetic groups to the degradation of different size fractions of DOM. Several members of Gammaproteobacteria preferentially utilize high molecular weight DOM, while members of the Alphaproteobacteria utilize preferentially low molecular weight DOM. Several members of the Alphaproteobacteria phylotypes that thrived in the LMW-DOM treatment are usually abundant in natural open ocean conditions (Giovanoni and Rappé

2000, DeLong et al. 2006; Guerrero-Feijóo et al. 2017), where the labile DOM is limited. The Gammaproteobacteria phylotypes that developed on the H+L-DOM treatment corresponded to characteristically opportunistic microbes, which usually grow when newly generated organic matter becomes available (Lauro et al. 2009; Landa et al. 2013). Additionally, the changes in community composition were strongly associated with changes in optical properties of DOM, suggesting that the diversity of DOM was critical to select the Flavobacteriaceae and Alphaproteobacteria members growing in LWM-DOM and Gammaproteobacteria phylotypes in H+L-DOM. Further studies are necessary to investigate functional genes involved in the bacterial utilization of different size classes of DOM in parallel with DOM composition identification (e.g, transcriptomics combined with proteomics). This approach combining different -omics could help to explain the usage of individual molecules of DOM by specific bacterial taxa, and could provide a better understanding of both DOM and microbes, necessary to predict the marine carbon cycle response to global change.



Chapter 5

High dark inorganic carbon fixation rates by chemolithoautotrophic microbes off the Galician coast (NW Iberian margin)

Abstract

Bulk dark dissolved inorganic carbon (DIC) fixation rates were determined and compared to microbial heterotrophic production in subsurface, meso- and bathypelagic Atlantic waters off the Galician coast (NW Iberian margin). DIC fixation rates were slightly higher than heterotrophic activity throughout the water column, however, more prominently in the bathypelagic waters. Microautoradiography combined with catalyzed reporter deposition fluorescence in situ hybridization (MICRO-CARD-FISH) allowed us to identify several microbial groups involved in dark DIC uptake. Noteworthy, the contribution of SAR406 (Marinimicrobia), SAR324 (Deltaproteobacteria) and *Alteromonas* (Gammaproteobacteria) to the bulk dark DIC fixation was significantly higher than that of SAR202 (*Chloroflexi*) and Thaumarchaeota, in agreement with their contribution to the microbial abundance. Q-PCR on the gene encoding for the ammonia monooxygenase subunit A (*amoA*) from two ecotypes revealed their depth-specified niche partitioning off the Galician coast. Taken together, our results indicate that chemoautotrophy is widespread among microbes in the dark ocean, particularly in bathypelagic waters. This chemolithoautotrophic biomass production in the dark ocean, depleted in bio-available organic matter, might play a substantial role in sustaining the dark ocean's food web.

5.1. Introduction

Over the past decade it has been recognized that dissolved inorganic carbon (DIC) fixation by the marine microbial community might be substantial in the meso- and bathypelagic waters (Herndl et al. 2005; Baltar et al. 2010; Varela et al. 2011). Marine chemolithoautotrophic microorganisms can incorporate inorganic carbon into organic compounds in the dark by harvesting energy from the oxidation of ammonium (Wuchter et al. 2006; Agogué et al. 2008; Beman et al. 2008), urea (Alonso-Sáez et al. 2012) or sulfur (Baltar et al. 2016) among other reduced inorganic compounds. Additionally, several metabolic pathways can potentially contribute to heterotrophic inorganic carbon fixation, known as the anaplerotic reaction (Dijkhuizen and Harder 1984; Erb 2011). A recent study showed an increase in DIC fixation in response to the addition of labile organic carbon in incubation experiments concomitant with an up-regulation of genes involved in DIC assimilation via anaplerotic pathways (Baltar et al. 2016). However, this anaplerotic reaction should vary considerably with substrate utilization (quality and quantity of organic substrate) and/or the microbial community composition. Therefore, dark DIC fixation may be relevant for both chemolithoautotrophic and heterotrophic microorganisms.

Using microautoradiography combined with catalyzed reported deposition fluorescence in situ hybridization (MICRO-CARD-FISH) the uptake of dissolved inorganic carbon at a single cell level can be measured. A few studies have used this approach to confirm the uptake of radiolabeled inorganic carbon by specific marine prokaryotic taxa (Kirchmann et al. 2007; Grote et al. 2008; Alonso-Sáez et al. 2010; Varela et al. 2011; Swan et al. 2011). More recently, omics analyses have revealed a large diversity of microbes containing the enzymatic machinery potentially involved in DIC assimilation (Glaubitx et al. 2010; Swan et al. 2011; DeLorenzo et al. 2012). Gene expression studies have sheds light on the mechanism of alternative DIC fixation pathways (Baltar et al. 2016). To the

best of our knowledge, these investigations have not been yet quantified the contribution of the different microbial members to the bulk dark ocean DIC fixation.

Despite advances in our understanding of the dark inorganic carbon assimilation, the energy sources used to sustain the chemolithoautotrophic activity in the open ocean remains enigmatic. Since mesophilic Thaumarchaeota were reported to be widely distributed in oceanic environments (Varela et al. 2008a, 2011), several studies have suggested that ammonia oxidation by ammonia-oxidizing Archaea (AOA) cannot explain the high DIC fixation rates in the dark ocean (Reinthaler et al. 2010; Middelburg 2011). Elevated dark DIC fixation rates were observed in ammonium-amended microcosm of mesopelagic North Atlantic waters (Baltar et al. 2016). The ability of ammonia-oxidizing Archaea to thrive even under extremely low-nutrient concentrations (such as those in the meso- and bathypelagic realm) has been explained by their carbon assimilation through the more energy efficient aerobic autotrophic pathway (Könneke et al. 2014).

Two distinct AOA ecotypes were detected in the Atlantic, differentiated by *amoA* gene sequence differences (Sintes et al. 2013). One AOA ecotype is more abundant in the upper mesopelagic waters and apparently geared towards utilizing high ammonia concentrations (HAC-AOA) while the other one numerically dominates the lower meso- and bathypelagic waters and it is presumably geared to use the rather low (LAC-AOA) ammonia concentrations, typically found in these deep waters (Sintes et al. 2013). Hence, these two AOA ecotypes exhibit a pronounced vertical distribution pattern in the North Atlantic (Sintes et al. 2013). These ecotype distribution together with the biogeographical patterns of AOA, determined along a latitudinal gradient and thought the water column of the Atlantic ocean, have tentatively suggested an influence of the epipelagic conditions (e.g. organic matter production) on the bathypelagic AOA communities (Sintes et al. 2015).

We hypothesized that the particular hydrographic conditions in the Atlantic off the Galician coast (NW Iberian Peninsula), a dynamic area characterized by seasonal upwelling events and subsequent sedimentation of organic matter into the mesopelagic waters further offshore, might lead to specific distribution patterns of microbial chemolithoautotrophy and consequently DIC fixation. The main questions to answer in this investigation were: (1) What is the magnitude of the DIC fixation compared to microbial heterotrophic production? (2) Which organismal groups dominate the chemolithoautotrophic microbial community? (3) Are there different ecotypes, based on different archaeal *amoA* genes, present in the water column?

5.2. Material and methods

5.2.1. Study area

Sampling was carried out during two cruises, BIO-PROF-1 (11-28 August 2011) and BIO-PROF-2 (11-20 September 2012) on board R/V Cornide de Saavedra from 43°N, 9°W to 43°N, 14°W off Cape Finisterre (NW Spain) (Figure 5.1). Water samples were collected with Niskin bottles mounted on a CTD (conductivity-temperature-depth) rosette sampler from the subsurface layer (SSL, 0-200 m depth), the Eastern North Atlantic Water (ENACW, 300-900 m depth), where the oxygen minimum zone (OMZ, 900 m depth) was found, the Mediterranean Water (MW, 1000 m depth), the Labrador Sea Water (LSW, 1800-2000 m depth), the Eastern North Atlantic Deep Water (ENADW, 2750 m depth) and the Lower Deep Water (LDW, 4000-4500 m depth). Samples for physico-chemical analysis were collected at a total of 43 stations (22 and 21 stations for BIO-PROF-1 and BIO-PROF-2, respectively) (Figure 5.1, Table 5.1; Guerrero-Feijóo et al. 2017). Samples for microbial analysis were collected at 5 stations (8, 11, 16, 108 and 111 Figure 5.1) to determine DIC fixation, heterotrophic activity, MICRO-CARD-FISH (only BIO-PROF-2) and qPCR on the thaumarchaeal 16S rRNA and *amoA* gene.

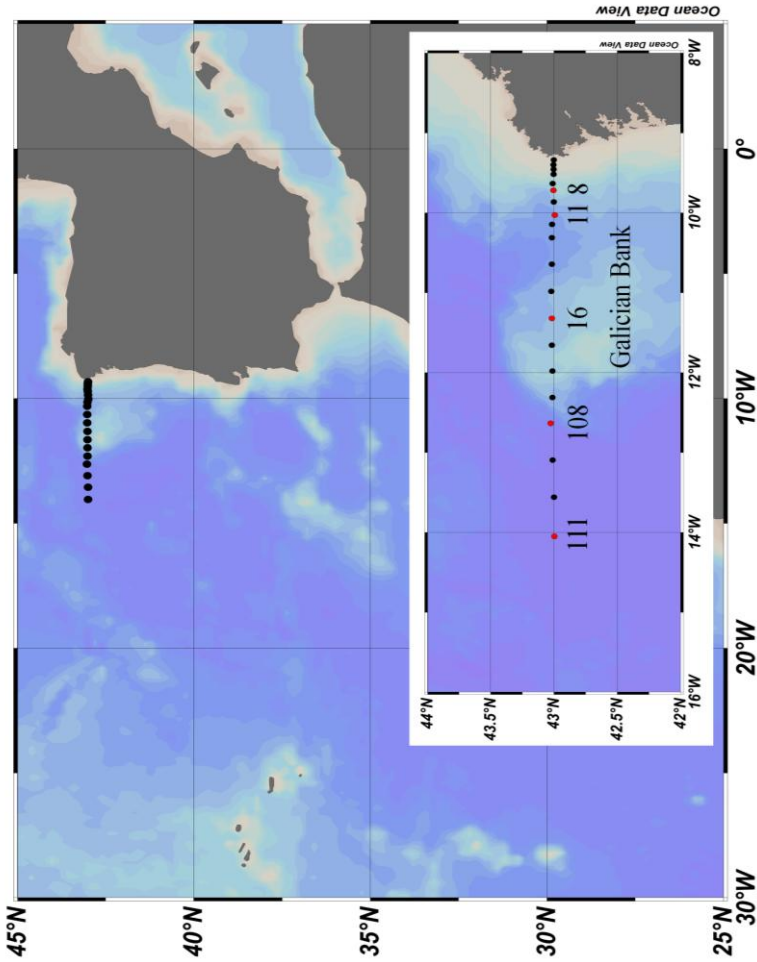


Figure 5.1. Map of the occupied stations in the Finisterre Section off the Galician coast (NW Iberian Peninsula). Dots represent all stations sampled for physico-chemical data. The key stations where the biological measurements were performed are also indicated and labeled in red (8, 11, 16, 108 and 111). Modified version of Guerrero-Feijóo et al. (2017).

Table 5.1. Physical and chemical characteristics of the water masses sampled in the Finisterre section off the Galician waters (NW Iberian Peninsula) in the North Atlantic during the BIO-PROF-1 and BIO-PROF-2 cruises. Mean±SD is given; n=267 for BIO-PROF-1 and n=245 for BIO-PROF-2. Abbreviations: ENACW-OMZ, Eastern North Atlantic Central Water – Oxygen Minimum Zone; MW, Mediterranean Water; LSW, Labrador Sea Water; ENADW, Eastern North Atlantic Deep Water; LDW, Lower Deep Water.

| Water masses | BIO-PROF-1 | | | | | BIO-PROF-2 | | | | |
|--------------|--|--|---|--|--|--|--|---|--|--|
| | Nitrate ($\mu\text{mol kg}^{-1}$) | Nitrite ($\mu\text{mol kg}^{-1}$) | Silicate ($\mu\text{mol kg}^{-1}$) | Phosphate ($\mu\text{mol kg}^{-1}$) | Phosphate ($\mu\text{mol kg}^{-1}$) | Nitrate ($\mu\text{mol kg}^{-1}$) | Nitrite ($\mu\text{mol kg}^{-1}$) | Silicate ($\mu\text{mol kg}^{-1}$) | Phosphate ($\mu\text{mol kg}^{-1}$) | Phosphate ($\mu\text{mol kg}^{-1}$) |
| SSL | 7.77±0.44 | 0.16±0.03 | 2.53±0.16 | 0.57±0.04 | 0.57±0.04 | 6.87±0.41 | 0.09±0.01 | 2.49±0.30 | 0.52±0.03 | 0.52±0.03 |
| ENACW-OMZ | 12.87±0.57 | 0.06±0.00 | 4.79±0.17 | 0.82±0.02 | 0.82±0.02 | 12.12±0.29 | 0.06±0.00 | 4.69±0.20 | 0.78±0.02 | 0.78±0.02 |
| MW | 17.55±0.48 | 0.05±0.00 | 8.68±0.20 | 1.06±0.02 | 1.06±0.02 | 15.12±0.39 | 0.06±0.00 | 7.87±0.21 | 0.93±0.02 | 0.93±0.02 |
| LSW | 19.33±0.43 | 0.05±0.00 | 15.79±0.42 | 1.22±0.02 | 1.22±0.02 | 17.19±0.22 | 0.07±0.02 | 13.04±0.26 | 1.16±0.01 | 1.16±0.01 |
| ENADW | 20.10±0.43 | 0.05±0.00 | 24.53±0.07 | 1.27±0.03 | 1.27±0.03 | 17.45±0.33 | 0.05±0.00 | 19.41±0.88 | 1.23±0.02 | 1.23±0.02 |
| LDW | 20.14±0.50 | 0.05±0.00 | 32.67±2.03 | 1.31±0.03 | 1.31±0.03 | 20.53±0.30 | 0.05±0.00 | 37.24±0.74 | 1.47±0.01 | 1.47±0.01 |

5.2.2. Bulk microbial heterotrophic production

Leucine incorporation (Leu incorp.) rates of the microbial communities within the subsurface and upper intermediate waters (up to 500m) were measured by adding 5 nmol L⁻¹ [³H]-leucine (final concentration, specific activity 160 Ci mmol L⁻¹, GE Healthcare, Amersham, Bucks, UK) to triplicate 1.2 mL samples and duplicate TCA (trichloroacetic acid)-killed blanks (5% final concentration) (Simon and Azam 1989). Samples and blanks were incubated in the dark at in situ temperature in temperature-controlled chambers for 2-6 h, depending on the expected activity. Incubations were terminated by adding TCA (5% final concentration) to the samples. Bacterial proteins were precipitated by two successive centrifugation steps (12350 g, 10 min), including a washing step with 1 mL of 5% TCA according to Kirchman (1985) with slight modifications (Smith and Azam 1992).

Leu incorp. of the lower intermediate and deep waters (below 1000m) was measured by adding 5 nmol L⁻¹ [³H]-leucine (final concentration, specific activity 160 Ci mmol L⁻¹, GE Healthcare, Amersham, Bucks, UK) to duplicate 40 mL samples and duplicate formaldehyde-killed blanks (2% final concentration) (Simon and Azam, 1989). Samples and blanks were incubated in the dark at in situ temperature in temperature-controlled chambers for 10 - 24 h, depending on the expected activity. Incubations were terminated by adding formaldehyde (2% final concentration) to the samples. After 10 min, the samples and the blanks were filtered onto 0.2 µm polycarbonate filters (25 mm filter diameter, Millipore). Subsequently, the filters were rinsed three times with 10 mL of 5% TCA. Thereafter, the filters were transferred into scintillation vials and dried at room temperature. Finally, scintillation cocktail was added to the vials, and after 18 h, the radioactivity was determined in a liquid scintillation counter (LKB Wallac). The mean disintegrations per minute (DPM) of the blanks were subtracted from the mean DPM of the respective samples and the resulting DPM converted into leucine incorporation rates.

We use 1.55 kg mol^{-1} to convert Leu incorp. into heterotrophic carbon biomass production (Kirchman 1993).

5.2.3. Bulk DIC (dissolved inorganic carbon) fixation

Water samples of 40 mL were collected in triplicate 50 mL glass bottles and two formaldehyde-fixed blanks and 100 μCi of [^{14}C]-bicarbonate added and incubated in the dark at in situ temperature for 72 h (Herndl et al. 2005). Incubations were terminated by adding formaldehyde (2% final concentration) to the samples, filtered onto 0.2- μm polycarbonate filters and rinsed three times with 10 mL of filtered seawater. Subsequently, the filters were fumed over concentrated HCl for 12 h and then transferred to scintillation vials. Scintillation cocktail was added and after 18 h, the radioactivity was determined in a liquid scintillation counter (LKB Wallac) for 10 min. The disintegrations per minute (DPM) of the formaldehyde-fixed blank were subtracted from the mean DPM of the respective samples and resulting DPM converted into DIC fixation rates.

5.2.4. MICRO-CARD-FISH with ^{14}C -bicarbonate

Duplicate samples (40 mL) were spiked with [^{14}C]-bicarbonate (100 μCi ; SA, 54.0 MCi mmol^{-1} ; Perkin Elmer) and incubated in the dark at in situ temperature for ≈ 72 h. After incubation, samples were fixed with paraformaldehyde (2% final concentration) and subsequently stored at 4°C in the dark for 12 – 18 h. Thereafter, the samples were filtered onto 0.2 μm polycarbonate filters (Millipore, GTTP, 25 mm diameter) supported by cellulose nitrate filters (Millipore, HAWP, 0.45 μm), rinsed twice with Milli-Q water, dried and stored in a microfuge vial at -20°C until further processing in the laboratory. The filters for catalyzed reported deposition fluorescence in situ hybridization (CARD-FISH) were embedded in low-gelling point agarose and incubated with lysozyme for Bacteria and specific bacterial groups or with proteinase-K for Thaumarchaeota following the method described in Teira et al. (2004). Filters were cut into sections

and hybridized with horseradish peroxidase (HRP)-labeled oligonucleotide probes (see details of the probe sequences and hybridization conditions used in the CARD-FISH in Dobal-Amador et al. 2016 and Guerrero-Feijoo et al. 2017), followed by tyramide-Alexa488 signal amplification. Autoradiographic development was conducted by transferring hybridized filter sections onto slides coated with photographic emulsion (type NTB-2 melted at 43°C for 1 h; Teira et al. 2004). Subsequently, the slides were placed in a dark box with a drying agent and exposed at 4°C for 15 d. Finally, the slides were developed and fixed using Kodak specifications (Dektol developer [1:1 dilution with Milli-Q water] for 2 min, followed by a Milli-Q water rinse for 2 min). Before completely dried, filter sections were removed and cells were counterstained with a DAPI mix and examined under a Nikon Eclipse 80i epifluorescence microscope equipped with an Hg-lamp and appropriate filter sets for DAPI, Cy3 and Alexa448. The silver grains in the autoradiographic emulsion were detected by switching to the transmission mode of the microscope. For each microscope field, we enumerated the DIC-positive cells of total microbes, Bacteria and Thaumarchaeota, and the specific bacterial groups SAR324 (Deltaproteobacteria), SAR406 (Marinimicrobia), and *Alteromonas* (Gammaproteobacteria) and SAR202 (Chloroflexi). Cells were classified as DIC-positive if at least three silver grains were associated with an individual cell. Around 50 DIC-positive cells were counted per sample. In the killed controls, < 1% of cells was associated with silver grains. We express the contribution of different groups as MICRO-CARD-FISH-positive cells divided by the total of prokaryotic abundance (MICRO-CARD-FISH₊/_g/DAPI counts) hence, indicating the number of active cells taking up DIC as a proportion of the total community.

5.2.5. DNA extraction

A volume of 10–15 L of water was filtered through sterile Sterivex 0.22 µm pore size filters (Millipore, USA). Subsequently, 1.8 mL of lysis buffer (40 mM EDTA, 50 mM Tris-HCl, 0.75 M sucrose) was immediately added to the

filters before storing them at -80°C until extraction. The DNA extraction was performed by adding lysozyme and sodium dodecyl sulphate (SDS) to the samples to lyse the cells. Proteins were removed from the lysis mixture by proteinase-K and chloroform/phenol extraction before DNA precipitation by isopropanol. The pellet was washed with 70% ethanol and resuspended in sterile TE buffer. DNA concentrations were quantified on a Nanodrop spectrophotometer.

5.2.6. Quantitative PCR

Quantitative PCR (q-PCR) was conducted to evaluate 16S rRNA gene abundance of Thaumarchaeota and the abundance of two ecotypes of ammonia oxidation Archaea: the low-ammonia concentration ecotype (LAC-AOA) and the high ammonia AOA ecotype (HAC-AOA) as previously described in Sintès et al. (2016). We used specific primers for 16S rRNA gene abundance MCGI-391F (5'AAGGTTARTCCGAGTGRTTTC) and MCGI-554R (5'TGACCACTTGAGGTGGCTG) (Coolen et al. 2007), as well as the specific primer set for archaeal amoA primers Arch-amoA- (5'CTGAYTGGGCYTGGACATC) for LAC- and HAC-amoA, Arch-amoA-rev (5'TTCTTCTTTGTTGCCAGTA) (Wuchter et al. 2006; Agogué et al. 2008; Sintès et al. 2013) for HAC-amoA and Arch-amoA-rev-New (5'TTCTTCTTCGTCGCCAATA) for LAC-amoA. Briefly, triplicate reactions were conducted on 5 times diluted DNA samples. Reaction samples contained 1x SYBR Green PCR master mix, forward and reverse primers and environmental DNA. The q-PCR program started with an initial denaturation at 95°C for 10 min; amplification: 50 cycles, at 95°C for 5 s, primer annealing temperature for 5 s and the extension at 72°C for 15 s, 80°C for 3 s with a plate read between each cycle; melting curve $65\text{-}95^{\circ}\text{C}$ with a read every 0.2°C held for 1 s between each read (Sintès et al. 2016). All analyses were carried out with a thermocycler (Roche Lightcycler 480 real time PCR).

4.3. Results

4.3.1. Water mass features

The main water masses in the Atlantic sampled along a section off the Galician coast (Figure 5.1; Table 5.1) are described in Guerrero-Feijóo et al. (2017). Briefly, the basic physico-chemical features of the main water masses encountered in the two research cruises (BIO-PROF-1 and BIO-PROF-2) are shown in Figure 5.2 A-F. The Lower Deep Water (LDW; 4000 m depth) was characterized by low temperature (Figure 5.2 A-B) and salinity (Figure 5.2 C-D) and high dissolved oxygen concentrations (Figure 5.2 E-F). The Eastern North Atlantic Deep Water (ENADW; 2750 m depth) was identifiable by slightly higher temperature than the LDW (2.5 – 3.5°C; Figure 5.2 A-B) and the highest oxygen concentrations of all water masses sampled (Figure 5.2 E-F). The intermediate water masses identified were Labrador Sea Water (LSW; 1800-2000 m), showing a minimum in salinity (Figure 5.2 C-D) and a relatively high oxygen concentration (Figure 5.2 E-F) and Mediterranean Water (MW; 1000 m depth) identifiable by the highest salinity values (Figure 5.2 C-D) of all water masses. The Eastern North Atlantic Central Water was found between 250 – 900 m depth and the Oxygen Minimum Zone (ENACW-OMZ) was located east of the Galician bank at around 900 m (Figure 5.2 E). Thereafter, the ENACW-OMZ and MW are referred to as mesopelagic waters (from 200 to 1000 m depth); and LSW, ENADW and LDW water masses shape the bathypelagic realm (from ≥ 1000 to ≈ 4500 m depth).

4.3.2. Bulk microbial heterotrophic production (MHP) vs. dark dissolved inorganic carbon (DIC) fixation

MHP and DIC fixation rates significantly decreased with depth through the water column (t-test, $p < 0.001$, $n = 43$ for MHP and $p < 0.001$, $n = 33$ for DIC fixation) (Figure 5.3). MHP rates decreased by 4 orders of magnitude from $149.9 \mu\text{mol C m}^{-3} \text{d}^{-1}$

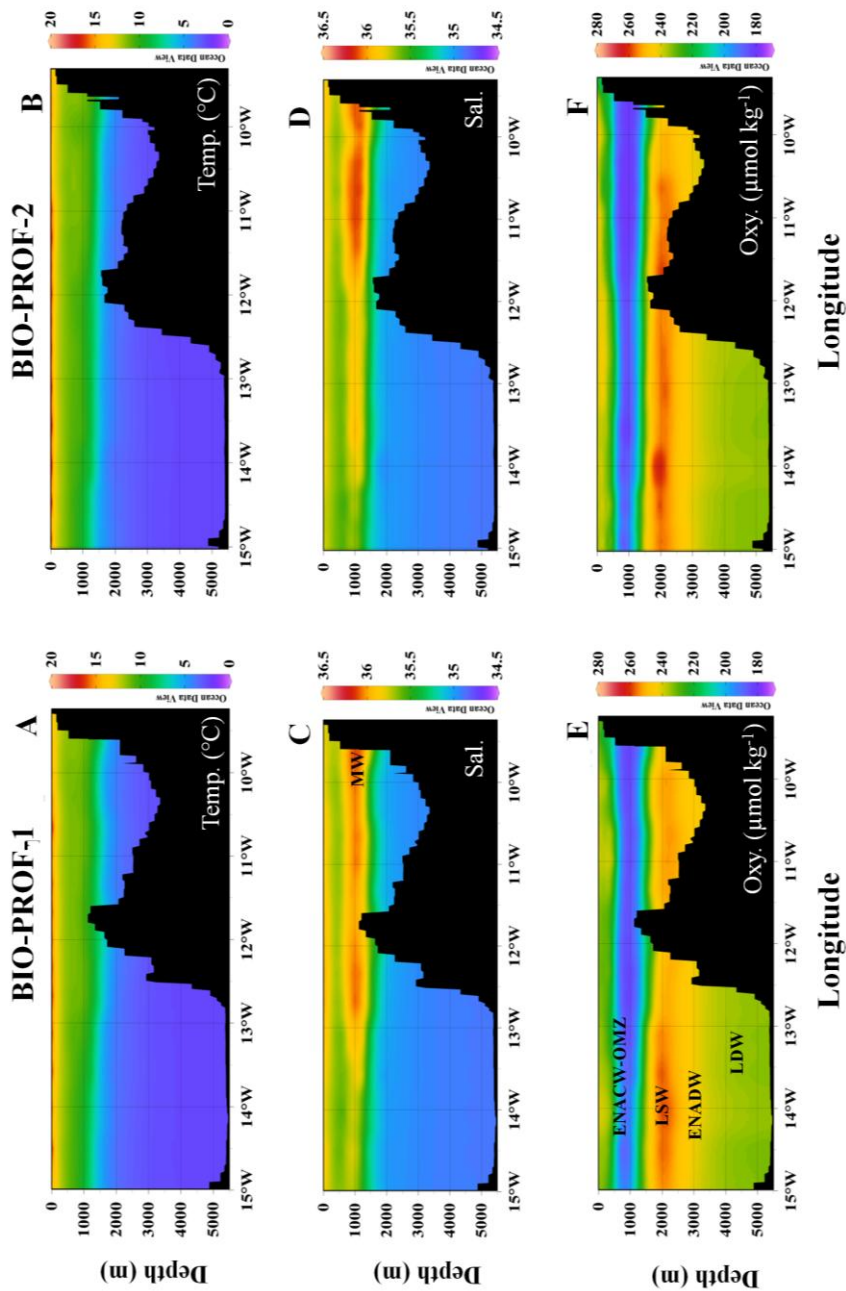


Figure 5.2. Temperature (A-B), salinity (C-D) and oxygen concentration (E-F) in the Finisterre Section off the Galician coast (NW Iberian Peninsula) during BIO-PROF-1 and BIO-PROF-2 cruises. Abbreviations see Table 5.1.

at 100 m depth to $0.01 \mu\text{mol C m}^{-3} \text{d}^{-1}$ at 4500 m depth (Figure 5.3). In contrast, dark DIC fixation rates declined only by one order of magnitude from $3.44 \mu\text{mol C m}^{-3} \text{d}^{-1}$ at 100 m depth to $0.30 \mu\text{mol C m}^{-3} \text{d}^{-1}$ at 4500 m depth (Figure 5.3). Overall, no significant differences were found between BIO-PROF-1 and BIO-PROF-2 cruises for both MHP and dark DIC fixation rates (t-test, $p=0.33$, $n=10$ for MHP and $p=0.16$, $n=10$ for DIC fixation) (Figure 5.3). While the maximum MHP was measured at the subsurface layer (200 m depth), the highest dark DIC fixation rates were measured in mesopelagic waters (up to $67.07 \mu\text{mol C m}^{-3} \text{d}^{-1}$ at 1005 m depth) (Figure 5.3). In general, the variability in both MHP and DIC fixation rates was higher in the mesopelagic than in the bathypelagic zone, and most of the water masses exhibited a slightly higher (although not statistically significant, t-test, $p=0.17$, $n=30$) DIC fixation than MHP, with the exception of the subsurface (down to 200m depth) where MHP always exceeded DIC fixation (Figure 5.3).

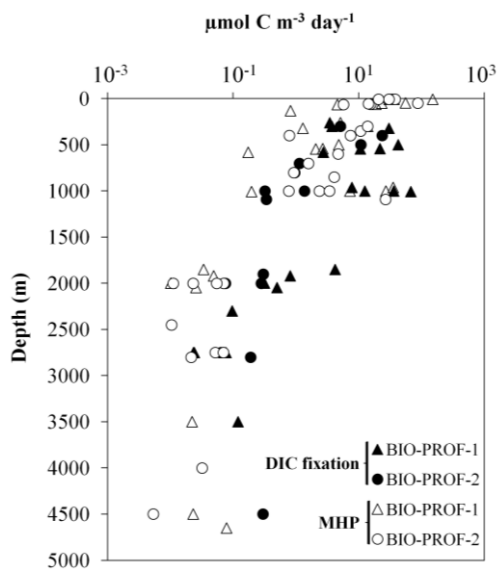


Figure 5.3. Microbial heterotrophic production (MHP, open triangles and circles) and dark DIC fixation rates (filled triangles and circles) in the Finisterre Section off the Galician coast (NW Iberian Peninsula) waters during BIO-PROF-1 and BIO-PROF-2 cruises.

5.3.3. Microbial groups involved in dark DIC uptake determined by MICRO-CARD-FISH

While the fraction of Bacteria taking up DIC was higher in subsurface and mesopelagic waters than in the bathypelagic (Figure 5.4 A), Thaumarchaeota exhibited the highest percentage of cells taking up DIC in mesopelagic waters (Figure 5.4 B). Specific bacterial groups exhibited significant differences with depth in the percentage of cells taking up DIC (t-test, $p < 0.05$, $n = 13$ for SAR324, SAR406 and *Alteromonas*, and $p < 0.05$, $n = 9$ for SAR202) (Figure 5.4 C-F). The highest

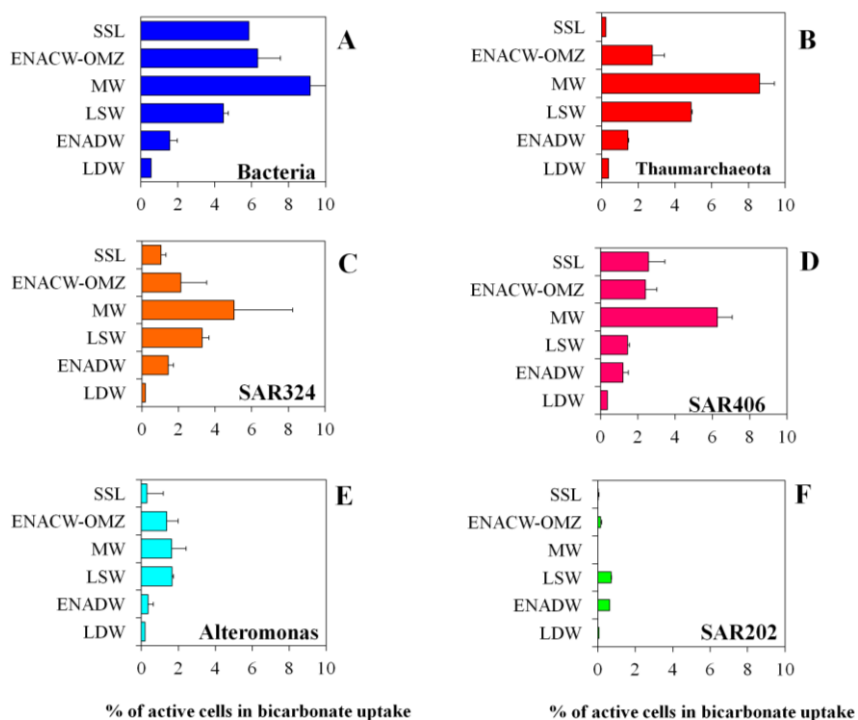


Figure 5.4. Percentage of active cells (expressed as % of DAPI cells) incorporating bicarbonate of major prokaryotic groups (A-B) and specific bacterial groups (C-F) within the main water masses sampled during BIO-PROF-2 cruise in the Finisterre Section off the Galician coast (NW Iberian Peninsula). For abbreviations see Table 5.1.

proportion of bacterial cells taking up DIC was detected in the MW, with the exception of *Alteromonas* which had the highest fraction of cell taking up DIC in the ENACW-OMZ (Figure 5.4 E). Very similar vertical trends were found for SAR324 and SAR406. Only $\approx 1\%$ of the SAR324 cells was taking up DIC in the subsurface layer, whereas this percentage increased to 5% in MW and subsequently decreased to $<1\%$ in the LDW (Figure 5.4 C). Similarly, SAR406 taking up DIC amounted to 3% in the subsurface layer and 6% in the MW, and remained rather stable deeper in the water column (Figure 5.4 D). Less than 5% of the cells identified as *Alteromonas* took up DIC (Figure 5.4 E). The lowest fraction of cells taking up DIC was found for SAR202 (0 - 1%) (Figure 5.4 F). No noticeable activity in DIC uptake was found in SAR11 (data not shown).

5.3.4. Contribution of specific microbial groups to the bulk DIC fixation

We calculated the relative contribution of different microbial groups taking up DIC as detected by MICRO-CARD-FISH to the bulk DIC fixation in the different water masses. While the contribution of Bacteria to bulk DIC fixation decreased with depth accounting for approximately 90% in the subsurface layer and 60% in bathypelagic waters (Figure 5.5 A), the contribution of Thaumarchaeota to bulk DIC fixation was rather low in the subsurface layer and upper mesopelagic waters and remained fairly constant in the lower meso- and bathypelagic waters comprising 40-50% of the bulk DIC fixation there (Figure 5.5 A). Overall, the percent contribution to bulk DIC fixation was significantly higher for Bacteria than for Thaumarchaeota (t-test, $p=0.02$, $n=13$).

The contribution of SAR324 to bulk DIC fixation increased from 15% in the subsurface layer to $\approx 60\%$ in ENADW (Figure 5.5 B). The contribution of SAR406 to the bulk DIC fixation did not show a clear trend with depth, accounting for up to $\approx 80\%$ of the bulk DIC fixation in the subsurface layer and $\approx 50\%$ in the MW and LDW (Figure 5.5 B). Although the fraction of *Alteromonas* cells taking up DIC compared to the

total microbial community taking up DIC was low (<5%; Figure 5.5 E), their contribution to bulk DIC fixation was up to $\approx 42\%$ in upper mesopelagic. In contrast, the contribution of SAR202 was always < 1% to the bulk DIC fixation (Figure 5.5 B).

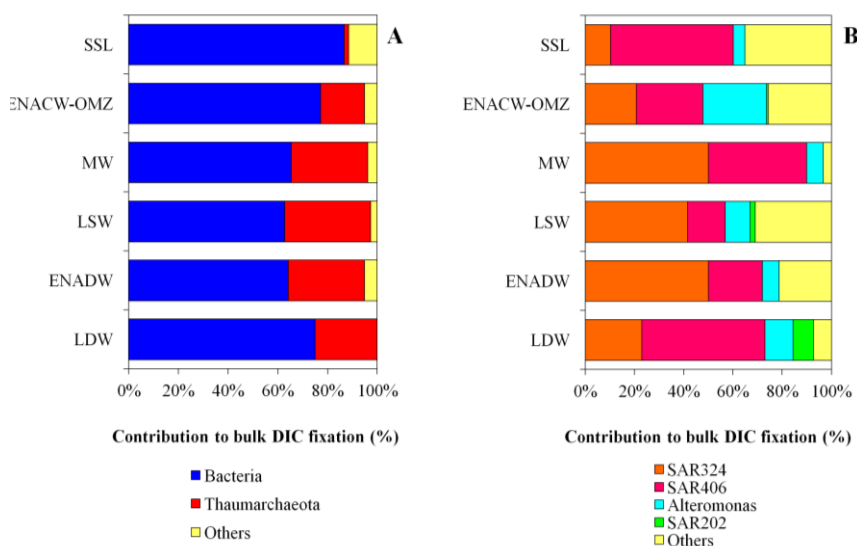


Figure 5.5. Contribution of major microbial groups (A) and specific bacterial groups (B) to the bulk DIC fixation within the main water masses sampled during BIO-PROF-2 cruise in the Finisterre Section off the Galician coast (NW Iberian Peninsula). For abbreviations see Table 5.1.

5.3.5. Vertical abundance and distribution of archaeal *amoA* genes

The abundance of both HAC- and LAC-*amoA* ecotypes and the thaumarchaeal 16S rRNA genes did not show significant differences between BIO-PROF-1 and BIO-PROF-2 (t-test, $p=0.06$, $n=13$ for HAC-*amoA*; $p=0.67$, $n=13$ for LAC-*amoA* and $p=0.05$, $n=12$ for Thaumarchaeota 16S rRNA). The archaeal HAC-*amoA* abundance was highest in the subsurface layer with an average of $1.6 \pm 0.2 \times 10^5$ and $0.4 \pm 0.3 \times 10^5$ copies mL^{-1} for BIO-PROF-1 and BIO-PROF-2, respectively, and decreased with depth to 36.2 copies mL^{-1} and 251.4 ± 121.4 copies mL^{-1} in LDW

for BIO-PROF-1 and BIO-PROF-2, respectively (Figure 5.6 A-B). The archaeal LAC-*amoA* abundance ranged from $2.0 \pm 1.7 \times 10^3$ copies mL⁻¹ for BIO-PROF-1 and 38.8 ± 34.8 copies mL⁻¹ for BIO-PROF-2 in the subsurface layer, with a slightly increase at the ENACW-OMZ ($2.6 \pm 1.4 \times 10^3$ for BIO-PROF-1), to 2.3×10^2 copies mL⁻¹ for BIO-PROF-1 in LDW. The ratio HAC/LAC was close to 1 in the subsurface layer and decreased abruptly with depth (Figure 5.6 A-B). Overall, HAC- dominated over LAC-*amoA* in the subsurface layer and intermediate waters (as ENACW-OMZ and MW), while LAC-*amoA* dominated the deep water masses LSW, ENADW and LDW.

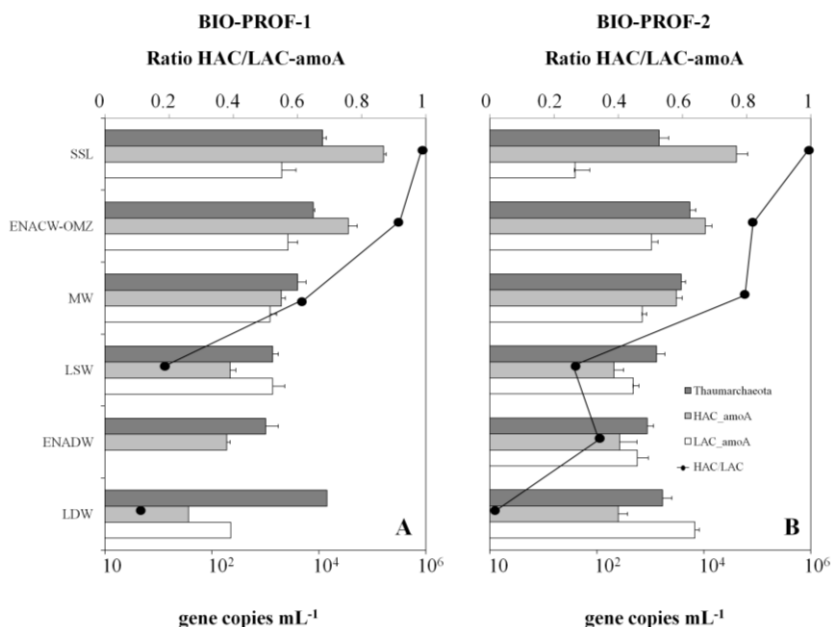


Figure 5.6. Vertical distribution of (A and B) archaeal *amoA* gene abundance obtained with the high-ammonia concentration primer set (HAC-*amoA*), with the low ammonia concentration primer set (LAC-*amoA*) and abundance of 16S rRNA gene of Marine Thaumarchaeota within the main water masses sampled during BIO-PROF-1 and BIO-PROF-2 cruise in the Finisterre section off the Galician coast (NW Iberian Peninsula). The ratio of high to low ammonia concentration *amoA* gene (HAC/LAC) is also shown.

5.4. Discussion

The notion on the relevance of dark DIC fixation in the ocean's global carbon cycle has progressively increased as DIC fixation rates were reported to be in the same order of magnitude as heterotrophic microbial production in the ocean's interior (Herndl et al. 2005; Reinthaler et al. 2010; Varela et al. 2011). Dark DIC fixation in the deep ocean represents a source of new organic matter potentially available for the deep water food web (Herndl and Reinthaler 2013). DIC fixation rates throughout the water column in the North Atlantic off the Galician coast are within the same order of magnitude as those previously reported for north Atlantic waters (Reinthaler et al. 2010; Baltar et al. 2010; Varela et al. 2011; Bergauer et al. 2013) and in the same range as microbial heterotrophic activity. DIC fixation and microbial heterotrophic production measured in this study were correlated (Spearman, $R=0.59$, $n=14$), which could be attributed on one side to the occurrence of DIC fixation by heterotrophs, via anaplerotic reactions, or to the stimulation of heterotrophic activity by newly produced organic matter. This could be associated with the presence of a variety of carboxylase genes involved in fatty acids biosynthesis, anaplerotic pathways or leucine catabolism (Alonso-Sáez et al. 2010).

The abundance and vertical distribution of the major prokaryotic groups (Bacteria and Archaea) were previously studied in this area (Guerrero-Feijóo et al. 2017), indicating that the contribution of Bacteria to the total prokaryotic community decreases from the euphotic zone to bathypelagic waters while the relative abundance of Thaumarchaeota increases with depth. Additionally, the contribution of the most abundant bacterial taxa to the total bacterial abundance was depth-specific, showing that the relative abundance of SAR11 and *Alteromonas* decreased with depth and the contribution of SAR202 and SAR324 was significantly higher in the deeper waters (Dobal-Amador et al. 2016). In the present study, dark DIC fixation of the bulk microbial community and of the most abundant deep-water bacterial phylotypes was determined by using the

MICRO-CARD-FISH approach. Chemolithoautotrophy of the SAR324 clade has been reported previously in mesopelagic waters (Swan et al. 2011). Off the Galician coast, the contribution of SAR324 to the bulk DIC fixation was high, particularly in the MW (Figure 5.5). SAR406 and *Alteromonas* were fixing DIC, although the contribution to bulk DIC fixation was 3-fold higher in SAR406 than in *Alteromonas*. The reason why SAR406 and *Alteromonas* take up DIC remains enigmatic, since the metabolic activity of both groups is poorly documented. Recent metagenomic analyses have found genes encoding different subunits of the carbon monoxide dehydrogenase associated with *Alteromonas* (Smedile et al. 2013). The high DIC uptake (particularly in the subsurface layers) by these taxa could be related to transporters of amino acids and TonB involved in the transport of carbohydrates (Baker et al 2013) and the availability of organic matter compounds easily degradable in the subsurface and upper mesopelagic waters off the Galician waters (Dobal-Amador et al. 2016; Guerrero-Feijóo et al. 2017), which might favor anaplerotic metabolism (Erb 2011; Sauer and Eikmanns 2005). In contrast to SAR406 and *Alteromonas*, most members of the SAR202 clade did not fix DIC or their activity was below the detection limit (see Figure 4.4). Although some members of the SAR 202 clade might be capable of fixing DIC (Yilmaz et al. 2016), previous studies indicated the heterotrophic lifestyle of SAR202 by utilizing recalcitrant as well as some labile organic compounds (Varela et al. 2008b; Landry et al. in press) which might explain the very low DIC uptake by SAR202 in this study (Figure 5.5 B).

Quantitative PCR data revealed that the vast majority of Thaumarchaeota in the dark waters off the Galician coast harbours the gene encoding the ammonia monooxygenase responsible for ammonia oxidation, and thus are likely chemolithoautotrophs. Early studies pointed towards the existence of different AOA clusters and their vertical segregation (Francis et al. 2005; Hallam et al. 2006) tentatively provoked by adaptation to low and high ammonia supply rates (Sintes et al. 2013). In agreement to the latter, our study also

found predominance of low ammonia concentration (LAC)-AOA in the dark waters off the Galician coast, likely related to very low energy supply as described by Sintes et al. (2013, 2015). In contrast, the high ammonia concentration (HAC)-AOA dominated the subsurface layer and upper mesopelagic (ENACW-OMZ and MW) waters off the Galician coast (Figure 4.6), indicated by their negative correlation with depth (Spearman, $R=-0.51$, $p<0.05$, $n=59$) and the positive correlation with high nitrite concentrations (Spearman, $R=0.33$, $p<0.05$, $n=59$). Additionally, the abundance of Thaumarchaeota and the HAC-amoA ecotype were positively related to DIC fixation rates (Spearman, $R=0.39$, $p<0.005$, $n=59$ and $R=0.71$, $p<0.0001$, $n=59$, respectively) suggesting, that potentially, the HAC-AOA might oxidize aerobically ammonia to fix inorganic carbon. Our results agree with previous findings showing that only a fraction of the AOA community oxidize ammonia (Smith et al. 2016), while the LAC-AOA might be utilizing other substrates (Smith et al. 2016). However, our work highlight the low contribution of Thaumarchaeota to the bulk DIC fixation compared to that of Bacteria, particularly in the subsurface layer and upper mesopelagic waters (SSL, ENACW-OMZ).

Overall, our results indicate that heterotrophic and autotrophic microbial production are in the same order of magnitude with dark DIC fixation mediated by a diverse group of microbes in the meso- and bathypelagic waters of the North Atlantic waters off the Galician coast. Also, we have shown that DIC fixation varies markedly with depth and among specific microbial groups. Additionally, evidence has been presented that two depth-specific ecotypes of thaumarchaeal genes of the amoA subunit encoding ammonia monooxygenase with presumably different substrate affinities are present. However, chemolithoautotrophic Bacteria are apparently responsible for the high DIC fixation rates measured in the North Atlantic.



Chapter 6

Conclusions

The **main conclusions** of this PhD thesis are:

1. Microbial (Archaea and Bacteria) abundance, activity, community composition and structure in the Atlantic ocean off the Galician coast are depth-stratified.
2. The mean microbial abundance in mesopelagic and bathypelagic waters is $\approx 25\%$ and $\approx 7\%$, respectively, of the mean prokaryotic abundance in the epipelagic waters. Microbial heterotrophic production decreases by 4 orders of magnitude from epipelagic to the bathypelagic layers, whereas autotrophic activity decreases only one order of magnitude with depth.
3. Bacteria are more abundant than Archaea throughout the water column. The relative abundance of SAR324 and SAR406 obtained with CARD-FISH and 454-pyrosequencing is similar. By contrast, SAR11 abundance seems to be overestimated while SAR202 and *Alteromonas* are underestimated with 454-pyrosequencing as compared to CARD-FISH.
4. Labile (FDOM-T) and refractory DOM (FDOM-M) compounds are the main DOM variables associated to the vertical stratification of microbial communities. SAR406, SAR202 and Rickettsiales are strongly positively related with refractory compounds, whereas Flavobacteriaceae, Rhodobacteraceae, Nitrospinaceae or SAR11 are linked to labile DOM compounds.
5. The different components of CDOM at 254, 340 and 365nm exhibit marked vertical variations. Nitrospinaceae is significantly linked to aCDOM₃₄₀, while Mariprofundaceae and Gemmatimonadetes correlate with aCDOM₃₆₅, suggesting that bacterial communities inhabiting deeper waters metabolize DOM with a higher degree of aromaticity.
6. Overall, Euryarchaeota-MGIII and Thaumarchaeota-MGI members inhabiting the bathypelagic realm are related to

refractory compounds and DOM with high degree of aromaticity, respectively. However, the archaeal communities inhabiting the intermediate waters are related to labile compounds.

7. Changes in bacterial activity and community composition in response to size-fractionated-DOM are associated to variations in optical properties of DOM.

8. High- and low- molecular weight DOM (H+L-DOM) provides more bioavailable organic compounds for bacterial communities than low molecular weight fraction of DOM (LMW-DOM) alone. However, LMW-DOM supports higher microbial diversity as compared to H+L-DOM.

9. Colwelliaceae, Shewanellaceae and Oleiphilaceae are selectively stimulated by H+L-DOM and are strongly linked with protein-like fluorescence, suggesting their preference for labile substances. Alternatively, Flavobacteriaceae, Rhodospirillales and Rhodobacteraceae increase their relative contribution to the microbial community in the LMW-DOM treatment, and are connected with refractory compounds.

10. Dark chemolithoautotrophic activity is mediated by a diverse group of microbes, with Bacteria, particularly SAR406, SAR324 and *Alteromonas* showing the highest percentage of actively uptaking inorganic carbon cells.

11. The distribution of two ecotypes of ammonia oxidizing Thaumarchaeota, harbouring low- and high- ammonia concentration of monooxygenase gene (LAC- and HAC-*amoA*, respectively) suggests widespread potential chemolithoautotrophic activity of this group. However, the contribution of Thaumarchaeota cells to the bulk dissolved inorganic carbon (DIC) uptaking cells was lower than that of bacteria.



Spanish summary / Resumen en español

1. Introducción

Los océanos cubren el 70% de la superficie de la Tierra y proporcionan el mayor hábitat para los organismos vivos, en particular para los microorganismos. Estos microorganismos marinos habitan tanto en las aguas superficiales como en las aguas más profundas y abisales del océano. El término “microorganismo” hace referencia a los organismos que son invisibles al ojo humano e incluye a los virus y miembros de los dominios Archaea, Bacteria y Eukarya.

Las arqueas y bacterias (Madigan et al. 2006) son organismos unicelulares (procariotas) que no difieren en apariencia morfológica (las bacterias poseen lípidos de membrana diferentes de las arqueas) pero presentan un amplio espectro de metabolismos. Estos microorganismos son un importante componente del plancton pelágico marino, contribuyendo más del 70% a la biomasa total del océano (Furhman et al. 1989) y $\approx 50\%$ a la actividad total (Aristeguí et al. 2009). La abundancia de los organismos procariotas (Bacteria y Archaea) desciende exponencialmente entre uno y dos órdenes de magnitud desde las aguas superficiales hasta las profundas (Aristeguí et al. 2009) y su distribución vertical presenta un patrón inverso. Mientras que las arqueas aumentan con la profundidad, las bacterias son más abundantes en la superficie. Adicionalmente, también se ha encontrado que la composición taxonómica de ambos dominios varía con la profundidad (Karner et al. 2001; Teira et al. 2006a; Varela et al. 2008ab; Dobal-Amador et al. 2016; Guerrero-Feijóo et al. 2017).

Los microorganismos desempeñan un papel crucial en los ciclos biogeoquímicos marinos produciendo materia orgánica y oxígeno necesario para sostener la vida, así como el almacenamiento, transporte y la renovación de los elementos biológicos clave (Falkowski et al. 2008). La tradicional división clásica de los ecosistemas marinos, basada por un lado en organismos productores de materia orgánica mediante autotrofia y por otro en consumidores de esta producción, debe reconsiderarse. Así por ejemplo, trabajos recientes han descubierto que diversos grupos de bacterioplancton usan la luz (Gomez-Consarnau et al. 2007) para sobrevivir cuando hay poca materia orgánica disponible. Por otro lado, en el océano profundo se ha descubierto la fijación de carbono inorgánico disuelto por parte de Bacteria y Crenarchaea (Varela et al. 2011; Swan et al. 2011). Así durante años se pensó que el océano profundo era un depósito de diversidad latente con baja actividad pero ahora sabemos que algunos grupos microbianos son más activos de lo que se pensaba.

La bomba biológica comienza en superficie donde el plancton autotrófico utiliza la luz para convertir CO₂ en carbono orgánico particulado produciendo biomasa. Este nuevo material puede seguir dos vías: (i) una considerable fracción es remineralizada en las aguas superficiales del océano y/o (ii) ser exportado al océano profundo entrando así en el denominado “bucle microbiano”, donde es remineralizado lentamente por diferentes procesos (Azam et al. 1983; Ducklow et al. 2001) y sirve como substrato para las poblaciones de microbios que habitan las aguas profundas (Azam et al. 1983; Ducklow and

Carlson 1992). Estudios recientes han descubierto que la estructura y funcionamiento de las comunidades microbianas marinas no sólo está relacionada con los factores físico-químicos sino que también con la calidad y cantidad de MOD (materia orgánica disuelta) (Cottrell and Kirchman 2000; Kirchman et al. 2004; Dobal-Amador et al. 2016; Guerrero-Feijóo et al. 2017). Sin embargo, esta materia orgánica sedimentada no es suficiente para satisfacer la demanda de carbono de los microorganismos del océano oscuro (Baltar et al. 2009), sugiriendo que la fracción de carbono inorgánico que fijan los microorganismos quimiolitotóxicos podría representar una fuente significativa de suministro de carbono autóctono en el océano profundo (Herndl and Reinthaler, 2013).

Los organismos quimiolitotóxicos oxidan amonio (Wuchter et al. 2006), urea (Alonso-Sáez et al. 2012) o azufre (Agogué et al. 2008; Baltar et al. 2016) para generar la energía necesaria para la fijación de CID (carbono inorgánico disuelto). Se han medido tasas de fijación de CID en el océano del mismo orden de magnitud que las de la actividad heterotrófica (Reinthaler et al. 2010; Varela et al. 2011). Este reciente descubrimiento, sumados al amplio espectro de distribución de arqueas en los ambientes marinos (DeLong 1998) han sugerido que la oxidación de amonio por las arqueas podría contribuir sustancialmente a explicar las elevadas tasas de fijación de CID del océano (Wuchter et al. 2006; Sintès et al. 2013). También se ha confirmado el consumo de CID por grupos de bacterias específicos (Swan et al. 2011; Guerrero-Feijóo et al. aceptado) que puede ser relevante para un amplio rango de filotipos

microbianos, incluyendo tanto grupos autotróficos como heterotróficos. Estos últimos podrían contribuir a las tasas de fijación de CID medidas a través de reacciones anapleróticas.

Trabajos recientes han encontrado que los microorganismos marinos representan el grupo biológico más importante en términos de diversidad filogenética y funcional (Sunagawa et al. 2015; Salazar et al. 2016). Tradicionalmente, el estudio de la diversidad estuvo limitado por el desarrollo tecnológico. Así, antes de la era “ómica” era típico tener información únicamente de los microorganismos cultivables, que representan menos del 1% de la diversidad total de las comunidades microbianas. En la década de los 90, las técnicas de huella dactilar, que necesitan de una extracción previa de ADN, permitieron obtener perfiles de la estructura de las comunidades microbianas (Singh et al 2006; Sun et al 2012; Dorst et al 2014). Entre ellas cabe destacar el análisis del polimorfismo en la longitud de fragmentos de restricción terminales (T-RFLP) (Moeseneder et al. 2001) y análisis automático del espaciador intergénico ribosomal (ARISA) (Borneman and Triplett 1997). Estas técnicas tienen regiones diana diferentes en el ADN de los microorganismos. ARISA tiene diana en la región del espaciador intergénico (ITS), que es más variable que el gen rRNA, en la que tiene diana la técnica de T-RFLP (Brown and Furhman 2005). Las ventajas de estas técnicas es que son robustas, altamente reproducibles y lleva poco tiempo obtener resultados, pero la principal desventaja es su falta de resolución para identificar qué grupo microbiano corresponde a cada unidad taxonómica operacional (OTU), así como su abundancia relativa (Bent and Forney 2008). Las técnicas de

secuenciación masiva han supuesto un avance importante, ya que determinan una gran diversidad filogenética microbiana a partir del ADN genómico de una muestra ambiental. A su vez, estas técnicas han evolucionado desde el método Sanger hasta métodos de secuenciación más baratos como pirosecuenciación-454 (Venter et al. 2004) y más recientemente Illumina (Singh et al. 2009). Estas metodologías nos permiten determinar la abundancia relativa de las comunidades microbianas, tanto los filotipos más abundantes como los más raros (Sogin et al. 2006; Huber et al. 2007), así como su identificación taxonómica. En esta tesis doctoral se utilizó el método de pirosecuenciación-454 para el estudio de la diversidad microbiana.

También existen técnicas cuantitativas con un alto poder de resolución, como PCR cuantitativa (qPCR), utilizada para amplificar y simultáneamente cuantificar de forma absoluta el producto de la amplificación de ADN de una muestra ambiental por fluorescencia. Por último, otra técnica cuantitativa, y la cual no requiere extracción de ADN, es la hibridización in situ fluorescente utilizada con sondas específicas (FISH por sus siglas en inglés Fluorescence in Situ Hybridization) (DeLong et al. 1989; Amann et al. 1990). Esta técnica fue mejorada debido a un problema de especial relevancia en los ecosistemas acuáticos, donde el pequeño tamaño y el crecimiento lento de los microorganismos subestiman la intensidad de la señal. Esta detección fluorescente se mejoró por la amplificación de la señal con tiramida, conocida como deposición catalizada (CARD-FISH) (Pernthaler et al. 2002), incrementando entre 10-20 veces la intensidad de la señal. Esta técnica puede ser combinada con

autoradiografía (MICRO-CARD-FISH) para estudiar las diferentes capacidades metabólicas de grupos específicos de comunidades microbianas. Gracias a este método, numerosos estudios han demostrado la incorporación de diferentes compuestos (tales como aminoácidos) por grupos específicos microbianos. Algunos resultados obtenidos por esta técnica muestran heterogeneidad en los patrones de actividad microbiana (Ouverney and Furhman 1999; Cottrell and Kirchman 2003; Teira et al. 2004) y más recientemente la capacidad quimilotoautotrófica de las arqueas y bacterias (Varela et al. 2011; Swan et al. 2011; Guerrero-Feijóo et al. aceptado).

Las interacciones entre los microorganismos y la MOD dependen de la bio-disponibilidad de la MOD, que varía desde altamente disponible (escalas de tiempo cortas minutos-días) hasta refractarias (escalas de tiempo largas siglos-milenios) (Williams and Druffel, 1987; Bauer et al 1992). Hay dos aspectos importantes a destacar que se han incluido en esta tesis doctoral con el fin de estudiar las interacciones entre microorganismos y la MOD, que son sus propiedades ópticas y/o el peso o tamaño molecular. Las propiedades ópticas de MOD son esenciales para determinar tanto la cantidad como la calidad del material orgánico utilizado como sustrato por los microorganismos. La MOD comprende una fracción coloreada conocida como MOD coloreada (del inglés CDOM; Coble, 1996), que absorbe a diferentes longitudes de onda en el visible y ultravioleta. Además, una fracción del CDOM puede emitir fluorescencia azul cuando es irradiada por luz ultravioleta CDOM fluorescente (FDOM; Coble 1996, 2007), dando lugar a sustancias que son

características de aminoácidos (Coble, 1996) y húmicas que son consideradas fotolábiles y biorefractarias (Chen and Bada 1992; Nieto et al. 2006). Los cambios en FDOM indican que hay procesos biológicos (Chen and Bada 1992; Nieto-Cid et al. 2006) y químicos (Moran et al. 2000; Nieto-Cid et al. 2006) actuando sobre la MOD. Operacionalmente, la MOD puede clasificarse por su peso molecular en alto (HMW-DOM, del inglés high molecular weigh-dissolved inorganic matter) o bajo peso molecular (LMW-DOM, del inglés low molecular weight-dissolved inorganic matter) que pueden influir en su bio-disponibilidad para las comunidades microbianas (Amon and Benner 1994; Khodse and Bhosle 2011; Benner and Amon, 2015). La diversidad y composición de la MOD es una de los principales factores ambientales que determinan la composición de la comunidad microbiana y, a su vez, el ciclo del carbono marino (Alonso-Sáez et al. 2007; Dobal-Amador et al. 2016; Guerrero-Feijóo et al. 2017).

El **principal objetivo** de esta tesis doctoral es profundizar en el conocimiento sobre la variabilidad vertical de la abundancia, la actividad (heterotrófica y autotrófica) y la composición taxonómica de la comunidad microbiana en relación con la concentración y composición elemental y molecular de la materia orgánica en las aguas epi-, meso- y batipelágicas cercanas a la costa Gallega (NO Península Ibérica).

Los **objetivos específicos** de esta tesis doctoral fueron:

(Capítulo 3) Estudiar el papel de la calidad y cantidad de la DOM en relación a la estructura de la comunidad de Archaea en comparación con la de Bacteria. Para ello se aplicó un método de regresión multivariada basada en matrices de similitud y permutaciones (DISTLM, del inglés distance-based linear models) que permitió estudiar las asociaciones entre las diferentes propiedades ópticas de la DOM y la estructura de la comunidad de Archaea y Bacteria obtenidas por T-RFLP y ARISA, respectivamente. Además, se aplicó un análisis de redundancia (RDA, del inglés redundancy analysis) para estudiar la asociación entre los diferentes índices de la MOD y grupos específicos de microorganismos obtenidos por pirosecuenciación-454.

(Capítulo 4) Evaluar la respuesta de las bacterias heterótrofas a la degradabilidad de materia orgánica disuelta filtrada y fraccionada por clases de tamaño. Para ello, se aisló una comunidad microbiana natural de agua mediterránea (1000 m de profundidad) y se evaluó la respuesta a la degradabilidad de MOD de bajo peso molecular (LMW-DOM) y la combinación de alto y bajo peso molecular (H+L-DOM). Durante 6 días se midió la abundancia y producción bacteriana en paralelo con las propiedades ópticas de la MOD, y estos parámetros se relacionaron con los cambios en la composición de la comunidad.

(Capítulo 5) Estudiar la actividad quimiolitotrófica de las comunidades microbianas, ya que se ha observado que es sustancialmente mayor de lo que se suponía hasta ahora, representando una fuente significativa de suministro de carbono

autóctono en el océano profundo. Mediante la combinación de la microautoradiografía con CARD-FISH, se ha investigado la actividad de varios grupos microbianos en la fijación oscura de CID. Se ha encontrado que la fijación oscura de CID está ampliamente distribuida entre diferentes grupos bacterianos, lo que sugiere una contribución significativa de las bacterias a la quimiolitotrofia global del océano oscuro.

2. Metodología

La estrategia de muestreo consistió en medidas “in situ” en dos campañas oceanográficas, BIO-PROF-1 (agosto 2011) y BIO-PROF-2 (septiembre 2012) y una aproximación experimental llevada a cabo durante la campaña oceanográfica MODUPLAN (agosto 2014) en un transecto perpendicular a la costa Gallega (NO de la Península Ibérica), caracterizado por una dinámica hidrográfica marcada por pulsos de afloramiento estacionales. En BIO-PROF-1 y BIO-PROF-2 se muestrearon verticalmente 22 y 21 estaciones, respectivamente, desde la superficie hasta >5000 m de profundidad y se obtuvieron perfiles verticales de temperatura, salinidad y oxígeno. Para la aproximación experimental llevada a cabo durante la campaña MODUPLAN se muestreó la profundidad de 1000 m de la estación 11.

Este estudio incluyó una aproximación multidisciplinar, en la que se caracterizaron variables ambientales (incluyendo variables físicas, químicas y biológicas) y el estudio de la variabilidad vertical en la abundancia, estructura y composición de las comunidades microbianas. Aplicamos una variedad de herramientas moleculares para estudiar la estructura de la

comunidad microbiana y su diversidad, incluyendo técnicas de análisis de huella genética ARISA y T-RFLP (Capítulo 3), pirosecuenciación (Capítulo 3 y 4), CARD-FISH (Capítulo 3 y 5), MICRO-CARD-FISH (Capítulo 5) y qPCR (Capítulo 5).

3. Patrón vertical de las propiedades ópticas de la materia orgánica en relación con las comunidades de Archaea y Bacteria en el océano del Atlántico Norte

Se estudió la abundancia, actividad y composición de la comunidad microbiana en las aguas eufóticas, intermedias y profundas de la costa de Galicia (NO de la Península Ibérica) en relación con la caracterización óptica de la materia orgánica disuelta (DOM). La estructura de las comunidades microbianas (Archaea y Bacteria) estuvo verticalmente estratificada. Entre la comunidad de Archaea, Euryarchaeota, y especialmente Thermoplasmata, dominó las aguas intermedias y su abundancia disminuía en profundidad, mientras que Thaumarchaeota, especialmente Grupo Marino I, fue el más abundante en las aguas profundas. La comunidad de bacterias estuvo dominada por el filo Proteobacteria en toda la columna de agua. No obstante, la presencia de Cyanobacteria y Bacteroidetes fue relevante en las aguas superficiales, mientras que SAR202 fue relativamente más abundante en las aguas más profundas. Tanto la composición microbiana como la abundancia no estuvieron significativamente correlacionadas con la cantidad de carbono orgánico disuelto, sin embargo revelaron fuertes conexiones con la calidad de la materia orgánica. La comunidad de Archaea estuvo

162

principalmente asociada con la fluorescencia de la MOD (sugiriendo respiración de MOD lábil y generación de compuestos refractarios), mientras que la comunidad de bacterias estuvo fuertemente asociada a la aromaticidad/edad de la MOD producida en la columna de agua. En resumen, nuestros datos indican que la composición de las comunidades microbianas se asocia con la composición de la MOD de cada masa de agua, sugiriendo que distintos taxones microbianos consumen y/o producen compuestos específicos de MOD.

4. Cambios en la actividad y composición de la comunidad bacteriana en respuesta al fraccionamiento por tamaños de la materia orgánica disuelta

Las bacterias heterotróficas juegan un papel fundamental en el reciclado de materia orgánica disuelta (MOD) de origen marino. Sin embargo, nuestra comprensión de las interacciones entre microorganismos y la MOD es limitada. En esta investigación, se estudió la respuesta de las bacterias a la degradabilidad de la MOD filtrada y fraccionada por clases de tamaño y la relación con sus propiedades ópticas. Para ello, se aisló una comunidad bacteriana del agua mediterránea (1000 m de profundidad) y se cultivó en (i) de agua prefiltrada por 0.1 μm (comunidad endógena bacteriana), (ii) materia orgánica de bajo peso molecular (LMW-DOM, por sus siglas en inglés low molecular weight) y (iii) la combinación de las fracciones de materia orgánica de alto y bajo peso molecular (H+L-DOM, por

sus siglas en inglés high + low molecular weight). La abundancia y actividad bacteriana fue consistentemente mayor en el tratamiento de H+L-DOM que en LMW-DOM al final del experimento, sugiriendo una diferente biodisponibilidad de las fracciones de MOD. Además, la composición de la comunidad bacteriana en los diferentes tratamientos experimentales varió debido a la exposición a diferentes fracciones de MOD. Colwelliaceae, Shewanellaceae y Oleiphilaceae fueron selectivamente estimuladas por el tratamiento de H+L-DOM. Estos resultados, asociados a la fluorescencia de las sustancias de origen proteico, sugieren su preferencia por las sustancias lábiles. Alternativamente, Flavobacteriaceae, Rhodospirillales y Rhodobacteraceae aumentaron relativamente en el tratamiento de LMW-DOM en comparación con los demás tratamientos (CONTROL y H+L-DOM). Nuestros resultados sugieren que el fraccionamiento por tamaños de la MOD, asociado a los cambios en las propiedades ópticas de la misma en los diferentes tratamientos, estimuló grupos bacterianos específicos.

5. Tasas elevadas de fijación de carbono inorgánico por microbios quimiolitotópicos en la costa gallega (NO de la Península Ibérica)

Se determinaron las tasas de fijación de carbono inorgánico disuelto (CID) y se compararon con la producción microbiana heterotrófica en aguas subsuperficiales, meso- y batipelágicas en la costa gallega (NO de la Península Ibérica). Las tasas de fijación de CID fueron más altas que la actividad heterotrófica en toda la columna de agua, sin embargo, fueron más

prominentes en las aguas batipelágicas. La microautoradiografía combinada con CARD-FISH (MICRO-CARD-FISH) nos permitió identificar varios grupos microbianos implicados en el consumo de CID. La contribución de SAR406 (Marinimicrobia), SAR324 (Deltaproteobacteria) y Alteromonas (Proteobacteria) a la fijación oscura de CID fue significativamente más elevada que para SAR202 (Chloroflexi) y/o Thaumarchaeota, de acuerdo con su contribución a la abundancia microbiana. La utilización de la técnica cuantitativa de PCR (qPCR) del gen que codifica la subunidad A de la enzima monooxigenasa del amonio (amoA) de dos ecotipos de Thaumarchaeota reveló patrones diferentes de distribución de ambos ecotipos en las aguas oceánicas del Atlántico Norte. En conjunto, nuestros resultados indican que la quimiolitotoautotrofia se da de forma generalizada entre los microorganismos del océano oscuro, particularmente en las aguas batipelágicas. Esta producción de biomasa quimiolitotoautotrófica en el océano oscuro, donde la materia orgánica bio-disponible es reducida, puede desempeñar un papel importante en el mantenimiento de las redes tróficas del océano profundo.

6. Conclusiones

Las principales conclusiones de esta tesis son:

1. La abundancia (Archaea and Bacteria), actividad, estructura y composición de las comunidades microbianas de las aguas oceánicas de Galicia está estratificada con la profundidad.

2. En promedio, la abundancia microbiana en las aguas mesopelágicas es $\approx 25\%$ de la abundancia procariota en las aguas epipelágicas y $\approx 7\%$ de la abundancia en las aguas batipelágicas. La producción microbiana heterotrófica desciende en 4 órdenes de magnitud desde las aguas epipelágicas hasta las más profundas, mientras que la actividad quimiolitotrófica desciende en un orden de magnitud con la profundidad.

3. Bacteria es más abundante que Archaea en toda la columna de agua. La abundancia relativa de SAR324 y SAR406 obtenida por CARD-FISH y 454-pirosecuenciación es similar. Sin embargo, la abundancia de SAR11 parece estar sobreestimada con pirosecuenciación-454 en comparación con el CARD-FISH. Por el contrario, SAR202 y *Alteromonas* fueron infraestimados usando pirosecuenciación comparativamente con CARD-FISH.

4. Los compuestos lábiles (FDOM-T) y refractarios (FDOM-M) son las principales variables asociadas a la estratificación vertical de las comunidades microbianas. SAR406, SAR202 y Rickettsiales revelaron fuertes correlaciones positivas con los componentes refractarios mientras que Flavobacteriaceae, Rhodobacteraceae, Nitrospinaceae y SAR11 están relacionados a los compuestos lábiles de la MOD.

5. Las diferentes fluorescencias de la MOD, CDOM a 254, 340 y 365 nm, exhibieron variaciones verticales muy marcadas. Nitrospinaceae estuvo significativamente asociado a aCDOM₂₅₄, mientras Mariprofundaceae and Gemmatimonadetes estuvieron significativamente correlacionados con aCDOM₃₆₅, sugiriendo

que las comunidades de bacterias que habitan las aguas más profundas metabolizan MOD con mayor grado de aromaticidad.

6. En general, las comunidades de Archaea que habitan las aguas más profundas, Euryarchaeota-MGIII y Thaumarchaeota-MGI, estuvieron correlacionadas con compuestos refractarios y MOD con alto grado de aromaticidad, respectivamente. Sin embargo, las comunidades de Archaea que habitan aguas intermedias estuvieron relacionadas con los compuestos lábiles.

7. Los cambios en la actividad y composición de las comunidades bacterianas en respuesta al fraccionamiento por tamaños de la MOD estuvieron correlacionados con variaciones en el espectro de propiedades ópticas de MOD después del procesamiento microbiano.

8. El tratamiento donde ambas fracciones de MOD estuvieron presentes, alto y bajo peso molecular (H+L-DOM), sostuvo compuestos orgánicos más biodisponibles para las comunidades de bacterias que la fracción de bajo peso molecular (LMW-DOM). No obstante, el tratamiento LMW-DOM presentó mayor diversidad que el tratamiento HMW-DOM.

9. Colwelliaceae, Shewanellaceae y Oleiphilaceae estuvieron selectivamente estimulados por H+L-DOM y mostraron una fuerte correlación con la fluorescencia proteica, lo que sugiere preferencia por sustancias muy lábiles. Alternativamente, el crecimiento de Flavobacteriaceae, Rhodospirillales y

Rhodobacteraceae en el tratamiento de LMW-DOM estuvo principalmente asociado a compuestos refractarios.

10. La actividad chemolitoautotrófica está mediada por un diverso grupo de microorganismos, especialmente Bacteria (en particular, SAR406, SAR324 y Alteromonas), mostrando el mayor porcentaje de células activas consumiendo carbono inorgánico.

11. Los dos ecotipos de Thaumarchaeota, de baja y alta afinidad por el gen de oxidación de amonio (LAC-/HAC-amoA, respectivamente) indicaron el potencial de la actividad quimiolitoautotrófica de este grupo. Sin embargo, la contribución de Thaumarchaeota a la fijación de carbono inorgánico disuelto (CID) fue menor que Bacteria.



Appendix

Chapter 3:

Supplementary Table 3.1. Probe sequences and formamide concentrations used for CARD-FISH analysis.

| Probe | Organism | Sequence (5' → 3') | FA* (%) | Reference |
|--------------|------------------|---------------------------|----------------|-----------------------|
| NON338 | Negative control | ACTCCTACGGGAGGCAGC | 55 | (Wallner et al. 1993) |
| Cren357 | Thaumarchaeota | TGACCACTTGAGGTGCTG | 20 | (Teira et al. 2004) |
| EUB338 I | Bacteria | GCTGCCCTCCCCTAGGAGT | 55 | (Amann et al. 1990) |
| EUB338 II | Bacteria | GCAGCCACCCCGTAGGTGT | 55 | (Daims et al. 1999) |
| EUB338 III | Bacteria | GCTGCCACCCCGTAGGTGT | 55 | (Daims et al. 1999) |

*Formamide (FA) concentration in percent of hybridization buffer

Supplementary Table 3.2. Values of Chao1 index richness for Archaea and Bacteria throughout the water column.

| Water masses | Archaea | Bacteria |
|--------------|---------|----------|
| EZ | 117 | 330 |
| ENACW-OMZ | 414 | 638 |
| MW | 57 | 422 |
| LSW | 45 | 476 |
| ENADW | 41 | 405 |
| LDW | 51 | 222 |

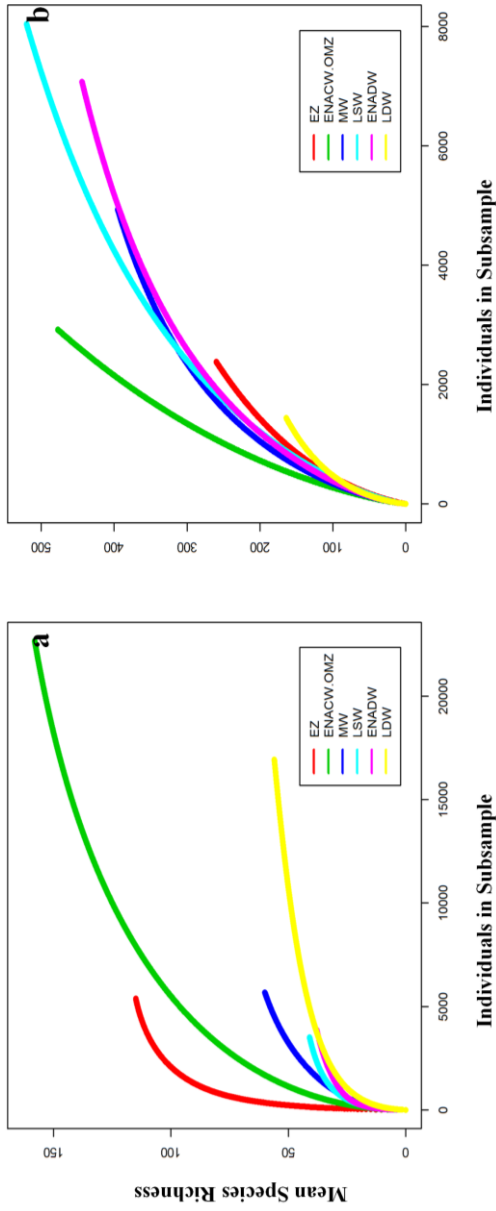
Supplementary Table 3.3. Marginal test parameters obtained for the relationship between the DOM-related variables and the archaeal community composition. P: represents the significance level; % Var.: the fraction of the variation in the community explained by each independent variable.

| Variables | Pseudo-F | P | %Var. |
|-----------|----------|--------------|-------|
| DOC | 4.4156 | 0.001 | 8.76 |
| FDOM-T | 4.9448 | 0.001 | 9.71 |
| FDOM-M | 7.1726 | 0.001 | 13.49 |
| aCDOM254 | 4.2841 | 0.001 | 8.52 |
| aCDOM340 | 1.7986 | 0.082 | 3.76 |
| aCDOM365 | 0.8652 | 0.548 | 1.85 |

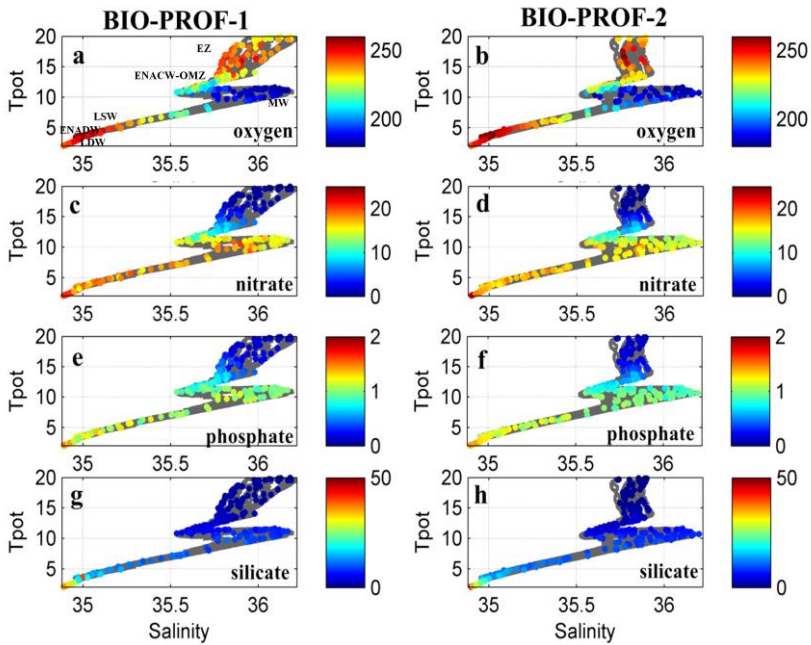
| | | | |
|--------------|--------|--------------|------|
| sCDOM275-295 | 2.3068 | 0.020 | 4.78 |
| Depth | 4.4522 | 0.001 | 8.82 |

Supplementary Table 3.4. Marginal test parameters obtained for the relationship between the DOM-related variables and the bacterial community composition. P: represents the significance level; % Var.: the percentage of variation explained by each independent variable.

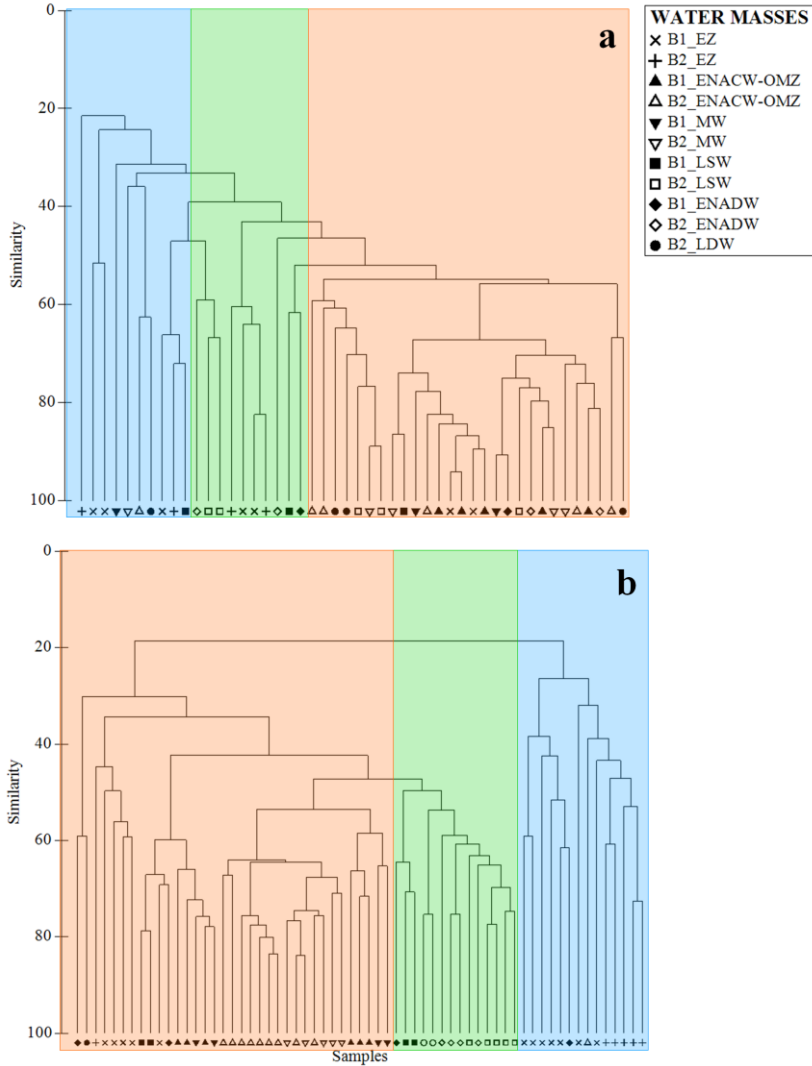
| Variables | Pseudo-F | P | %Variation |
|------------------|-----------------|--------------|-------------------|
| DOC | 7.123 | 0.001 | 10.46 |
| FDOM-T | 6.2658 | 0.001 | 9.32 |
| FDOM-M | 10.541 | 0.001 | 14.73 |
| aCDOM254 | 5.4039 | 0.001 | 8.14 |
| aCDOM340 | 3.6261 | 0.003 | 5.61 |
| aCDOM365 | 3.2062 | 0.005 | 4.99 |
| sCDOM275-295 | 2.4193 | 0.020 | 3.81 |
| Depth | 7.3835 | 0.001 | 10.80 |



Supplementary Figure 3.1.1. Rarefaction analyses of the archaeal (a) and bacterial (b) 16S rRNA gene sequences clustered at 97% similarity.



Supplementary Figure 3.2. Potential temperature (Tpot, °C) - salinity diagrams every 2 dbars for the BIOPROF-1 (Left) and BIOPROF-2 (Right), with superimposed values from discrete depths of: (a, b) dissolved oxygen; (c, d) nitrate; (e, f) phosphate; (g, h) silicate. All in $\mu\text{mol kg}^{-1}$.

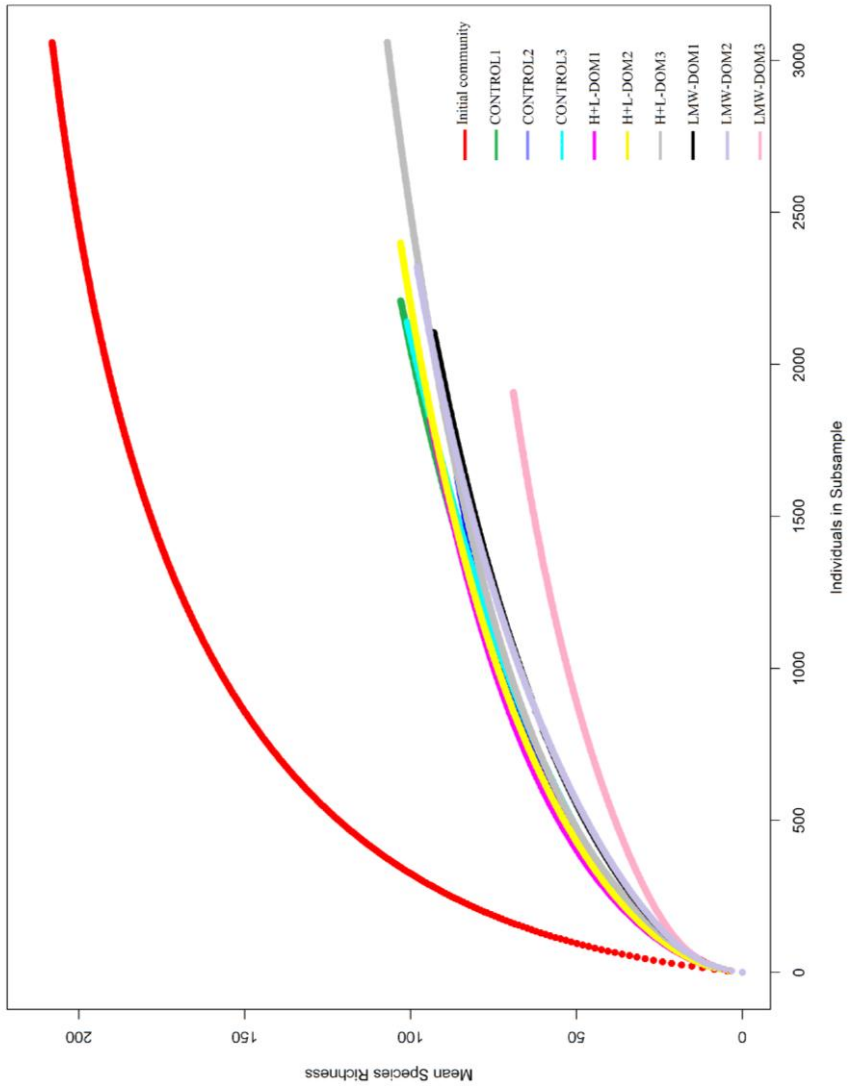


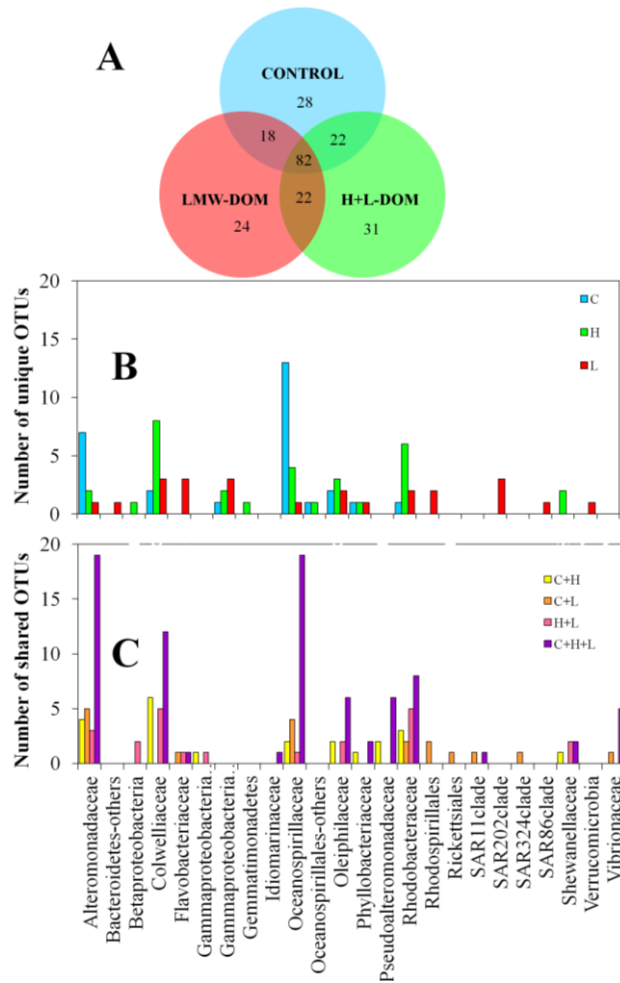
Supplementary Figure 3.3. Cluster analysis based on the Bray Curtis similarity matrix obtained by (a) T-RFLP and (b) ARISA fingerprinting of archaeal and bacterial communities, respectively. For watermass abbreviations see Table 1. B1: BIO-PROF-1 cruise and B2: BIO-PROF-2 cruises.

Chapter 4:

Supplementary Table 4.1. Change in the average (triplicate experiments) concentration of nitrate+nitrite ($\text{NO}_3^- + \text{NO}_2^-$) and phosphate (PO_4^{3-}) in the environmental initial community and in the different treatments at the end of the experiment. The treatments were: 0.1 μm filtered seawater (CONTROL), low molecular weight DOM fraction (LMW-DOM) and the combination of low and high molecular weight DOM fractions at the original ratio (H+L-DOM). Three replicates were measured at each time point.

| Treatment | $\text{NO}_3^- + \text{NO}_2^-$ (μM) | PO_4^{3-} (μM) |
|-----------|--|---|
| CONTROL | -0.23 ± 0.05 | -0.03 ± 0.02 |
| H+L-DOM | -0.24 ± 0.09 | -0.03 ± 0.02 |
| LMW-DOM | 0.18 ± 0.10 | 0.01 ± 0.04 |





Supplementary Figure 4.2. Changes in the bacterial community composition excluding the initial community: (A) Venn diagram showing the number of unique and shared OTUs between treatments, (B) number and taxonomy of unique OTUs in CONTROL, H+L-DOM and LMW-DOM and (C) number and taxonomy of shared OTUs between treatments. Abbreviations: C, CONTROL; H, H+L-DOM; L, LMW-DOM; C+H, CONTROL + H+L-DOM, C+L; CONTROL + LMW-DOM, H+L, H+L-DOM + LMW-DOM, C+H+L, CONTROL + H+L-DOM + LMW-DOM.



References

- Agogué H, Lamy D, Neal PR, et al. (2011) Water mass-specificity of bacterial communities in the North Atlantic revealed by massively parallel sequencing. *Mol Ecol* 20: 258-278.
- Agogué H, Brink M, Dinasquet J, Herndl GJ (2008) Major gradients in putatively nitrifying and non-nitrifying *Archaea* in the deep North Atlantic. *Nature* 456: 788-791.
- Alonso-Sáez L, Waller AS, Mende DR, et al. (2012) Role for urea in nitrification by polar marine *Archaea*. *Proc Natl Acad Sci USA* 109: 17989-17994.
- Alonso-Sáez L, Galand PE, Casamayor EO, et al. (2010) High bicarbonate assimilation in the dark by Arctic bacteria. *ISME J* 4: 1581-1590.
- Alonso-Sáez L, Gasol JM (2007) Seasonal variations in the contributions of different bacterial groups to the uptake of low-molecular-weight compounds in Northwestern Mediterranean Coastal Waters. *Appl Environ Microbiol* 73: 3528-3535.
- Álvarez-Salgado XA, Miller AEJ (1998) Simultaneous determination of dissolved organic carbon and total dissolved nitrogen in seawater by high temperature catalytic oxidation: conditions for precise shipboard measurements. *Mar Chem* 62: 325–333.
- Alonso C, Pernthaler J (2006) *Roseobacter* and SAR11 dominate glucose uptake in coastal North Sea waters. *Environ Microbiol* 8:2022-2030.
- Amman RI, Binder BJ, Olson RJ et al. (1990) Combination of 16S rRNA-targeted oligonucleotide probes with flow cytometry for analyzing mixed microbial populations. *App Environ Microbiol* 56: 1919- 1925.

References

- Amon RMW (2016) Carbon cycle: Ocean dissolved organics matter. *Nat Geosci* 9: 864-865.
- Amon RMW, Benner R (1996) Bacterial utilization of different size classes of dissolved organic matter. *Limnol Oceanogr* 41:41-51.
- Amon RMW, Benner R (1994) Rapid cycling of high-molecular-weight dissolved matter in the ocean. *Nature* 369:549-552.
- Anderson MJ (2001) A new method for non-parametric multivariate analysis of variance, *Austral. Ecology* 26: 32–46.
- Aristegui J, Gasol JM, Duarte CM et al. (2009) Microbial oceanography of the dark ocean's pelagic realm. *Limnol Oceanogr* 54: 1501-1529.
- Anderson MJ, Gorley RN, Clarke KR (2008). PERMANOVA+ for PRIMER: Guide to Software and Statistical Methods. PRIMER-E, Plymouth, UK.
- Arnosti C, Steen AD, Ziervogel K, et al. (2011) Latitudinal gradients in degradation of marine dissolved carbon. *PLoS ONE* 6:e28900.
- Azam F, Fenchel T, Field JG et al. (1983) The ecological role of water-column microbes in the sea. *Mar Ecol Prog Ser* 10: 257-263.
- Baker BJ, Sheik CS, Taylor CA, et al. (2013) Community transcriptomic assembly reveals microbes that contribute to deep-sea carbon and nitrogen cycling. *ISME J* 7: 1962-1973.
- Baltar F, Lundin D, Palovaara J et al. (2016) Prokaryotic Responses to Ammonium and Organic Carbon Reveal Alternative CO₂ Fixation Pathways and Importance of

- Alkaline Phosphatase in the Mesopelagic North Atlantic. *Front Microbiol* **7**: 1670. doi: 10.3389/fmicb.2016.01670.
- Baltar F, Aristegui J, Sintès E, et al. (2010) Significance of non-sinking particulate organic carbon and dark CO₂ fixation to heterotrophic demand in the mesopelagic northeast Atlantic. *Geophys Res Lett* **37**, L09602.
- Bauer JE, Williams PM, Druffel ERM (1992) ¹⁴C activity of dissolved organic carbon fractions in the north-central Pacific and Sargasso Sea. *Nature* **357**: 667-670.
- Beman JM, Popp BN, Francis CA (2008) Molecular and biogeochemical evidence for ammonia oxidation by marine *Crenarchaeota* in the Gulf of California. *ISME J* **2**: 429-441.
- Benner R, Amon RMW (2015) The size-reactivity continuum of major bioelements in the ocean. *Annu Rev Mar Sci* **7**:185-205.
- Bent SJ, Forney LJ (2008) The tragedy of the uncommon: understanding limitations in the analysis of microbial diversity. *ISME J* **2**: 689-695.
- Bergauer K, Sintès E, van Bleijswijk J, et al. (2013) Abundance and distribution of archaeal acetyl-CoA/propionyl-CoA carboxylase genes indicative for putatively chemoautotrophic Archaea in the tropical Atlantic's interior. *FEMS Microbiol Ecol* **84**: 461-473
- Borneman J, Triplett EW (1997) Molecular microbial diversity in soils from eastern Amazonia: evidence for unusual microorganisms and microbial populations shifts associated with deforestation. *Appl Environ Microbiol* **63**: 2647-2653.

References

- Brown MV, Furlan JA (2005) Marine bacterial microdiversity as revealed by internal transcribed spacer analysis. *Aquat Microb Ecol* 41: 15-23.
- Buchan A, LeClerc GR, Gulvik CA, Gonzalez JM (2014) Master recyclers: features and functions of bacteria associated with phytoplankton blooms. *Nat Rev Microbiol* 12:686-698.
- Bustin SA (2000) Absolute quantification of mRNA using real-time reverse transcription polymerase chain reaction assays. *J Molec Endocrinol* 25: 169-193.
- Caporaso JG, Kuczynski J, Stombaugh J, et al. (2010) QIIME allows analysis of high-throughput community sequencing data. *Nat Methods* 7:335-336.
- Cardinale M, Brusetti L, Quatrini P, et al. (2004) Comparison of different primer sets for use in automated ribosomal intergenic spacer analysis of complex bacterial communities. *Appl Environ Microbiol* 70: 6147-6156.
- Carlson CA, Hansell DA (2015) DOM sources, sinks, reactivity, and budgets. In *Biogeochemistry of Marine Dissolved Organic Matter*, Hansell & Carlson, 2015. doi.org/10.1016/B978-0-12-405940-5.00010-8. Elsevier Inc.
- Carlson CA (2002) Production and Removal Processes. In: Hansell DA, Carlson CA (eds), *Biogeochemistry of marine dissolved organic matter*. Academic Press: San Diego, USA, pp 91–151.
- Chakravorty S, Helb D, Burday M, et al. (2007) A detailed analysis of 16S ribosomal RNA gene segments for the diagnosis of pathogenic bacteria. *J Microbiol Methods* 59: 330-339.

- Chao A (1987) Estimating the population size for capture-recapture data with unequal catchability. *Biometrics* 43: 783-791.
- Chauhan A, Cherrier J, Williams, HN (2009) Impact of sideways and bottom-up control factors on bacterial community succession over a tidal cycle. *Proc Natl Acad Sci USA* 106: 4301-4306.
- Chen RF, Bada JL (1992) The fluorescence of dissolved organic matter in seawater. *Mar Chem* 37: 191-221.
- Christian RR, Capone DG (2002) Overview of issues in aquatic microbial ecology. In: Hurst CJ, Crawford RL, Knudsen GR, McInerney MJ, Stetzenbach LD (eds). *Manual of Environmental Microbiology*. 2nd edn. ASM Press: Washington, pp 323-328.
- Coble PG (2007) Marine optical biogeochemistry: The chemistry of ocean color. *Chem Rev* 107: 402-418.
- Coble PG (1996) Characterization of marine and terrestrial DOM in seawater using excitation-emission matrix spectroscopy. *Mar Chem* 51: 325-346.
- Coolen MJL, Abbas B, van Bleijswijk J, et al. (2007) Putative ammonia-oxidizing Crenarchaeota in suboxic waters of the Black Sea: a basin-wide ecological study using 16S ribosomal and functional genes and membrane lipids. *Environ Microbiol* 9: 1001-1016.
- Cottrell MT, Kirchman DL (2003) Contribution of major bacterial groups to bacterial biomass production (thymidine and leucine incorporation) in the Delaware estuary. *Limnol Oceanogr* 48: 168-178.

References

- Cottrell MT, Kirchman DL (2000) Community composition of marine bacterioplankton determined by 16S rRNA gene clone libraries and Fluorescence In Situ Hybridization. *Appl Environ Microbiol* 66: 5116-5122.
- Covert JS, Moran MA (2001) Molecular characterization of estuarine bacterial communities that use high- and low-molecular weight fractions of dissolved organic matter. *Aquat Microb Ecol* 25: 127-139.
- Daims H, Brühl A, Amann R, et al. (1999) The Domain-specific probe EUB338 is insufficient for the detection of all Bacteria: Development and evaluation of a more comprehensive probe set. *Syst Appl Microbiol* 22: 434-444.
- DeLong EF, Béjà O (2010) The light-driven proton pump proteorhodopsin enhances bacterial survival during tough times. *PLoS Biology* 10: 101371.
- DeLong EF, Preston CM, Mincer T, et al. (2006) Community genomics among stratified microbial assemblages in the ocean's interior. *Science* 311:496–503.
- DeLong EF (1998) Everything in moderation: archaea as “non-extremophiles”. *Curr Opin Genet Dev* 8: 649-654.
- DeLong EF (1992) Archaea in coastal marine environments. *Proc Natl Acad Sci USA* 89: 5685-5689.
- DeLong EF, Wickham GS, Pace NR (1989) Phylogenetic stains: ribosomal RNA-based probes for the identification of single cells. *Science* 243: 1360-1363.
- DeLorenzo S, Bräuer SL, Edgmont CA, et al. (2012) Ubiquitous dissolved inorganic carbon assimilation by marine bacteria

- in the Pacific Northwest Coastal Ocean as determined by stable isotope probing. *PLoS ONE* 7: e46695.
- Dijkhuizen L, Harder W (1984) Current views on the regulation of autotrophic carbon dioxide fixation via the Calvin cycle in bacteria. *Antonie van Leeuwenhoek* 50: 473-487.
- Dinasquet J, Kragh T, Schroter ML, et al. (2013) Functional and compositional succession of bacterioplankton to a gradient in bioavailable dissolved organic carbón. *Environ Microbiol* 15: 2616-2628.
- Dobal-Amador V, Nieto-Cid M, Guerrero-Feijóo E, et al. (2016) Vertical patterns of bacterial abundance, activity and community composition in the dark waters of the Galician coast (NW Spain). *Deep Sea Res Part I* 114: 1-11.
- Dorst J, Bissett A, Palmer AS, et al. (2014) Community fingerprinting in a sequencing world. *FEMS Microbiol Ecol* 89: 316-330.
- Ducklow H, Carlson C, Church M, et al. (2001) The seasonal development of the bacterioplankton bloom in the Ross Sea, Antarctica. *Deep Sea Res P II* 48: 4199-4221.
- Ducklow HW, Carlson CA (1992) Oceanic bacterial production. In: *Advances in Microbial ecology*. Springer 113-181p.
- Erb TJ (2011) Carboxylases in natural and syntethic microbial pathways. *Appl Environ Microbiol* 77: 8466-8477
- Falkowski PG, Fenchel T, DeLong EF (2008) The microbial engines that drive Earth's biogeochemical cycles. *Science* 320: 1034-1039.
- Fernández-Gómez B, Richter M, Schüler M, et al. (2013) Ecology of marine Bacteroidetes: a comparative genomics approach. *ISME J* 7:1026-1037.

References

- Ferrera I, Arístegui J, González JM, et al. (2015) Transient changes in bacterioplankton communities induced by the submarine volcanic eruption of El Hierro (Canary Islands). *PloS One* 10: e0118136.
- Field CB, Behrenfeld MJ, Randerson JT, Falkowski P (1998) Primary production of the biosphere: integrating terrestrial and oceanic components. *Science* 281: 237-240.
- Francis CA, Roberts KJ, Beman JM, et al. (2005) Ubiquity and diversity of ammonia-oxidizing archaea in water columns and sediments of the ocean. *Proc Natl Acad Sci USA* 102: 14683–14688.
- Frank AH, Garcia JA, Herndl GJ, Reinthaler T (2016) Connectivity between surface and deep waters determines prokaryotic diversity in the North Atlantic Deep Water. *Environ Microbiol* DOI: 10.1111/1462-2920.13237
- Furhman JA, Cram JA, Needham DM (2015) Marine microbial community dynamics and their ecological interpretation. *Nat Rev Microbiol* 13: 133-146.
- Fuhrman JA, Hewson I, Schwalbach MS, et al. (2006) Annually reoccurring bacterial communities are predictable from ocean conditions. *Proc Natl Acad Sci USA* 103: 13104-13109.
- Furhman JA, Sleeter TD, Carlson CA, Proctor LM (1989) Dominance of bacterial biomass in the Sargasso Sea and its ecological implications. *Mar Ecol Prog Ser* 57: 207-217.
- Galand PE, Lovejoy C, Amilton AK, et al. (2010) Archaeal diversity and gene for ammonia oxidation are coupled to ocean circulation. *Environ Microb* 11: 971-980.

- Galand PE, Casamayor EO, Kirchman DL, Lovejoy C (2009) Ecology of the rare microbial biosphere of the Arctic Ocean. *Proc Natl Acad Sci USA* 106: 22427-22432.
- Gallagher JM, Carton MW, Eardly DF, Patching JW (2004) Spatio-temporal variability and diversity of water column prokaryotic communities in the eastern North Atlantic. *FEMS Microbiol Ecol* 47:249-262.
- García-Martínez J, Acinas SG, Anton AI, Rodríguez-Valera F (1999) Use of the 16S--23S ribosomal genes spacer region in studies of prokaryotic diversity. *J Microbiol Methods* 36: 55-64
- Gasol JM, Arístegui J (2007) Cytometric evidence reconciling the toxicity and usefulness of CTC as a marker of bacterial activity. *Aquat Microb Ecol* 46:71-83.
- Gasol JM, Zweifel U, Peters F, et al. (1999) Significance of Size and Nucleic Acid Content Heterogeneity as Measured by Flow Cytometry in Natural Planktonic Bacteria. *Appl Environ Microbiol* 65: 104475-104483.
- Ghiglione JF, Galand PE, Pommier T et al. (2012) Pole-to-pole biogeography of surface and deep marine bacterial communities. *Proc Natl Acad Sci USA* 109: 17633-17638.
- Giovanonni S, Rappé M (2000) Evolution, diversity and molecular ecology of marine prokaryotes. In Kirchman DL (ed.) *Microbial Ecology of the Oceans*, 1st edn. New York: John Wiley and Sons Inc., pp 47-84.
- Giovanonni SJ, Rappé MS, Vergin, KL, Adair NL (1996) 16S rRNA genes reveal stratified open ocean bacterioplankton populations related to the green non-sulfur bacteria. *Proc Natl Acad Sci USA* 93: 7979-7984.

References

- Glaubitx S, Labrenz M, Jost G, Jürgens K. (2010) Diversity of active chemolithoautotrophic prokaryotes in the sulfidic zone of a Black Sea pelagic redoxcline as determined by rRNA-based stable isotope probing. *FEMS Microbiol Ecol* 74: 32.41.
- Glöckner FO, Gasol JM, McDonough N, et al. (2012) Marine microbial diversity and its role in ecosystem functioning and environmental change. Marine Board Position Paper 17. Calewaert JB and McDonough N (Eds). Marine Board-ESF, Ostend, Belgium.
- Goldberg SM, Johnson J, Busam D, et al. (2006). A Sanger/pyrosequencing hybrid approach for the generation of high-quality draft assemblies of marine microbial genomes. *Proc Natl Acad Sci USA* 103, 11240-11245.
- Gomez-Alvarez V, Teal TK, Schmidt TM (2009) Systematic artifacts in metagenomes from complex microbial communities. *ISME J* 3: 1314-1317.
- Gómez-Consarnau L, Lindh MV, Gasol JM, Pinhassi J (2012) Structuring of bacterioplankton communities by specific dissolved organic carbon compounds. *Environ Microbiol.* 14:2361-2378.
- Gómez-Consarnau L, González JM, Coll-Jadó M, et al. (2007) Light stimulates growth of proteorhodopsin-containing marine Flavobacteria. *Nature* 445: 210-213.
- Gordon DA, Giovannoni SJ (1996) Detection of stratified microbial populations related to *Chlorobium* and *Fibrobacter* species in the Atlantic and Pacific Oceans. *Appl Environ Microbiol* 4: 1171-1177.

- Green SA, Blough NV (1994) Optical absorption and fluorescence properties of chromophoric dissolved organic matter in natural waters. *Limnol Oceanogr* 29: 1903-1916.
- Grégori G, Citterio S, Ghiani A, et al. (2001) Resolution of viable and membrane-comprised bacteria in freshwater and marine waters based on analytical flow cytometry and nucleic acid double staining. *Appl Environ Microbiol* 67:4662-4670.
- Grote J, Jost G, Labernz M, et al. (2008) Epsilonproteobacteria Represent the Major Portion of Chemoautotrophic Bacteria in Sulfidic Waters of Pelagic Redoxclines of the Baltic and Black Seas. *App Environ Microbiol* 74: 7546-7551.
- Guerrero-Feijóo E, Nieto Cid M, Sintes E, Varela MM (submitted) Changes in bacterial activity and community composition in response to size-fractionated dissolved organic matter. *ISME J*
- Guerrero-Feijóo E, Sintes E, Herndl GJ, Varela MM (accepted) High dark inorganic carbón fixation rates by active chemolithoautotrophic microbes off the Galician margin (NW Iberian margin). *Environ Microbiol*
- Guerrero-Feijóo E, Nieto-Cid M, Dobal-Amador V, et al. (2017) Optical properties of dissolved organic matter shape the microbial communities inhabiting the euphotic, intermediate and deep waters off the Galician coast (NW Iberian margin). *FEMS Microbiol Ecol* DOI: <http://dx.doi.org/10.1093/femsec/fiw224>
- Guerrero-Feijóo E, Nieto-Cid M, Sintes E, Varela MM (2015) Bacterial activity and community composition response to the size-reactivity of dissolved organic matter. *Personnel*

References

- communication. *SAME14 Second EMBO Conference*. Uppsala. Sweden.
- Haas BJ, Gevers D, Earl AM, et al. (2011) Chimeric 16S rRNA sequence for formation and detection in Sanger and 454-pyrosequenced PCR amplicons. *Genome Res* 21: 494-504.
- Hallam SJ, Mincer TJ, Schleper C, et al. (2006) Pathways of carbon assimilation and ammonia oxidation suggested by environmental genomic analyses of marine Crenarchaeota. *PLoS Biol* 4: 520-536.
- Hansell D (2013) Recalcitrant dissolved organic fractions. *Annu Rev Mar Sci* 5:421-445.
- Hass BJ, Gevers D, Earl AM, et al. (2011) Chimeric 16S rRNA sequence formation and detection in Sanger and 454-pyrosequenced PCR amplicons. *Genome Res* 21:494-504.
- Hansell DA, Carlson CA, Repeta DJ, Schlitzer R (2009) Dissolved organic matter in the ocean: A controversy stimulates new insights. *Oceanography* 22: 202-211.
- Hansen HP, Koroleff F (1999). Determination of nutrients. In: Grasshoff K, Kremling, K, Ehrhardt, M. (ed), *Methods of Seawater Analysis*, 3rd edition Wiley-VCH Verlag GmbH.
- Helms JR, Stubbins A, Ritchie JD, et al. (2008) Absorption spectral slopes and slope ratios as indicators of molecular weight, source and photobleaching of chromophoric dissolved organic matter. *Limnol Oceanogr* 51: 2170-2180.
- Herlemann DPR, Labrenz M, Jürgens K, et al. (2011) Transitions in bacterial communities along the 2000 km salinity gradient of the Baltic Sea. *ISME J* 5:1571-1579.
- Herndl GJ, Reinthaler T (2013) Microbial control of the dark end of the biological pump. *Nat Geosci* 6: 718-724.

- Herndl GJ, Reinthaler T, Teira E, et al. (2005) Contribution of Archaea to total prokaryotic production in the deep Atlantic Ocean. *Appl Environ Microbiol* 71: 2303-2309.
- Hill MO (1973) Diversity and evenness: a unifying notation and its consequences. *Ecology* 54: 427-432.
- Huber JA, Welch DBM, Morrison HG, et al (2007) Microbial population structures in the deep marine biosphere. *Science* 318: 97-100.
- Jiao N, Herndl GJ, Hansell DA, et al. (2010) Microbial production of recalcitrant dissolved organic matter: long-term carbon storage in the global ocean. *Nat Rev Microbiol* 8: 593-599.
- Kaiser K, Benner R (2009) Biochemical composition and size distribution of organic matter at the Pacific and Atlantic time-series stations. *Mar Chem* 133: 63-77.
- Kaneko R, Nagata T, Suzuki S, Hamasaki K (2016) Depth-dependent and seasonal variability in archaeal community structure in the subarctic and subtropical western North Pacific. *J Oceanogr* 72: 427-438.
- Karner MB, DeLong EF, Karl DM (2001) Archaeal dominance in the mesopelagic zone of the Pacific Ocean. *Nature* 409: 507-510.
- Khodse VB, Boshle NB (2011) Bacterial utilization of size-fractionated dissolved organic matter. *Aquatic Microb Ecol* 64:299-309.
- Kirchman DL, Elifantz H, Dittel AI, et al. (2007) Standing stocks and activity of Archaea and Bacteria in the western Arctic ocean. *Limnol Oceanog* 52:495-507.
- Kirchman DL, Dittel AI, Findlay, SEG, Fische D (2004) Changes in bacterial activity and community structure in response to

References

- organic matter in the Hudson River, New York. *Aquat Microb Ecol* 34: 243-257.
- Kirchman DL (2002) The ecology of Cytophaga-Flavobacteria in aquatic environments. *FEMS Microbiol Ecol* 39: 91-100.
- Kirchman DL (2001) Measuring bacterial biomass production and growth rates from leucine incorporation in natural aquatic environments. In: Paul JH (ed) *Methods in microbiology*, Academic Press 227-237pp.
- Kirchman DL (1993) Leucine incorporation as a measure of biomass production by heterotrophic bacteria. In: Kemp, P.F., Sherr, B.F., Sherr, E.B., Cole, J.J. (Eds.), *Handbook of Methods in Aquatic Microbial Ecology*. Lewis Publishers, Boca Raton, pp. 509–512.
- Kirchman DL, Knees E, Hodson R (1985) Leucine incorporation and its potential as measure of protein synthesis by bacteria in natural aquatic system. *Appl Environ Microbiol* 49: 599-607.
- Könneke M, Schubert DM, Brown PC, et al. (2014) Ammonia-oxidizing archaea use the most energy-efficient aerobic pathway for CO₂ fixation. *Proc Natl Acad Sci USA* 111: 8239-8244.
- Könneke MB, DeLong EF, Karl DM (2005) Isolation of an autotrophic ammonia-oxidizing marine archaeon. *Nature* 437: 543-546.
- Kujawinski EB (2011) The impact of microbial metabolism on marine dissolved organic matter. *Ann Rev Mar Sci* 3:567-599.

- Lam P, Jensen MM, Lavik G, et al. (2007) Linking crenarchaeal and bacterial nitrification to anammox in the Black Sea. *Proc Natl Acad Sci USA* 104: 7104-7109.
- Lami R, Cottrell MT, Campbell B, Kirchman DL (2009) Light-dependent growth and proteorhodopsin expression by Flavobacteria and SAR11 in experiments with Delaware coastal waters. *Environ Microbiol* 11: 3201-3209.
- Landa M, Cottrell MT, Kirchman DL et al. (2014) Phylogenetic and structural response of heterotrophic bacteria to dissolved organic matter of different composition in a continuous culture study. *Environ Microbiol* 16: 1668-1681.
- Landa M, Cottrell MT, Kirchman DL, et al. (2013) Changes in bacterial diversity in response to dissolved organic matter supply in a continuous culture experiment. *Aquat Microb Ecol* 69:157-168.
- Landry Z, Swan BK, Herndl GJ, et al. (in press) SAR202 genomes from the dark ocean predict pathways for the oxidation of recalcitrant dissolved organic matter. *MBio*8: e00413-17. doi:10.1128/mBio.00413-17.
- Langdon C (2010) Determination of dissolved oxygen in seawater by winkler titration using the amperometric technique. IOCCP Report N° 14, ICPO publication series N 134.
- Lauro FM, McDougald D, Thomas T et al. (2009) The genomic basis of trophic strategy in marine bacteria. *Proc Natl Acad Sci USA* 106:15527-15533.
- Lauro FM, Bartlett DH (2008) Prokaryotic lifestyles in deep sea habitats. *Extremophiles* 12: 15-25.
- Lekunberri I, Sintés E, De Corte D, et al. (2013) Spatial patterns of bacterial and archaeal communities along the Romanche

References

- Fracture Zone (tropical Atlantic). *FEMS Microbiol Ecol* 85: 537-552.
- Leuko S, Goh F, Ibáñez-Peral R et al. (2008) Lysis efficiency of standard DNA extraction methods for *Halococcus* spp. in an organic rich environment. *Extremophiles* 12:301-8.
- Locey KJ, Lennon JT (2016) Scaling laws predict global microbial diversity. *Proc Natl Acad Sci USA* 113: 5970-5975.
- Logue JB, Stedmon CA, Kellerman A, et al. (2016) Experimental insights into the importance of aquatic bacterial community composition to the degradation of dissolved organic matter. *ISME J* 10:533-545.
- Lønborg C, Nieto-Cid M, Hernando-Morales V, et al. (2016) Photochemical alteration of dissolved organic matter and the subsequent effects on bacterial carbon cycling and diversity. *FEMS Microbiol Ecol* 92, doi: 10.1093/femsec/fiw048
- Lønborg C, Álvarez-Salgado XA (2014) Tracing dissolved organic matter cycling in the eastern boundary of the temperate North Atlantic using absorption and fluorescence spectroscopy. *Deep-Sea Res I* 85: 35-46.
- Lopez-Garcia P, Lopez-Lopez A, Moreira D, Rodriguez-Valera F (2001) Diversity of free-living prokaryotes from a deep-sea site at the Antarctic Polar Front. *FEMS Microbiol Ecol* 36: 193-202.
- Madigan MT, Martinko JM, Brock TD (2006) Brock biology of microorganisms. Pearson Prentice Hall, Upper Saddle River, NJ.

- Margulies M, Egholm M, Altman WE, et al. (2005) Genome sequencing in microfabricated high-density picolitre reactors. *Nature* 437: 376-380.
- Martín-Cuadrado AB, López-García P, Alba JC, et al. (2007) Metagenomics of the Deep Mediterranean, a Warm Bathypelagic Habitat. *PloS ONE* 2: e914.
- Martínez-Pérez AM, Álvarez-Salgado XA, Arístegui J, Nieto-Cid M (2017) Deep-ocean dissolved organic matter reactivity along the Mediterranean Sea: does size matter? *Sci Rep* 7: 5687. doi:10.1038/s41598-017-05941-6
- Mende DR, Waller AS, Sunagawa S, et al. (2012) Assessment of metagenomic assembly using simulated next generation sequencing data. *PloS One* 7: e31386.
- Meyer JL, Edwards RT, Risley R (1987) Bacterial growth on dissolved organic carbon from a blackwater river. *Microb Ecol* 13: 13-29.
- Middelburg JJ (2011) Chemoautotrophy in the ocean. *Geophys Res Lett* 38: L24604. doi:10.1029/2011GL049725
- Moesender MM, Winter C, Arrieta JM, Herndl GJ (2001) Terminal-restriction fragment length polymorphism (T-RFLP) screening of a marine archaeal clone library to determine the different phylotypes. *J Microbiol Methods* 44: 159-172.
- Moran MA, Sheldon WM, Zepp RG (2000) Carbon loss and optical property changes during long-term photochemical and biological degradation of estuarine dissolved organic matter. *Limnol Oceanogr* 45: 1254-1264.

References

- Morán XAG, Clavo-Díaz A (2009) Single-cell vs. bulk activity properties of coastal bacterioplankton over an annual cycle in a temperate ecosystem. *FEMS Microbiol Ecol* 67:43-56.
- Moreira D, Rodríguez-Varela F, López-García P (2004) Analysis of a genome fragment of a deep-sea uncultivated Group II euryarchaeote containing 16S rDNA, a spectinomycin-like operon and several energy metabolism genes. *Environ Microbiol* 6: 959–969
- Morris RM, Rappé MS, Connon SA, et al. (2002) SAR11 clade dominates ocean surface bacterioplankton communities. *Nature* 420: 806-810.
- Nelson CE, Carlson CA (2012) Tracking differential incorporation of dissolved organic carbon types among diverse lineages of Sargasso Sea bacterioplankton. *Environ Microbiol* 14: 1500-1516.
- Nieto-Cid M, Alvarez-Salgado XA, Perez FF (2006) Microbial and photochemical reactivity of fluorescent dissolved organic matter in a coastal upwelling system. *Limnol Oceanogr* 51: 1391-1400.
- Nikard MP, Cottrell MT, Kirchman DL (2014) Uptake of dissolved organic carbon by gammaproteobacterial subgroups in coastal waters of the West Antarctic Peninsula. *Appl Environ Microbiol* 80: 3362-3368.
- Ouverney CC, Furhman HA (1999) Combined microautoradiography–16S rRNA probe technique for determination of radioisotope uptake by specific microbial cell types in situ. *App Environ Microbiol* 65: 1746-1752.

- Paillet J, Arhan M, McCartney MS (1998) Spreading of Labrador Sea water in the eastern North Atlantic. *J Geophys Res Oceans* 103: 10223-10239.
- Palovaara J, Akram N, Baltar F, et al. (2014) Stimulation of growth by proteorhodopsin phototrophy involves regulation of central metabolic pathways in marine planktonic bacteria. *Proc Natl Acad Sci* 111: 3650-3658.
- Pernthaler A, Pernthaler J, Amann R (2002) Fluorescence in situ hybridization and catalyzed reporter deposition for the identification of marine bacteria. *Appl Environ Microbiol* 68: 3094-3101.
- Pham VD, Konstantinidis KT, Palden T, DeLong EF (2008) Phylogenetic analyses of ribosomal DNA-containing bacterioplankton genome fragments from a 4000 m vertical profile in the North Pacific Subtropical Gyre. *Environ Microbiol* 10: 2313-2330.
- Pinhassi J, Sala MM, Havskum H, et al. (2004) Changes in bacterioplankton composition under different phytoplankton regimens. *Appl Environ Microbiol* 70:6753-6766.
- Pinhassi J, Berman T (2003) Differential growth response of colony-forming α - and γ -proteobacteria in dilution culture and nutrient addition experiments from Lake Kinneret (Israel), the eastern Mediterranean Sea, and the Gulf of Eilat. *Appl Environ Microbiol* 69: 199–211
- Pomeroy LR (1974) The ocean's food web, a changing paradigm. *Bioscience* 24: 499-504.
- Prieto E, González-Pola C, Lavín S, et al. (2013) Seasonality of intermediate waters hydrography west of the Iberian

References

- Peninsula from an 8 year semiannual time series of an oceanographic section. *Ocean Sci* 9: 411-429.
- Quince C, Lanzén A, Curtis TP, et al. (2009) Accurate determination of microbial diversity from 454 pyrosequencing data. *Nature Meth* 6: 639.
- Reeder J, Knight R (2010) Rapidly denoising pyrosequencing amplicon reads by exploiting rank-abundance distributions. *Nat Methods* 7: 668 – 669.
- Reinthaler T, van Aken H, Herndl GJ (2010) Major contribution of autotrophy to microbial carbon cycling in the North Atlantic's interior. *Deep-Sea Res P II* 57:1572–1580.
- Ruiz-Villarreal M, González-Pola C, del Rio GD, et al. (2006) Oceanographic conditions in North and Northwest Iberia and their influence on the Prestige oil spill. *Mar Pollut Bull* 53: 220-238.
- Salazar G, Cornejo-Castillo FM, Benítez-Barrios V, et al. (2016) Global diversity and biogeography of deep-sea pelagic prokaryotes. *ISME J* 10: 596-608.
- Sanger F, Nicklen S, Coulson AR (1977) DNA sequencing with chain-terminating inhibitors. *Proc Natl Acad Sci* 74, 5463-5467.
- Sauer U, Eikmanns BJ (2005) The PEP-pyruvate-oxaloacetate node as the switch point for carbon flux distribution in bacteria. *FEMS Microbiol Rev* 29: 765-794.
- Schloss PD, Westcott SL, Ryabin T, et al. (2009) Introducing MOTHUR: Open-source, platform-independent, community-supported software for describing and comparing microbial communities. *Appl Environ Microbiol* 75:7537-7541.

- Schmidt TM, DeLong EF, Prace NR (1991) Analysis of a marine picoplankton community by 16S rRNA gene cloning and sequencing. *J Bacteriol* 173: 4371-4378.
- Sheik CS, Jain S, Dick GJ (2014) Metabolic flexibility of enigmatic SAR324 revealed through metagenomics and metatranscriptomics. *Environ Microbiol* 16: 304–317.
- Simon M, Azam F (1989) Protein content and protein synthesis rates of planktonic marine bacteria. *Mar Ecol Progr Ser* 51: 201–13.
- Singh BN, Singh BR, Singh RL ,et al. (2009) Oxidative DNA damage protective activity, antioxidant and anti-quorum sensing potentials of *Moringa oleifera*. *Food Chem Toxicol* 47: 1109-1116.
- Singh BN, Munro S, Reid E, et al. (2006) Investigating microbial community structure in soils by physiological, biogeochemical and molecular fingerprinting methods. *Eur J Soil Sci* 57: 72-82.
- Sintes E, De Corte D, Haberleitner E, Herndl GJ (2016) Geographic Distribution of Archaeal Ammonia Oxidizing Ecotypes in the Atlantic Ocean. *Front Microbiol* doi: 10.3389/fmicb.2016.00077.
- Sintes E, De Corte D, Ouillon N, Herndl GJ (2015) Macroecological patterns of archaeal ammonia oxidation in the Atlantic Ocean. *Mol Ecol* 24: 4931-4942.
- Sintes E, Bergauer K, De Corte D, et al. (2013) Archaeal amoA gene diversity points to distinct biogeography of ammonia-oxidizing Crenarchaeota in the ocean. *Environ Microbiol* 15: 1647-1658.

References

- Sjöstedt J, Martiny JB, Munk P, Riemann L (2014) Abundance of broad bacterial taxa in the Sargasso Sea explained by environmental conditions but not water mass. *Appl Environ Microbiol* 80: 2786-2795.
- Smedile F, Messina E, La Cono V, et al. (2013) Metagenomic analysis of hadopelagic microbial assemblages thriving at the deepest part of Mediterranean Sea, Matapan-Vavvilov Deep. *Environ Microbiol* 15:167-192.
- Smith JM, Damashek J, Chavez FP, Francis CA (2016) Factors influencing nitrification rates and the abundance and transcriptional activity of ammonia-oxidizing microorganisms in the dark northeast Pacific Ocean. *Limnol Oceanogr* doi: 10.1002/lno.10235.
- Smith DC, Azam F (1992) A simple, economical method for measuring bacterial protein synthesis rates in seawater using 3 H-leucine. *Mar Microb Food Webs* 6: 107–114.
- Sogin ML, Morrison HG, Huber JA, et al. (2006) Microbial diversity in the deep sea and the underexplored “rare biosphere”. *Proc Natl Acad Sci USA* 103: 12115-12120.
- Sokal RR, Rohlf FJ (2013) *Biometry: The principles and practice of statistics in biological research*. WH Freeman and Co: New York.
- Stedmon CA, Nelson NB (2015) The optical properties of DOM in the ocean. In: Hansell DA, Carlson CA (eds). *Biogeochemistry of Marine Dissolved Organic Matter*, 2nd edn. Academic Press/Elsevier. 481-508p. doi.org/10.1016/B978-0-12-405940-5.00010-8.

- Sun MY, Dafforn KA, Brown MV, Johnston EL (2012) Bacterial communities are sensitive indicators of contaminant stress. *Mar Pollut Bull* 64: 1029-1038.
- Sunagawa S, Coelho LP, Chaffron S, et al. (2015) Ocean plankton. Structure and function of the global ocean microbiome. *Science* 348: 1261359.
- Swan BK, Martinez-Garcia M, Preston CM (2011) Potential for chemolithoautotrophy among ubiquitous bacteria lineages in the dark ocean. *Science* 333: 1296-1300.
- Teira E, Hernando-Morales V, Guerrero-Feijóo E, Varela MM (2017) Leucine, starch and bicarbonate by specific bacterial groups in surface shelf waters off Galicia (NW Spain). *Environ Microbiol* 19: 2379-2390.
- Teira E, Lebaron P, van Aken H, Herndl GJ (2006a) Distribution and activity of Bacteria and Archaea in the deep waters masses of the North Atlantic. *Limnol Oceanogr* 54: 2131-2144.
- Teira E, van Aken H, Veth, et al. (2006b) Archaeal uptake of enantiomeric amino acids in the meso- and bathypelagic waters of the North Atlantic. *Limnol Oceanogr* 54: 60-69.
- Teira E, Reinthaler T, Pernthaler A, et al. (2004) Combining catalyzed reporter deposition-fluorescence in situ hybridization and microautoradiography to detect substrate utilization by bacteria and archaea in the deep ocean. *Appl Environ Microbiol* 70: 4411-4414.
- Van de Peer Y, Rensing SA, Maier UG, De Wachter R (1996) Substitution rate calibration of small subunit ribosomal RNA identifies chlorarachniophyte endosymbionts as

References

- remnants of green algae. *Proc Natl Acad Sci USA* 93: 7732-7736.
- Varela MM, van Aken H, Sintès E, et al. (2011) Contribution of Crenarchaeota and Bacteria to autotrophy in the North Atlantic interior. *Environ Microbiol* 13: 1524-1533.
- Varela M, van Aken H, Herndl GJ (2008a) Abundance and activity of Chloroflexi-type SAR202 bacterioplankton in the meso- and bathypelagic waters of the (sub)tropical Atlantic. *Environ Microbiol* 10: 1903-1911.
- Varela M, van Aken H, Sintès E, Herndl GJ (2008b) Latitudinal trends of Crenarchaeota and Bacteria in the meso- and bathypelagic waters of the eastern north Atlantic. *Environ Microbiol* 10: 110-124.
- Venter JC, Remington K, Heidelberg JF, et al. (2004) Environmental genome shotgun sequencing of the Sargasso Sea. *Science* 304: 66-74.
- Wallner G, Amman R, Beisker W (1993) Optimizing fluorescent in situ hybridization 696 with rRNA-targeted oligonucleotide probes for flow cytometric identification of 697 microorganisms. *Cytometry*;14: 136–143.
- Walsh E, Smith D, Sogin M, D'Hondt S (2015) Bacterial and archaeal biogeography of the deep chlorophyll maximum in the South Pacific Gyre. *Aquat Microb Ecol* 75: 1-13.
- Wang Q, Garrity GM, Tiedje JM et al. (2007) Naive Bayesian classifier for rapid assignment of rRNA sequences into the new bacterial taxonomy. *Appl Env Microbiol* 73:5261-5267.
- West NJ, Obernosterer I, Zemb O, Lebaron P (2008) Major differences of bacterial diversity and activity inside and

- outside of a natural iron-fertilized phytoplankton bloom in the Southern Ocean. *Environ Microbiol* 10:738-756.
- Whitman WB, Coleman DC, Wiebe WJ (1998) Prokaryotes: the unseen majority. *Proc Natl Acad Sci USA* 95: 6578-6583.
- Williams PM, Druffel ER (1987) Radiocarbon in dissolved organic matter in the central North Pacific Ocean. *Nature* 330: 6145.
- Williams P (1981) Incorporation of microheterotrophic processes into the classical paradigm of the planktonic processes into the classical paradigm of the planktonic food web. *Kiel Meeresforsch* (in press).
- Wuchter C, Abbas B, Coolen MJL, et al. (2006) Archaeal nitrification in the ocean. *Proc Natl Acad Sci USA* 103: 12317-12322.
- Yamamoto M, Takai K (2011) Sulfur metabolisms in epsilon- and gamma-Proteobacteria in deep-sea hydrothermal fields. *Front Microbiol* 2: 1-8.
- Yamashita Y, Tanoue E (2003) Chemical characterization of protein-like fluorophores in DOM in relation to aromatic amino acids. *Mar Chem* 82: 255-271.
- Yilmaz P, Yarza P, Rapp JZ, Glöckner FO (2016) Expanding the world of marine bacterial and archaeal clades. *Front Microbiol* 6: 1524.
- Yokokawa T, De Corte D, Sintès E, Herndl GJ (2010) Spatial patterns of bacterial abundance, activity and community composition in relation to water masses in the eastern Mediterranean Sea. *Aquat Microb Ecol* 59: 185-195.

References

Zehr JP, Ward BB (2002) Nitrogen cycling in the ocean: new perspectives on processes and paradigms. *Appl Environ Microbiol* 68: 1015-1024.



Acknowledgements

Para finalizar esta tesis toca escribir los agradecimientos. Tengo que decir que esta tesis no es únicamente mía, si no de todas esas personas que me han acompañado durante esta etapa. Sin sus ánimos, su apoyo y sus consejos esto no sería posible. Me siento afortunada de haberme encontrado con personas tan maravillosas durante esta etapa.

Empezando por las Rías Altas:

Quiero expresar mi más sincero agradecimiento a mi patrona, Marta Varela, que me brindó la oportunidad de iniciarme en el mundo de la Ecología Microbiana. Gracias por contagiarme el entusiasmo, la pasión por el trabajo y guiarme durante este camino, por tu apoyo incondicional, tus cuidadosas planificaciones y concienzudas correcciones. Debo agradecerte enormemente por haber removido cielo y tierra para que mi estancia en el instituto fuese más larga y un largo etc...

También debo agradecer enormemente a Eva Sintés. Por tu implicación, tus consejos y todas las ideas interesantes que has aportado a este trabajo y por todo el apoyo y la ayuda que me has dado. Cuando viajé a Viena para realizar mi estancia predoctoral me recibiste con los brazos abiertos. Aunque fue una estancia breve, hiciste que me sintiese muy cómoda. Gracias por ayudarme tanto y especialmente en la etapa final, gracias por conseguir sacar hueco para mí con todo el lío que has tenido.

Me gustaría agradecer al Instituto Español de Oceanografía de A Coruña toda la ayuda durante esta travesía. Muchas gracias a toda la gente que del grupo Medio Marino que de una forma u

otra me han acompañado en esta aventura de aprendizaje y crecimiento profesional: Marta Álvarez, Antonio Bode, Manuel Ruíz (“el chico”), Angelucho (“el padre”), Conchi (“la pitonisa”), Fátima (“la patronita”), Elena (“la princess de los océanos”), Jorge, José (“máster chef”), Mónica, María Jesús, Gelines, Carlota (“la fashion victim”), Pedrito... y a los que no son del grupo Jose Luis, Sole, Joaquín, Pedro... gracias por hacerme sentir tan arropada.

No me olvido del “gallinero”, mi segunda casa, lugar donde se ha incubado gran parte de esta tesis. Gracias a mis compis por compartir tantos momentos conmigo y por aguantarme en los momentos de máximo estrés: Ángel, Inés, Carmen, Henar, Susi.

Gracias a la gente que a pesar de su breve paso por el gallinero u otras dependencias del insti hicimos buenas migas, porque con compañía se trabaja mejor: Ale, Alba, Eva, Tania (mi mouchi), Noelia, Iraia.

Isa Herraiz, la vecina más próxima al gallinero. Gracias por tu apoyo, nuestras largas charlas, por tus consejos, nuestros coffees, tardes de shopping y surffing.

Ángel, muchas gracias por tu amistad, por aguantarme, por enseñarme a mantener la calma en los momentos de estrés exponencial, por ser mi instructor de surf, de buceo, por preocuparte siempre por mi bienestar, sabes que cuentas con mi amistad para siempre. Y como no...muchas gracias también a tu

media naranja, la Mery, que ella siempre sabe sacarme una sonrisa.

Inesita, cuando te fuiste el gallinero se quedó muy vacío, pero a pesar de la distancia siempre has estado bien cerca. Muchísimas gracias por todo tu apoyo, tu positividad y por los grandes consejos que me has dado.

Alejandrina, gracias por todos los ánimos, por escuchar siempre mis monólogos infinitos, por entenderme.

Mouchi, tu siempre ahí tan pendiente de mí, eres una grandísima persona. Doy gracias por haberte conocido y compartido tantas cosas juntas.

A la chiquilla siempre pegada al citómetro, mi Patronita, te estoy muy muy muy agradecida y ya lo sabes. Qué te voy a decir que tú no sepas ya. Eres una de las personas con las que más momentos he compartido en la Coru, nuestras comilonas y tardes gochas, el shopping, tus enseñanzas sobre el mundo miyuki, tu amistad, tu gratitud, tu generosidad, tu apoyo, las risas juntas, todas esas cosas que espero seguir compartiendo contigo.

Mi pitonisa, ¿pensabas que te librabas de una dedicatoria especial? jaja, muchísimas gracias por todos tus sabios consejos, por darme la mano, y por el cariño con el que siempre me has tratado. Echo de menos “la silla”. Sii te aburres de los ciliados y los flagelados siempre puedes abrir tu propia consulta, ya tu sabeh... jaja. Te echo mucho de menos!

Gracias a la gente que conocí durante mi paso por la Coru, que me sacaron de marcha en los momentos cruciales... Ale, Vitiño, San, Cris cantante, Dani, Patri, Miti, Cris, tito Mark....

..... *haciendo unas breves paradas:*

I would like to thank Gerhard Herndl for giving me the opportunity to visit your lab. Although my research stay at the University of Vienna was not too long, it was a great experience. Also, thank you for your comments on the manuscript.

Gracias a Pep y Vanessa Balagué por la estancia en el ICM. Gracias a esta estancia me inicié en el mundo de la bioinformática y aprendí a procesar secuencias de 454, gracias Vane por enseñarme tanto en tan poco tiempo. Por la rapidez contestando a los e-mails y resolviendo mis dudas.

.... *Cruzando el charco:*

Mis chicas, Antonia y Mery, muchas gracias por todo vuestro apoyo, por estar ahí, los gabinetes de crisis, os quiero mucho. Gracias por acompañarme mis mexicanitas!!!

.... *Gracias a la financiación y soporte técnico:*

Por supuesto, gracias a los proyectos BIO-PROF y MODUPLAN, que han financiado esta tesis, los congresos y las estancias.

Quiero agradecer a los tripulantes del B. O. Sarmiento de Gamboa por el apoyo logístico durante la campaña MODUPLAN.

Gracias a los compis de la campaña MODUPLAN por hacer la travesía y los muestreos más amenos (Ángel, Martita, Esther, Marta, Antonio, Carlota, Manuel, Gelines, Elena, Menchu, Alonso, Eva T, Eva S, Chie, Lisi, José, Mar, Vanesa, David....espero no olvidarme de nadie!!).

Gracias al CESGA por el soporte técnico prestado para la realización de los análisis de secuenciación.

..... y finalizando por mis queridas Rías Baixas:

Gracias a Mar Nieto-Cid, otro pilar importante en el desarrollo de esta tesis doctoral. Gracias por darle sentido a las relaciones de los microbes con la DOM, por compartir tu valioso conocimiento de las propiedades ópticas de la DOM, mil gracias por tu amabilidad y tu apoyo (otra vez, :P).

A Mar Nieto-Cid y Pepe Álvarez-Salgado, gracias por el soporte con la materia orgánica disuelta vinculados al proyecto BIO-PROF y MODUPLAN.

Al equipo materia orgánica (Mar, Vane, David) por la ayuda prestada durante la campaña MODUPLAN para la realización de los experimentos de peso molecular.

A NICANOR team, por nuestras noches coruñesas de tapeo y cerveceo, por nuestras charlas.

A la chavalada del Grupo de Oceanografía Biológica de la UVigo (coloquialmente, GOBIDOS). Gracias por los buenos momentos compartidos, por las risas, las fiestas, congresos, excursiones, conciertos... Martita, Mery, mi superamiga Marina, Victor Hernando (por tus correcciones y charlas científicas), Toño, Little Nicanor (Victor Moreira), Esther, Antero, Otero...

Superamiga, la luarquesa, muchas gracias por escucharme siempre que lo he necesitado, por aportarme tantas buenas vibraciones, desprendes alegría y positividad!!! Nos quedan pendientes unas sidrinas y un rico cachopo para celebrar el depósito de esta tesis.

A mis chicas del piso camelias: Martita, Belén y Ele. Muchas gracias por todo el apoyo durante estos años (y los que nos quedan), vosotras siempre hacéis que lo complicado sea sencillo, gracias por aguantar mis dilemas y por nuestros debates... Martita, gracias por todo, por tu apoyo, los ánimos, por nuestras conversaciones sobre ecología microbiana, por los skypes para ayudarme a practicar las comunicaciones orales para los congresos, etc....Ah! la siguiente eres tú, y allí estaremos nosotras para apoyarte!! Ele...te mereces un monumento, aguantar a tres tesistas llocas!!! Belén, gracias por animarme, ya sabes cuál es el mejor modo de hacerlo, un rico guacamole soluciona todos los problemas e incrementa mi productividad (ya sabes, Guacalén

SA). Chicas os quiero muchísimo!!! Sin vosotras estaría perdida!!! Muchas gracias por estar siempre ahí!!!

A los pajaritos de Varys, Irene y Pascual, más que mis amigos sois como mis hermanos, os quiero un montón. Gracias por los momentos compartidos, por las noches de desenfreno acompañadas de mañanas de ibuprofeno, mis consejeros, que deciros... gracias por vuestra amistad. Gracias Pascu, por tus pascualadas con las que me has sacado más de una sonrisa e Irene, gracias por poner la cordura que nos falta a Pascu y a mí.

Gracias a mis chic@s: Pili, Ana Manzana, Vic, Chou, Fer, Samu, Laura, por las cerves, las cenas, las fiestas, por vuestros ánimos y ayuda.

Como no, gracias a la parte más importante, la familia. Muchas gracias a mis padres y hermanos, por vuestra paciencia infinita y vuestro apoyo incondicional. Gracias por animarme y aguantarme especialmente en la etapa final... A Lila y Willy que siempre tienen un mimiño para mí.

A Iván, gracias por acompañarme durante el viaje más duro, por poner luz en los días más grises, por ayudarme a superar los obstáculos, por estar siempre ahí.

Gracias a todos!!!



